The three dimensional structure of the apicoplast

A comprehensive study of the apicoplast architecture
in relation to lipid trafficking and protein translocation

De drie dimensionale structuur van de apicoplast

Een uitgebreide studie van de architectuur van de apicoplast
in relatie tot lipide transport en eiwit translocatie.

(met een samenvatting in het Nederlands)

Proefschrift

ter verkrijging van de graad van doctor aan de Universiteit Utrecht
op gezag van de rector magnificus, prof. dr. J.C. Stoof,
ingevolge het besluit van het college voor promoties
in het openbaar te verdedigen op
woensdag 28 januari 2009 des middags te 12.45

door

Cveta Borisova Tomova

Geboren op 18 juni 1976 te Ruse (Bulgarije)

Promotor: Prof. dr. A.J. Verkleij

Co-promotor: Dr. B.M. Humbel

To *Stefka Petkova Tomova*
Boris Ivanov Tomov

The research described in this thesis was performed at the division of Cellular Architecture and Dynamics, Institute of Biomembranes, University Utrecht, the Netherlands.

Print: Gildeprint, Enschede

Table of contents

Chapter 1

GENERAL INTRODUCTION

GENERAL INTRODUCTION

Plastids are a remarkably diverse set of organelles with distinct morphology and physiological functions. The two most prominent organelles are the mitochondria and the chloroplasts. Both are responsible for the two life-defining, biochemical pathways: the oxidative phosphorylation and the photosynthesis, respectively. The functions of mitochondria and plastids are not restricted to these two fundamental processes only, but extend to amino acid, carbohydrate and lipid metabolism and apoptosis. Virtually, these organelles are an indispensable part of the eukaryotic cells since the moment they were incorporated in an event called endosymbiosis. This incorporation of free living bacteria by a heterotrophic cell imposed the establishment of sophisticated machinery, which enables the transport of metabolites between the newly acquired organelles and the host cell. As a consequence of their origin, the biogenesis of these organelles became directly linked to the developmental fate of their host cells, being entirely dependant on the import of nuclear encoded proteins. How the substrates required for the metabolic processes that these organelles harbour are transported to their functional site is a key question. Understanding this transport mechanism will give the possibility to regulate the functionality of these organelles and to control the complicated processes, which are the basis of the fragile balance between health and diseases.

Next to mitochondria and chloroplasts, evolution has given rise to even more complex organelles known as secondary plastids. These plastids are bound by three or four membranes and are to be found in numerous organisms, mainly algae, but also in a very remarkable group of protozoan, intracellular parasites of the phylum Apicomplexa. These parasites are of great medical and veterinary importance. For example, the coccidian genus *Eimeria* causes a variety of intestinal diseases in poultry and cattle, the genus *Plasmodium* is the causative of malaria, one of the humankind's most prevalent health problems. Other members of this phylum include the human pathogens *Cryptosporidium* as well as the animal pathogens *Sarcocystis*. *Toxoplasma* also belongs to the phylum Apicomplexa and is capable of infecting and replicating within virtually any nucleated mammalian or avian cell (Dubey, 1998; Wong and Remington, 1993).

The phylum Apicomplexa has a characteristically polarized cell structure and a complex cytoskeletal and organellar arrangement at their apical end (Dubey et al., 1998) and a complex life cycle. The *Toxoplasma* life cycle is divided between feline and non-feline host-infections, which are correlated with sexual and asexual replication, respectively. The asexual part consists of two distinct stages depending on whether the infection is in the acute or chronic phase. The tachyzoite stage defines the rapidly growing form of the parasite found during the acute phase of toxoplasmosis.

The tachyzoite is crescent shaped, approximately 2 by 5 μm (Fig. 1), with a pointed anterior end and a rounded posterior end. The tachyzoite consists of various organelles, including a certain combination of structures called the apical complex. This complex includes: pellicle, subpellicular microtubules, apical rings, polar rings, conoid, rhoptries,

micronemes, dense granules and a multiple-membrane-bound plastid-like organelle the apicoplast, which has also been referred to as Golgi adjunct (Dubey et al., 1998; Dubremetz and Swartzman, 1993; Köhler et al., 1997; Sheffield and Melton, 1968).

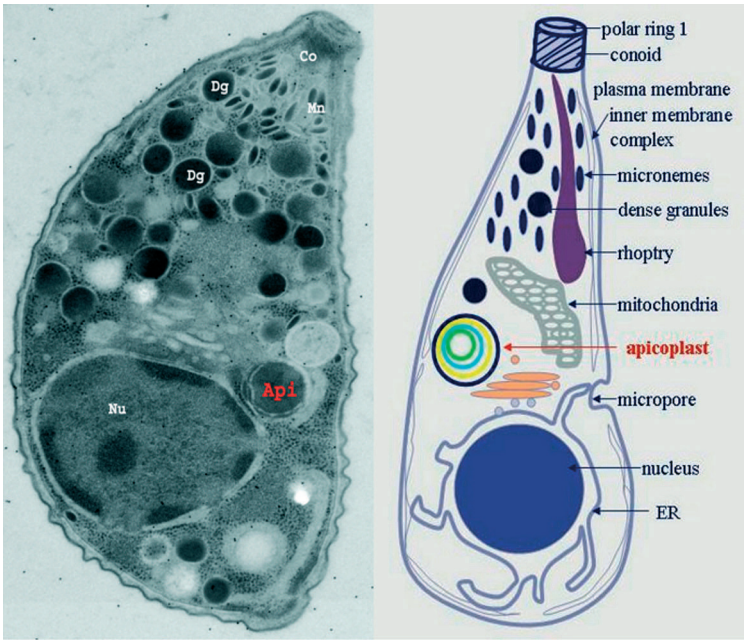

Figure 1 Micrograph and schematic drawing of a *Toxoplasma gondii* tachyzoite.

The pellicle consists of three membranes, a plasma membrane and two closely apposed membranes that form an inner membrane complex (IMC) (Morrissette et al., 1997; Sulzer et al., 1974; Vivier and Petitprez, 1972). Polar ring 1 is an electron-dense thickening of the inner membrane complex at the anterior end of the tachyzoite. Polar ring 2 give rise to twenty-two subpellicular microtubules running longitudinally almost the entire length of the cell just beneath the inner membrane complex. The Conoid (Co) consists of six to eight microtubular elements, arranged in a gentle spiral, forming a compressed spring. The Rhoptries are club-shaped organelles with excretory function, each consisting of an anterior narrow neck that extends into the interior of the conoid, and a saclike, posterior end. The Micronemes (Mn) are rod-like structures, which occur mostly at the anterior end of the parasite. Nucleus (Nu), Dense granules (Dg), Apicoplast (Api).

Asexual Life Cycle

Tachyzoites enter host cells by actively penetrating through the host cell plasmalemma or by phagocytosis (Dubremetz and Swartzman, 1993; Joiner, 1993; Morisaki et al., 1995; Silva et al., 1982). After entering the host cell, the tachyzoite becomes surrounded by a parasitophorous vacuole (PV), derived from both the parasite and the host cell (Joiner et al., 1994). They replicate inside the host cell by repeated endodyogeny (Sheffield and Melton, 1968) until they exit the cell to infect neighbouring cells. In the infected animal, tachyzoites differentiate into bradyzoites and form tissue cysts. These cysts are found predominantly in the central nervous system and muscle tissue, where they may reside for the life of the host. The development of tissue cysts throughout the body defines the

chronic stage of the asexual cycle. Cysts that are ingested through eating infected tissue are ruptured as they pass through the digestive tract, causing bradyzoite release. These bradyzoites can then infect the epithelium of the intestinal lumen, where they differentiate back to the rapidly dividing tachyzoite stage for dissemination throughout the body, thereby completing the asexual cycle.

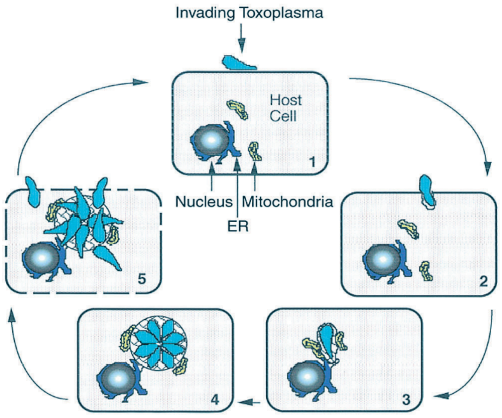

Figure 2 The *Toxoplasma* lytic cycle. (according to (Black and Boothroyd, 2000))

This diagram depicts the five steps responsible for the acute phase of toxoplasmosis. step 1: Attachment of *Toxoplasma* tachyzoite to the host cell. step 2: The parasite makes contact, at its apical end, with the host surface to initiate invasion. step 3: During the invasion the PV is formed and modified by secretion of the rhoptries and, later, the dense granules. The newly formed PV immediately recruits host mitochondria and ER. step 4: The parasites undergo several rounds of replication. step 5: Host cell egress is typically a destructive process that lyses the host cell and releases motile parasites. These parasites quickly invade neighboring cells to complete the cycle.

Pathogenicity of *Toxoplasma gondii*

The acute disease phase is associated with the rapidly dividing form of the parasite the 'tachyzoite', and the chronic phase with the presence of parasite tissue cysts containing the slowly dividing form or 'bradyzoite'. The tissue cysts can persist for the life of the host with no apparent ill-effects in healthy individuals. A significant proportion of the adult human population has been infected by the parasite, depending on lifestyle and geographic location.

Although human infections are usually relatively benign and lead to lifelong immunity, acute *T. gondii* infection during pregnancy in the nonimmune host can cause congenital transmission resulting in serious birth defects (affecting up to 0.1% of live births in some locations (Remington and Desmonts, 1995). The severity of congenital infections depends on the stage of pregnancy when the acute infection occurred, and spontaneous abortions or neurological disorders such as blindness and mental retardation can result. Furthermore, the reactivation of the latent chronic infection in immunocompromised individuals (e.g. the AIDS community) can cause a life-threatening toxoplasmosis. Within this latter patient group, *Toxoplasma* is a frequent cause of intracerebral focal lesions

resulting in toxoplasmic encephalitis (Luft, 1993; Luft and Remington, 1992). No therapy currently exists to treat the chronic infection stage of the disease (Ajioka et al., 2001; Jacobs et al., 1960).

Origin of the Apicoplast

The apicomplexan plastid, the apicoplast, has derived by "secondary endosymbiosis" (Fig. 3). Endosymbiosis is an evolutionary process, which gave rise to a remarkable variety of plastid-bearing organisms. They all, despite their diverse morphology and physiology, originated from a single successful incorporation of a cyanobacterium-like ancestor into and a eukaryotic phagotroph (Delwiche and Palmer, 1997). The product of this primary symbiotic event, an alga, has been itself engulfed and retained by another free living eukaryote in a process referred to as secondary endosymbiosis. This event had established the formation of eukaryotic hosts with a photosynthetic capacity such as Cryptophytes, Heterokonts, Euglenoids, Dinoflagellates (Douglas, 1998; Palmer and Delwiche, 1996). The same secondary symbiotic event led to the formation of a very specific group of protozoan parasites belonging to the phylum Apicomplexa. They have apparently lost the capacity to photosynthesize but retained a vestigial, DNA-containing plastid (Delwiche, 1997; McFadden, 1997; Köhler, 1997; Douglas, 1998; Dzierszinski, 1999; Bhattacharya, 2007).

Both the phylogeny of the apicoplast genome and the structure of this organelle (surrounded by multiple membranes) support this hypothesis (McFadden and Roos, 1999).

The most crucial step in the establishment of a new complex system, as is the output of a secondary endosymbiosis, is the regulation of metabolic exchange. This process established a new mechanism for balancing the dependence and maintenance of the plastid by its host. A key step in this process was the gene transfer from the pro-plastid to the nucleus of the host cell, which subsequently required the development of a way for protein re-targeting to the plastid. An important indication for the secondary endosymbiotic

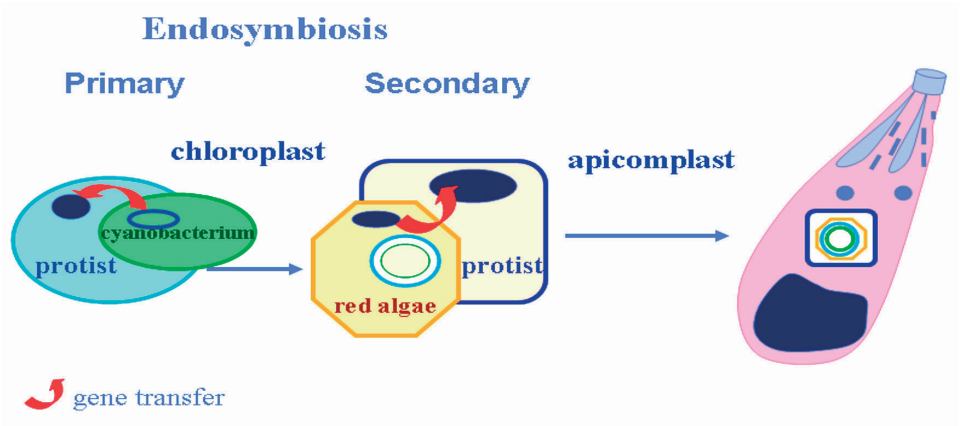

Figure 3 Schematic drawing of secondary endosymbiosis and the origin of Apicomplexa.

origin of the apicoplast is the number of membranes surrounding this organelle. The number of membranes is a very conservative character that does not change easily in evolution (Cavalier-Smith, 1999). The ultra-structure of the apicoplast is of crucial importance for the origin of the plastid and is directly related to its function. The number of membranes surrounding the apicoplast and the relation of this plastid with the other membranous compartments of the protozoan parasite is a key question for understanding the transport of metabolites to and from the apicoplast. Therefore the first step in this research was to elucidate the architecture of this organelle in its native state and in three dimensions.

Apicoplast function

The function of the apicoplast has been debated since its discovery (Gleeson, 2000; Wilson, 2002; Wilson et al., 1994). Early guesses, which were based on what was known about similar relict plastids in non-photosynthetic plants suggested that it was involved in the synthesis of haem for mitochondrial respiration, fatty-acid synthesis and starch storage (Köhler et al., 1997), and the production of aromatic amino acids (Palmer, 1992). Whatever the function, it was apparent soon after its discovery that the apicoplast is indispensable to the parasite (Fichera and Roos, 1997; Mazumdar et al., 2006)

Immediately after apicoplast inactivation (either pharmacological or genetic), parasites replicate normally in the first infectious cycle, but in the subsequent host cell the parasites die. This phenomenon is known as the delayed-death effect. Exactly what causes the "delayed death" still remains an open question. It became obvious that the apicoplast is crucial for a viable infection process. It has been postulated that the apicoplast provides substantial components, that are crucial for the successful invasion of the host cell and presumably involved in the generation of the parasitophorous vacuole (Fichera and Roos, 1997; Ralph et al., 2004).

Genome sequences of P. falciparum and *Toxoplasma gondii* predicted that most of the genes encoding apicoplast proteins have roles in anabolic functions belong to the proteins involved in fatty-acid synthesis (Waller et al., 1998) and non-mevalonate isopentenyl diphosphate synthesis (Jomaa et al., 1999).

Toxoplasma expresses enzymes associated with both type I (cytosolic) and type II (plastid) fatty-acid-synthesis pathways (Crawford et al., 2003), while *Plasmodium* harbours only a type II fatty acid synthesis pathway in the apicoplast.

Apicoplast metabolic pathways

The apicoplast pathways are reconstructed from the metabolic pathways of plant chloroplasts and bacteria as models in combination with the list of apicoplast proteins that have been predicted using bioinformatics. These pathways are different from the vertebrate host of the parasite, and provide insight into apicoplast function. The apicoplast apparently imports trioses that are converted to either fatty acids or isopentenyl diphosphate IPP (isoprenoid precursors) by the DOXP (1-deoxy-D-xylulose-5-phosphate) synthesis

pathway (Fig. 4). These acyl products are likely to be exported for use elsewhere in the parasite cell, perhaps even in formation of the parasitophorous vacuole within the host. Numerous nuclear encoded and apicoplast-targeted proteins, for example some type II FAS enzymes like ACP (Jelenska et al., 2001), malonyl-CoA transacylase (FabD), β-ketoacyl-ACP synthase III (FabH) (Prigge et al., 2003; Waller et al., 1998; Waller, 2003; Waters, 2002), enoyl-ACP reductase (FabI), β-ketoacyl-ACP reductase (FabG) (Pillai, 2003) and β-hydroxyacyl-ACP dehydratase (FabZ) (Sharma et al., 2003) are imported to join the handful of endogenously produced proteins for these activities.

The main carbon substrate for plastid fatty-acid synthesis is acetyl-CoA, which can either be generated from acetate, by the action of acetyl-CoA synthetase, or from pyruvate by the pyruvate dehydrogenase complex (PDHC). Plastid PDHC comprises four distinct subunits (E1α, E1β , E2 and E3), each of them seems to originate from the cyanobacterial ancestor of plastids (Schnarrenberger and Martin, 2002). These cyanobacterial-like subunits are also found in P. falciparum and *T. gondii*, and localization studies show that all substrates for PDHC, as well as the TPP and lipoic acid cofactors, are synthesized and assembled within the apicoplast (Fleige et al., 2007). ACP is the core protein of type II fatty-acid biosynthesis and holds the growing acyl chain on its phosphopantotheine prosthetic group.

Products of the fatty acid and isopentenyl diphosphate pathways have possible functions within the apicoplast, but these two pathways and the haem pathway also produce compounds that are likely to be essential for the whole parasite cell. Haem is required for mitochondrial respiration. Isoprenoids are required for mitochondrial ubiquinones, many prenylated proteins and for the synthesis of GPI and N-glycosylated proteins. Fatty acids are probably exported to the ER, where they are likely to be incorporated into phospholipids, perhaps together with the numerous fatty acids scavenged from the host. A common theme for these metabolic functions is the production and modification of lipids or lipid-bound proteins. All the pathways are likely to be crucial for the interaction between the parasite and the host, particularly in the establishment and regulation of the parasitophorous vacuole.

The metabolic products of the apicoplast synthesis are to be transported to different sites of the protozoan cell. This implies the existence of a highly specialized, trafficking system. What are the morphological sites involved in this system and what is the molecular mechanism regulating the specificity of metabolite recognition and translocation remains unknown. A major unit of such a specialized transport system in the eukaryotic cells is the endoplasmic reticulum (ER) as being both a significant site of lipid metabolism and a highly efficient lipid delivery network with diverse functional domains. It is accepted that ER participates in transport of acyl-lipids to plastids, but it is also possible that such lipid trafficking is accomplished in the opposite direction. Although the precise mechanism of lipid translocation is not defined yet one favoured hypothesis is that lipid transport takes place at specialized membrane contact sites (MCS) (Holthuis and Levine, 2005;

Voelker, 2003). Our investigation of the relation between the apicoplast outer membrane and the apposing ER membrane revealed the existence of such MCS between these two organelles.

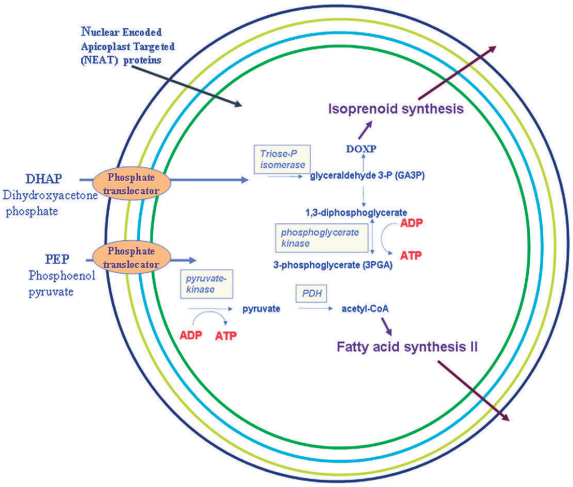

Figure 4 Overview of apicoplast metabolic pathways.

Posttranslational translocation of Nuclear-Encoded-Apicoplast-Targeted Prteins

Plastids are dependent on many hundreds of nuclear-encoded proteins that are targeted back to the organelle. The majority of proteins located in the mitochondria and in the plastids of plants and algae are encoded in the nuclear genome and targeted post-translationally to these organelles. Therefore, in eukaryotic cells N-terminal sequence extensions, called transit peptides, mediate accurate targeting of nuclear-encoded proteins into either mitochondria or plastids of plants and algae (Bruce, 2001; Waller et al., 1998), as well as into the relict plastids (apicoplasts) of parasites (Foth et al., 2003; Roos et al., 1999). Transit peptides (both plastid and mitochondrial) are enriched with basic residues (Jarvis and Soll, 2002), but their primary sequence and length are highly diverse, and no consensus motifs exist. Plastid transit peptides are not known to assume any consistent secondary structure (von Heijne and Nishikawa, 1991). Nevertheless, in plant cells, these two different classes of transit peptides direct the corresponding proteins from the cytoplasm into either the mitochondrion or the plastid with high fidelity.

In contrast to mitochondria and most plant plastids the secondary plastid is enclosed by multiple membranes, the outermost of which is apparently a derivative of the original phagocytic vacuole. As a result, the first step of targeting proteins to secondary plastids is entry into the endomembrane system, which is achieved by courtesy of an N-terminal signal peptide that precedes the transit peptide (Apt et al., 2002; Bhaya and Grossman, 1991; DeRocher et al., 2000; Ishida et al., 2000; van Dooren et al., 2001; Waller et al., 2000; Wastl and Maier, 2000; Yung and Lang-Unnasch, 1999; Yung et al., 2001). In these organisms, plastid-targeting leader sequences thus consist of two separate parts, i.e. they are bipartite (Roos et al., 1999; Waller et al., 2000). Once inside the endomem-

brane system, the signal peptide is cleaved off and the transit peptide then mediates a diversion from the default endomembrane secretion pathway into the plastid (van Dooren et al., 2001).

Besides being indicative of an endosymbiotic origin, the number of enveloping membranes is relevant to the molecular access of the apicoplast proteins from the cytosol to the plastid compartment. The mechanisms and molecules that mediate import of large amounts of cargo proteins across the four membranes surrounding the plastid remains elusive.

A summery of the currently existing models proposed to explain how nuclear-encoded proteins bound for the plastid lumen get across the membranes in plastids with four membranes like the apicoplast of parasite *Toxoplasma gondii* is presented in Figure 5.

In this study we clarified two important steps in the translocation process: The vesicular transport of proteins to the apicoplast and the existence of translocation complexes in the inner most membrane.

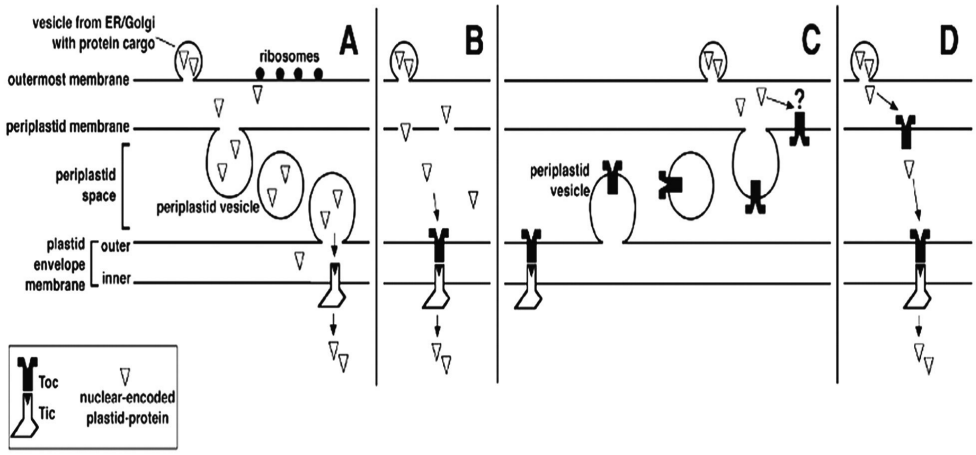

Figure 5 Schema representing four models (according to (Foth and McFadden, 2003)).

Proteins can reach the outermost plastid membrane in two possible ways: First, via vesicles that originate from somewhere along the secretory pathway (left side of panel A). Second option, nuclear-encoded plastid proteins are translated on ribosomes present on the outermost plastid membrane itself, which is continuous with the ER and the nuclear envelope (right side of panel A, and omitted in the other panels). (A) Gibbs (Gibbs, 1981) suggested that vesicles originating from the periplastid membrane fuse with the outer plastid envelope membrane, thus carrying the protein cargo across the periplastid space. (B) The simplest scenario postulates the presence of unspecific pores in the periplastid membrane that allow proteins to freely cross this membrane (Cavalier-Smith, 1999; Kroth and Strotmann, 1999). (C) (Cavalier-Smith, 1999) hypothesis suggests that periplastid vesicles may exchange (galacto)lipids as well as proteins between the outer plastid envelope membrane and the periplastid membrane. (D) Van Dooren (van Dooren et al., 2001) proposed dual targeting of the Toc complex components to both the outer plastid envelope membrane and the periplastid membrane.

Aim and Outline

The aim of this work was to elucidate the morphological features of the apicoplast and to correlate the obtained data with its cellular functions. The task of identifying the number of membranes surrounding this complex organelle, a debated issue ever since its discovery, and to follow the relation between these membranes with each other and with the neighbouring organelles was a challenging task. The most important condition to study the morphology of any biological sample is to preserve the structure in a state that is as close as possible to the native state.

Conventional methods of preparing biological samples for electron microscopy (chemical fixation, dehydration, embedding in resin at high temperature, sectioning and staining with heavy metals) have been invaluable for studies of cell morphology (Glauert, 1975; Hayat, 1989). However, these conventional methods have their limitations, especially for studies of membranous structures and their continuities by electron tomography. The ultra-structural determination and subsequent interpretation of the acquired data becomes difficult and dubious. Low temperature sample preparation and processing (cryomethods) can overcome some of these problems (Dubochet et al., 1983; Ebersold et al., 1981; Murk et al., 2003). Such preparations are likely to represent living cells more accurately because the sample is fixed within milliseconds allowing improvement of the ultrastructural observations.

Therefore we chose to combine high-pressure freezing (HPF), freeze substitution (FS) and resin embedding as a method that had proved to preserve lipids to a high degree and the morphology of subcellular structures (Ebersold et al., 1981; Humbel and Schwarz, 1989; Verkleij et al., 1985; Weibull et al., 1984). Further we examined the samples by electron tomography (ET) to elucidate the cellular ultra-structure of the apicoplast in its three dimensions.

1. *High-pressure freezing and freeze-substitution*

High-pressure freezing (Moor and Reiche, 1968) is generally acknowledged as the method of choice for cryo-fixation of biological samples up to a thickness of about 200 µm without the use of cryo-protectants. This enables us to study complex biological samples with improved ultra-structural preservation.

Frozen-hydrated cells can be examined directly in the EM by using a low temperature specimen holder, or they can subsequently be fixed by “freeze-substitution”.

During freeze-substitution, a technique developed for morphological studies (van Harreveld and Crowell, 1964), the frozen aqueous phase is removed by an organic solvent at low temperature (typically in the range -80 to -90°C). Finally the sample is warmed to room temperature and embedded by routine methods. The substitution solvent (such as acetone or methanol) contains fixatives, usually aldehydes, osmium tetroxide and uranyl acetate. The reagents included in FS protocols are typically the same as those used for aqueous phase fixation and staining, but can generate significantly different staining patterns following FS. In the present study we faced the problem that some membranes, including

those of the apicoplast were poorly visible on high-pressure frozen and freeze-substituted samples. The problem is complicated and controversial and some of its aspects will be addressed in Chapter 6. We applied different substitution cocktails, which yield different staining and contrast pattern in our samples. The FS with 0.1% uranyl acetate in acetone and subsequent low-temperature embedding in Lowicryl (Carlemalm et al., 1982) proved to be the most suitable approach for the purposes of this study. It allowed us to overcome the limitations that the other FS processing impelled in obtaining high-resolution data.

This specific sample processing is beneficial not only in terms of structure preservation and terms of contrast, but also suitable for immunocytochemical studies. Achieving this was a milestone in our attempt to elucidate the protein import pathway from the ER to the apicoplast.

Protein detection by immunocytochemistry at the ultra-structural level requires that the processing method does not alter an antigen beyond recognition by its specific antibody. For the majority of antigens, routine fixation and processing protocols for electron microscopy will not allow subsequent immunocytochemistry. The simplest approach is to apply mild fixation (e.g. low concentrations of formaldehyde with or without very low concentrations of glutaraldehyde) for relatively short periods of time (30–60 min.). The commonly used method today of thawed cryosections (Tokuyasu, 1980; Tokuyasu, 1986) reviewed by (Griffiths, 1993) relies on such sample stabilization. However, two potential problems with fixation in aldehydes remain. The first is that the antigen/antibody binding is reduced and there is always uncertainty over how much antigen has been lost. The second problem is that chemical fixation is slow, thus giving the possibility of redistribution of cellular constituents during the fixation process. Rapid freezing followed by freeze-substitution and low temperature embedding overcomes these two problems and offers an effective alternative to chemical fixation techniques for immunolabelling studies (Humbel et al., 1983; Humbel and Müller, 1986).

In general, the effects of fixatives at substitution temperatures are uncertain, therefore for immunocytochemical studies it is suggested fixatives to be avoided by freeze-substitution in solvent only (Monaghan and Robertson, 1990) followed by embedding in a low-temperature resin (Lowicryl), polymerised at low temperature by UV light.

2. *Electron tomography*

Electron tomography is a method for generating 3D images on the basis of multiple 2D projection images of a 3D object, obtained over a wide range of viewing directions (Fig. 6 steps 1, 2). The sought-after 3D image is generated in a computer by back-projecting each 2D image with appropriate weighting (Frank, 1992; Koster et al., 1997). Each image displays only one slice from the many that comprise the reconstruction, therefore, the structure and position of complex features can be followed in the neighbouring slices (Fig. 6 step 3). The features of interest can be traced through the tomogram, marking their contours (manually) on many successive slices in the 3D volume and finally creating a model (Fig. 6 steps 4, 5). Such models are viewed as a 3D representation.

Both tomograms and models can be zoomed, panned, tilted and rotated for easy viewing and can be used for quantitative structural analysis. ET provides highly informative images of functionally significant cellular structures. In addition, due to the fact that each image represents a slice that is only a few nanometers thick, defined by the size of the voxels in the reconstruction, the resolution along the viewing axis is almost as good as the resolution in the image itself.

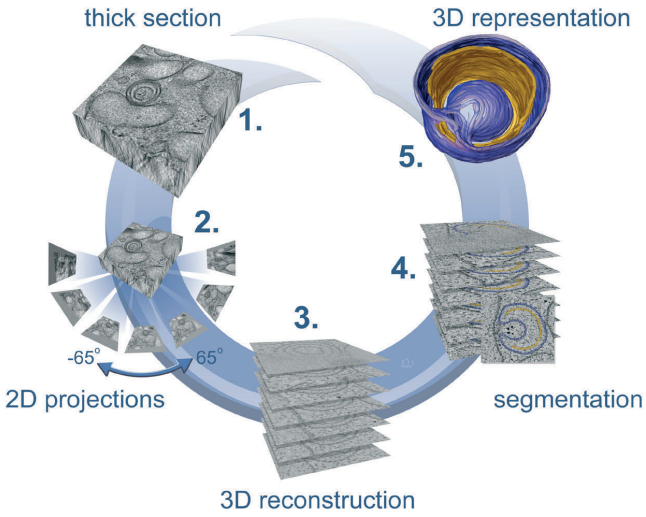

Figure 6 Schematic representation of the technique Electron Tomography
(courtesy of Misjaël N. Lebbink)

Chapter 2 Apicoplast Membranes – how many?
Since the discovery of the apicoplast the question of the number of membranes surrounding this plastid was one of the most convoluted issues. It was believed that the apicoplast in *Toxoplasma* and *Plasmodium* was bounded by only three (or even two) membranes (Hopkins et al., 1999; Köhler, 2005; McFadden et al., 1996; McFadden and Waller, 1997). It is nowadays commonly accepted that there are in fact four membranes (Tomova et al., 2006).
Chapter 3 What is the relation between ER and the apicoplast in *Toxoplasma gondii* and what are the possible functional aspects?
In this chapter we aimed to investigate the exact relation between the apicoplast and the ER. Associations of the apicoplast with the ER have been reported in P. falciparum (Aikawa, 1966; Tonkin et al., 2006) and *Sarcocystis* sp. (Tomova et al., 2006). The nature of this association is of high importance. The question whether the ER comes close to the apicoplast outer membrane without fusing with it; or whether the hydrophobic faces of the neighbouring bilayers are connected, so that the two membranes are continues, is both an indication for the evolutionary identity of the plastid and a key step in understanding the transport of nuclear encoded proteins. In order to ensure accurate morphological characterisation of the observed contact sites we performed numerous measurements in

high-resolution tomograms using the IMOD software package. We defined the structural features of these MCS and we proposed the functional aspect of it, namely an important part of the complex lipid traffic in the parasite cell.

Chapter 4 Where does *Tg*Tic20 localize in the apicoplast of *Toxoplasma gondii* and what is the importance of this protein for the biogenesis of the apicoplast?

Four membranes surround the apicoplast of *T. gondii*. To characterise proteins involved in protein import across these membranes, we performed comparative genomic analyses to identify proteins with possible roles in apicoplast protein import. In this study we identify a divergent *T. gondii* homologue of the plant Tic20 protein (*Tg*Tic20). We demonstrate that Tic20 of *Toxoplasma gondii* is an integral protein of the innermost plastid membrane. We engineer a conditional null-mutant and show that *Tg*Tic20 is essential for parasite growth. To functionally characterize this mutant we developed several independent biochemical import assays that reveal that loss of *Tg*Tic20 leads to severe impairment of plastid protein import. *Tg*Tic20 is the first experimentally validated protein import factor identified in apicoplast of *T. gondii* (van Dooren et al., 2008).

Chapter 5 How do nuclear encoded proteins tackle four biological membranes in *Toxoplasma gondii*?

In this chapter we focus on the possible mechanisms of translocation of proteins through four membranes with different evolutionary origin and thus different morphology. We followed the localization of the two most substantially studied stromal proteins acyl carrier protein (ACP) and ferrodoxin NADP reductase (FNR) (immunocytochemically) in high pressure frozen samples to obtain the most reliable information regarding the exact distribution of these proteins within the parasite cell and the plastid sub-compartments.

To validate these results and to obtain invaluable information regarding membrane continuities and the protein distribution in a three dimensional volume we also performed electron tomography. Based on our new results we propose a hypothesis how the proteins cross the four membranes of the apicoplast.

References

Aikawa, M. 1966. The fine structure of the erythrocytic stages of three avian malarial parasites, *Plasmodium fallax*, *Plasmodium lophurae* and *Plasmodium cathemerium*. American Journal of Tropical Medicine and Hygiene. 15:449–471.

Ajioka, J.W., Fitzpatrick, J.M. and Reitter, C.P. 2001. *Toxoplasma gondii* genomics: shedding light on pathogenesis and chemotherapy. Expert Reviews in Molecular Medicine. 6:1-19.

Apt, K.E., Zaslavkaia, L., Lippmeier, J.C., Lang, M., Kilian, O., Wetherbee, R., Grossman, A.R. and Kroth, P.G. 2002. In vivo characterization of diatom multipartite plastid targeting signals. Journal of Cell Science. 115:4061-4069.

Bhaya, D. and Grossman, A. 1991. Targeting proteins to diatom plastids involves transport through an endoplasmic reticulum. Molecular and General Genetics. 229:400-404.

Black, M.W. and Boothroyd, J.C. 2000. Lytic Cycle of *Toxoplasma gondii*. Microbiology and Molecular Biology Reviews. 64:607–623.

Bruce, B.D. 2001. The paradox of plastid transit peptides: conservation of function despite divergence in primary structure. Biochimica et Biophysica Acta. 1541:2-21.

Carlemalm, E., Garavito, R.M. and Villiger, W. 1982. Resin development for electron microscopy and an analysis of embedding at low temperature. Journal of Microscopy. 126:123-143.

Cavalier-Smith, T. 1999. Principles of protein and lipid targeting in secondary symbiogenesis: euglenoid, dinoflagellate, and sporozoan plastid origins and the eukaryotic family tree. Journal of Eukaryotic Microbiology. 46:347-366.

Crawford, M.J., Zhu, G. and Roos, D.S. 2003. Both type I and type II fatty acid synthases in *Toxoplasma gondii*, abstr. 14C. In Molecular Parasitology Meeting XIV.

Delwiche, C.F. and Palmer, J.D. 1997. The origin of plastids and their spread via secondary endosymbiosis. Plant Systematics and Evolution. Suppl. 11:53-86.

DeRocher, A., Hagen, C.B., Froehlich, J.E., Feagin, J.E. and Parsons, M. 2000. Analysis of targeting sequences demonstrates that trafficking to the *Toxoplasma gondii* plastid branches off the secretory system. Journal of Cell Science. 113:3969–3977.

Douglas, S.E. 1998. Plastid evolution: origins, diversity, trends. Current Opinion in Genetics & Development. 8:655-661.

Dubey, J.P. 1998. Advances in the life cycle of *Toxoplasma*. International Journal of Parasitology. 28:1019–1024.

Dubey, J.P., Lindsay, D.S. and Speer, C.A. 1998. Structures of *Toxoplasma gondii* Tachyzoites, Bradyzoites, and Sporozoites and Biology and Development of Tissue Cysts. Clinical Microbiology Reviews. 11:267–299.

Dubochet, J., McDowall, A.W., Menge, B., Schmid, E.N. and Lickfeld, K.G. 1983. Electron microscopy of frozen-hydrated bacteria. Journal of Bacteriology. 155:381-390.

Dubremetz, J.F. and Swartzman, J.D. 1993. Subcellular organelles of *Toxoplasma gondii* and host cell invasion. Res. Immunol. 144:31-33.

Ebersold, H.R., Cordier, J.L. and Lüthy, P. 1981. Bacterial mesosomes: method dependent artifacts. Archives of Microbiology. 130:19-22.

Fichera, M.E. and Roos, D.S. 1997a. A plastid organelle as a drug target in apicomplexan parasites. Nature. 390:407–409.

Fichera, M.E. and Roos, D.S. 1997b. A plastid organelle as a drug target in apicomplexan parasites. Nature. 390:407-409.

Fleige, T., Fischer, K., Ferguson, D.J., Gross, U. and Bohne, W. 2007. Carbohydrate metabolism in the *Toxoplasma gondii* apicoplast: localization of three glycolytic isoenzymes, the single pyruvate dehydrogenase complex, and a plastid phosphate translocator. Eukaryotic Cell. 6:984–996.

Foth, B.J., Ralph, S.A., Tonkin, C.J., Struck, N.S., Fraunholz, M., Roos, D.S., Cowman, A.F. and McFadden, G.I. 2003. Dissecting apicoplast targeting in the malaria parasite *Plasmodium falciparum*. Science. 299:705-708.

Frank, J. 1992. Electron Tomography: Three-dimensional imaging with the transmission

electron microscope. Plenum Press, New York, London.
Glauert, A. M. 1975. Fixation, dehydration and embedding of biological specimens. In: Practical Methods in Electron Microscopy, Vol. 3, Glauert, A. M., (ed.). Elsevier, Amsterdam.
Gleeson, M.T. 2000. The plastid in Apicomplexa: what use is it? International Journal of Parasitology. 30:1053–1070.
Griffiths, G. 1993. Fine Structure Immunocytochemistry. Springer-Verlag, Berlin, Heidelberg.
Hayat, M. A., 1989. Principles and Techniques of Electron Microscopy. Biological Applications, 3rd edn.,Hayat M. A., (ed.). Macmillan, London and CRC Press, Boca Raton, Florida, pp. 377-106.
Holthuis, J.C.M. and Levine, T.P. 2005. Lipid Traffic: Floppy Drives and a Superhighway. Nature Reviews Molecular Cell Biology. 6:209-220.
Hopkins, J., Fowler, R., Krishna, S., Wilson, I., Mitchell, G. and Bannister, L. 1999. The plastid in *Plasmodium falciparum* asexual blood stages: a three-dimensional ultrastructural analysis. Protist. 150:283-295.
Humbel, B., Marti, T. and Müller, M. 1983. Improved structural preservation by combining freeze substitution and low temperature embedding. In Beiträge zur elektronenmikroskopischen Direktabbildung von Oberflächen. Vol. 16. G. Pfefferkorn, editor, Antwerpen. 585-594.
Humbel, B. and Müller, M. 1986. Freeze substitution and low temperature embedding. In The Science of Biological Specimen Preparation 1985. M. Müller, R.P. Becker, A. Boyde, and J.J. Wolosewick, editors. SEM Inc., AMF O'Hare. 175-183.
Humbel, B.M. and Schwarz, H. 1989. Freeze-substitution for immunochemistry. In Immuno-Gold Labeling in Cell Biology. A.J. Verkleij and J.L.M. Leunissen, editors. CRC Press, Boca Raton. 115-134.
Ishida, K., Cavalier-Smith, T. and Green, B., R. 2000. Endomembrane structure and the chloroplast protein targeting pathway in Heterosigma akashiwo (Raphidophyceae, Chromista). Journal of Phycology. 36:1135-1144.
Jacobs, L., Remington, J.S. and Melton, M.L. 1960. The resistance of the encysted form of *Toxoplasma gondii*. Journal of Parasitology. 46:11-12.
Jarvis, P. and Soll, J. 2002. Toc, Tic, and chloroplast protein import. Biochimica et Biophysica Acta. 1590:177-189.
Jelenska, J., Crawford, M.J., Harb, O.S., Zuther, E., Haselkorn, R., Roos, D.S. and Gornicki, P. 2001. Subcellular localization of acetyl-CoA carboxylase in the apicomplexan parasite *Toxoplasma gondii*. Proceedings of the National Academy of Science of the Unated States of America. 98:2723-2728.
Joiner, K. 1993. Cell entry by *Toxoplasma gondii*: all paths do not lead to success. Research Immunology. 144:34-48.
Joiner, K.A., Beckers, C.J.M., Bermudes, D., Ossorio, P.N., Schwab, J.C. and Dubremetz, J.F. 1994. Structure and function of the parasitophorous vacuole membrane surrounding *Toxoplasma gondii*. Ann. N. Y. Acad. Sci. 730:1-6.
Jomaa, H., Wiesner, J., Sanderbrand, S., Altincicek, B., Weidemeyer, C., Hintz, M., Türbachova, I., Eberl, M., Zeidler, J., Lichtenthaler, H.K., Soldati, D. and Beck, E. 1999. Inhibitors of the nonmevalonate pathway of isoprenoid biosynthesis as antimalarial drugs. Science. 285:1573-1576.
Köhler, S. 2005. Multi-membrane-bound structures of Apicomplexa: I. the architecture of the *Toxoplasma gondii* apicoplast. Parasitology Research. 96:258-272.
Köhler, S., Delwiche, C.F., Denny, P.W., Tilney, L.G., Webster, P., Wilson, R.J.M., Palmer, J.D. and Roos, D.S. 1997. A plastid of probable green algal origin in apicomplexan parasites. Science. 275:1485–1489.
Koster, A.J., Grimm, R., Typke, D., Hegerl, R., Stoschek, A., Walz, J. and Baumeister, W. 1997. Perspectives of molecular and cellular electron tomography. Journal of Structural Biology. 120:276-308.
Luft, B.J., Hafner, R., Korzun, A. H., Leport, C., Antoniskis, D., Bosler, E. M., Bourland, D.

D., Uttamchandani, R., Fuhrer, J., Jacobson, J., et al. 1993. Toxoplasmic encephalitis in patients with the acquired immunodeficiency syndrome. N. Engl. J. Med. 329:995-1000.
Luft, B.J. and Remington, J.S. 1992. Toxoplasmic encephalitis in AIDS. Clin. Infect. Dis. 15:211-222.
Mazumdar, J., Wilson, E.H., Masek, K., Hunter, C.A. and Striepen, B. 2006. Apicoplast fatty acid synthesis is essential for organelle biogenesis and parasite survival in *Toxoplasma gondii*. Proceedings of the National Academy of Science of the Unated States of America. 103:13192–13197.
McFadden, G.I., Reith, M.E., Munholland, J. and Lang-Unnasch, N. 1996. Plastid in human parasites. Nature. 381:482.
McFadden, G.I. and Roos, D.S. 1999. Apicomplexan plastids as drug targets. Trends in Microbilogy. 7:328-333.
McFadden, G.I. and Waller, R.F. 1997. Plastids in parasites of humans. Bioessays. 19:1033-1040.
Monaghan, P., Perusinghe, N. and Müller, M. 1998. High-pressure freezing for immunocytochemistry. Journal of Microscopy. 192:248-258.
Monaghan, P. and Robertson, D. 1990. Freeze-substitution without aldehyde or osmium fixatives: ultrastructure and implications for immunocytochemistry. J Microsc. 158:355-363.
Moor, H. and Reiche, U. 1968. Snap freezing under high pressure: A new fixation technique for freeze etching. In Europian Conference on Electron Microscopy. Vol. 2. S. Bocciarelli, editor, Rome. 33-34.
Morisaki, J.H., Heuser, J.E. and Sibley, L.D. 1995. Invasion of *Toxoplasma gondii* occurs by active penetration of the host. Journal of Cell Science. 108:2457–2464.
Morrissette, N.S., Murray, J.M. and Roos, D.S. 1997. Subpellicular microtubules associate with an intramembranous particle lattice in the protozoan parasite *Toxoplasma gondii*. Journal of Cell Science. 110:35-42.
Murk, J.L.A.N., Posthuma, G., Koster, A.J., Geuze, H.J., Verkleij, A.J., Kleijmeer, M.J. and Humbel, B.M. 2003. Influence of aldehyde fixation on the morphology of endosomes and lysosomes: Quatitative analysis and electron tomography. Journal of Microscopy. 212:81-90.
Palmer, J.D. 1992. Green ancestry of malarial parasites? Current Biology. 2:318–320.
Palmer, J.D. and Delwiche, C.F. 1996. Second-hand chloroplasts and the case of the disappearing nucleus. Proceedings of the National Academy of Science of the Unated States of America. 93:7432-1435.
Pillai, S.e.a. 2003. Pillai, S. et al. Functional characterization of β-ketoacyl-ACP reductase (FabG) from *Plasmodium falciparum*. Biochemical and Biophysical Research Communications. 303:387–392.
Prigge, S.T., He, X., Gerena, L., Waters, N.C. and Reynolds, K.A. 2003. The initiating steps of a type II fatty acid synthase in *Plasmodium falciparum* are catalyzed by *pf*ACP, *pf*MCAT, and *pf*KASIII. Biochemistry. 42:1160–1169.
Ralph, S.A., van Dooren, G.G., Waller, R.F., Crawford, M.J., Fraunholz, M.J., Foth, B.J., Tonkin, C.J., Roos, D.S. and McFadden, G.I. 2004. Methabolic Maps and Functions of the *Plasmodium falciparum* Apicoplast. Nature Reviews | Microbiology. 2:204-216.
Remington, J.S. and Desmonts, G. 1995. Toxoplasmosis. In In Infectious Diseases of the Fetus and Newborn Infant. J.S.a.K. Remington, J.O, editor. Saunders, W.B., Philadelphia, PA, USA. 140-267.
Roos, D.S., Crawford, M.J., Donald, R.G., Kissinger, J.C., Klimczak, L.J. and Striepen, B. 1999. Origin, targeting, and function of the apicomplexan plastid. Current Opinion in Microbiology. 2:426-432.
Schnarrenberger, C. and Martin, W. 2002. Evolution of the enzymes of the citric acid cycle and the glyoxylate cycle of higher plants. A case study of endosymbiotic gene transfer. European Journal of Biochemistry. 269:868–883.

Sharma, S.K., Kapoor, M., Ramya, T.N., Kumar, S., Kumar, G., Modak, R., Sharma, S., Surolia, N. and Surolia, A. 2003. Identification, characterization and inhibition of *Plasmodium falciparum* β-hydroxyacyl-acyl carrier protein dehydratase (FabZ). Journal of Biological Chemistry. 278:45661–45671.

Sheffield, H.G. and Melton, M.L. 1968. The fine structure and reproduction of *Toxoplasma gondii*. Journal of Parasitology. 54:209–226.

Silva, S.R.L., Meirelles, S.S. and de Souza, W. 1982. Mechanism of entry of *Toxoplasma gondii* into vertebrate cells. J. Submicrosc. Cytol. 14:471–482.

Sulzer, A.J., Strobel, P.L., Springer, E.L., Roth, I.L. and Callaway, C.S. 1974. A comparative electron microscopic study of the morphology of *Toxoplasma gondii* by freeze-etch replication and thin sectioning technic. Journal of Protozoology. 21:710–714.

Tokuyasu, K.T. 1980. Immunochemistry on ultrathin frozen sections. Histochemical Journal. 12:381-403.

Tokuyasu, K.T. 1986. Cryosections for immunohistochemistry. Journal of Electron Microscopy. 35:1977-1978.

Tomova, C., Geerts, W.J.C., Müller-Reichert, T., Entzeroth, R. and Humbel, B.M. 2006. New comprehension of the apicoplast of *Sarcocystis* by transmission electron tomography. Biology of the Cell. 98:535–545.

Tonkin, C.J., Struck, N.S., Mullin, K.A., Stimmler, L.M. and McFadden, G.I. 2006. Evidence for Golgi-independent transport from the early secretory pathway to the plastid in malaria parasites. Molecular Microbiology. 61:614–630.

van Dooren, G.G., Marti, M., Tonkin, C.J., Stimmler, L.M., Cowman, A.F. and McFadden, G.I. 2005. Development of the endoplasmic reticulum, mitochondrion and apicoplast during the asexual life cycle of *Plasmodium falciparum*. Molecular Microbiology. 57:405-419.

van Dooren, G.G., Schwartzbach, S.D., Osafune, T. and McFadden, G.I. 2001. Translocation of proteins across the multiple membranes of complex plastids. Biochimica et Biophysica Acta. 1541:34-53.

van Dooren, G.G., Tomova, C., Agrawal, S., Humbel, B.M. and Striepen, B. 2008. *Toxoplasma gondii* Tic20 is essential for apicoplast protein import. Proceedings of the National Academy of Science of the Unated States of America. 105:13574–13579.

van Harreveld, A. and Crowell, J. 1964. Electron microscopy after rapid freezing on a metal surface and substitution fixation. Anatomical Record. 149:381-386.

Verkleij, A.J., Humbel, B., Studer, D. and Müller, M. 1985. 'Lipidic particle' systems as visualized by thin-section electron microscopy. Biochimica et Biophysica Acta. 812:591-495.

Vivier, E. and Petitprez, A. 1972. Donne´es ultrastructurales comple´mentaires, morphologiques et cytochimques, sur *Toxoplasma gondii*. Protistologica. 8:199–221.

Voelker, D.R. 2003. New perspectives on the regulation of intermembrane glycerophospholipid traffic. Journal of Lipid Research. 44:441-449.

von Heijne, G. and Nishikawa, K. 1991. Chloroplast transit peptides: The perfect random coil? Federation of European Biochemical Societies Letters. 278:1-3.

Waller, R.F., Keeling, P.J., Donald, R.G.K., Striepen, B., Handman, E., Lang-Unnasch, N., Cowman, A.F., Besra, G.S., Roos, D.S. and McFadden, G.I. 1998. Nuclear-encoded proteins target to the plastid in *Toxoplasma gondii* and *Plasmodium falciparum*. Proceedings of the National Academy of Science USA. 95:12352-12357.

Waller, R.F., Reed, M.B., Cowman, A.F. and McFadden, G.I. 2000. Protein trafficking to the plastid of *Plasmodium falciparum* is via the secretory pathway. EMBO Journal. 19:1794–1802.

Waller, R.F.e.a. 2003. A type II pathway for fatty acid biosynthesis presents drug targets in *Plasmodium falciparum*. Antimicrobial Agents Chemotherapy. 47:297–301.

Wastl, J. and Maier, U., G. 2000. Transport of proteins into cryptomonads complex plastids. Journal of Biological Chemistry. 275:23194-8.

Waters, N.C.e.a. 2002. Functional characterization of the acyl carrier protein (*Pf*ACP) and β-ketoacyl ACP synthase III (*Pf*KASIII) from *Plasmodium falciparum*. Molecular & Biochemical Parasitology. 123:85–94.

Chapter 2

New Comprehension of the Apicoplast of *Sarcocystis* by Transmission Electron Tomography

Cveta Tomova[1], Willie J.C. Geerts[2], Thomas Müller-Reichert[3], Rolf Entzeroth[1] and Bruno M. Humbel[2]

[1]Institut fur Zoologie/Spezielle Zoologie, Technische Universitat, Dresden, Germany
[2]Electron Microscopy and Structural Analysis, Department of Biology, Faculty of Sciences, Utrecht University,The Netherlands
[3]Max Planck Institute of Molecular Cell Biology and Genetics, Electron Microscopy Facility, Dresden, Germany

Biology of the Cell (2006) Vol 98 (9), pp 535-545

New Comprehension of the Apicoplast of *Sarcocystis* by Transmission Electron Tomography

Cveta Tomova, Willie J.C. Geerts, Thomas Müller-Reichert,
Rolf Entzeroth and Bruno M. Humbel

Abstract

Apicomplexan parasites (like *Plasmodium*, *Toxoplasma*, *Eimeria* and *Sarcocystis*) contain a distinctive organelle, the apicoplast, acquired by a secondary endosymbiotic process analogous to chloroplasts and mitochondria. The apicoplast is essential for long-term survival of the parasite. This prokaryotic origin implies that molecular and metabolic processes in the apicoplast differ from those of the eukaryotic host cells and therefore offer options for specific chemotherapeutic treatment.

We studied the apicoplast in high-pressure frozen and freeze-substituted cysts of *Sarcocystis* sp. from roe-deer (*Capreolus capreolus*) to get better insight in apicoplast morphology. We observed that the apicoplast contains four continuous membranes. The two inner membranes have a circular shape with a constant distance from each other and it seems that large-sized protein complexes are located between them. The two outer membranes have irregular shapes. The periplastid membrane also contains large-sized protein complexes, while the outer membrane displays protuberances into the parasite cytoplasm. In addition it is closely associated to the endoplasmic reticulum by 'contact sites'

Introduction

Sarcocystis is a worldwide-distributed Apicomplexan parasite. It is found in many domestic and wildlife species, including humans (Levine, 1973). It has an obligatory heteroxenous life cycle with herbivores as intermediate and carnivores as definitive hosts. Omnivores, such as humans serve as both intermediate and definitive hosts. Typically the Apicomplexan parasites, including *Plasmodium*, *Toxoplasma*, *Eimeria* and *Sarcocystis*, possess a distinctive organelle the apicoplast. This organelle is essential for long-term parasite survival (Fichera and Roos, 1997; He et al., 2001a).

It is commonly accepted that the apicoplast was acquired by secondary endosymbiosis (Gibbs, 1978; Delwiche and Palmer, 1997; McFadden, 1999; McFadden, 2001), an event in which a non-photosynthetic eukaryote initially engulfed a cyanobacteria-like prokaryotic cell followed by subsequent engulfment of this alga by the apicomplexan ancestor (for review see: Cavalier-Smith, 1999; Van Dooren et al., 2001).

The apicoplast is indispensable for survival of the parasite but its exact role is still unclear. The plastid is known to play a role in lipid metabolism by hosting the mevalonate-independent isoprenoid biosynthesis and fatty acid type II biosynthesis. (McFadden and Waller, 1997; Waller et al., 1998; Jomaa et al., 1999; Wilson, 2002). Apicoplast malfunctioning or complete absence of the plastid is not instantly lethal to apicomplexan parasites, rather, it causes a 'delayed-death' phenotype instead. These parasites remain viable for a while and continue replicating but are unable to successfully re-invade another host cell and die soon thereafter (Fichera et al., 1995; Fichera and Roos, 1997; He et al., 2001a).

The apicoplast has its own genome (35 kb DNA-like circles, McFadden et al., 1996; Wilson et al., 1996), but the majority of the apicoplast proteome is encoded in the parasite nuclear genome. The products of these parasite genes are post-translationally modified and targeted to the organelle by a bipartite N-terminal leader sequence, which is proteolytically cleaved (Nielsen et al., 1997).

The prokaryotic nature of the apicoplast opens great potential for new drug development for chemotherapeutic treatment of severe infectious diseases like malaria, toxoplasmosis and coccidiosis in both human and livestock. For efficient drug targeting it is important to have accurate knowledge on the interaction between the apicoplast and the parasite cell, e.g., what are the pathways for importing polypeptides into the plastid. In literature, however, there are contradicting reports on the ultrastructure of the apicoplasts. The information concerning the ultrastructure of the apicoplast is incomplete and based on thin (sometimes serial) sections from chemically fixed material. It is, however, known that chemical fixation destabilises membranous structures (Ebersold et al., 1981; Dubochet et al., 1983; Murk et al., 2003) and during dehydration and resin embedding most of the lipids are lost. Only preparation methods based on cryofixation are able to preserve membranous structures. The first choice in terms of optimal preservation would be imaging of the cysts in the frozen-hydrated state (Dubochet et al., 1988), however, the cysts are

Furthermore, artefact-free thick cryosections justifying tomographic investigations cannot be produced (Al-Amoudi et al., 2005). The next best option is freeze-substitution, a hybrid-method of cryofixation and resin embedding. It was demonstrated that with freeze-substitution and resin embedding most of the lipids can be preserved to a high degree (Verkleij et al., 1985; Weibull and Christiansson, 1986; Humbel and Schwarz, 1989) and that cellular organelles do not change their morphology (Ebersold et al., 1981; Murk et al., 2003).

Therefore, we choose to combine high-pressure freezing, freeze-substitution, resin embedding, and electron tomography to elucidate the cellular ultrastructure of the parasites and to develop models of the apicoplast and to establish a hypothesis on the import of proteins.

Results

The ultrastructural preservation of the cysts was very good (Fig. 1A) and no intracellular ice crystal formation of detectable size was observed. At low magnification the plasma membranes of the individual parasites can be clearly distinguished. Internal parasite structures like the nucleus (Nu), dense granules (Dg), micronemes (Mn) and rhoptries (Rh) can be clearly seen. t is even possible to distinguish a density gradient in the amylopectin granules (Am). At higher magnification (Fig. 1B) the membranes of the apicoplast (Ap) are visible. Both the cytoplasm of the parasite and the lumen of the apicoplast have a homogeneous protein distribution pattern, which is typical for a well preserved ultrastructure.

In total more than 20 double tilt tomograms were recorded and analyzed. In the approx. 6 nm thin slices of the tomograms we clearly identified four continuous membranes surrounding the plastid (Fig. 2).

The two innermost membranes (IMs), thought to be derived from a primary symbiont, are very regular, oval shaped with a constant distance of 4-6 nm from each other (Fig. 2). They have no protuberances or other deformations. Patches of lighter mass densities between the two inner membranes interrupt the profile of the two inner membranes in a regular pattern. The patches seem to form disks of a regular size and shape of about 15-20 nm thick and 60-80 nm in diameter.

The third membrane is thought to be a relict plasma membrane of the eukaryotic endosymbiont. It is known as the ‘periplastid membrane’ (Cavalier-Smith, 1999). The space between the second and third membrane, the periplastid space, generally is 10-15 nm in thickness, however, sometimes the periplastid membrane seems to touch the second inner membrane (Fig. 2). This membrane also contains patches similar to those in the inner membranes (Fig. 2). These patches do not seem to bridge membranes.

The outermost membrane is believed to derive from the endomembrane system of the heterotrophic protists itself (Douglas, 1998). In some areas, the membrane forms prominent protuberances into the cytoplasm (Figure 2A). Apart from the protuberances, it is equidistant to the third membrane. In the reconstructed tomograms, these protuberances have diverse

shape and size (Figures 2A and 2B). Some apicoplasts have a bilobed appearance, also of different shapes and sizes (Figures 2C and 2D).

An important observation in the tomograms was the close proximity of the apicoplast to the ER (endoplasmic reticulum), visible as tubules dotted with ribosomes (Figures 2B, 2D and 3A). At some places, the ER touches the forth membrane of the apicoplast (Figures 2D and 3A), most probably forming 'contact points' between the ER and the outermost membrane. The size, shape, number and spatial distribution of the contact points between the outermost membrane and the ER varied.

The models presented give an overview of the results observed in the present study. The close proximity of the ER to the apicoplast is illustrated in Figure 3(B). It can be clearly demonstrated that the four membranes are individual structures and each continuous in three dimensions (Figure 4). Though sometimes touching each other, they do not cross over. The equidistance of the two innermembranes and the variable distance of the two outer membranes are evident. The protuberances of the fourth membrane sometimes are

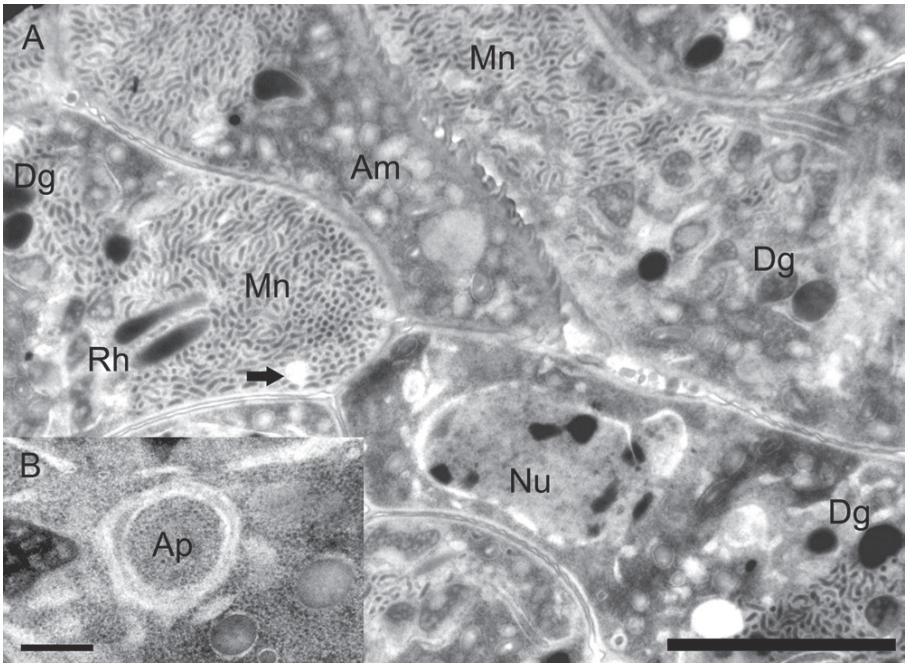

Figure 1 Structural preservation of the morphology of the *Sarcosystis*

(A) Low-magnification electron micrograph of part of a cyst containing the cystozoites of *Sarcocystis* after high-pressure freezing and freeze-substitution to illustrate the well preserved morphology. Section is 80 nm thick. Black arrow indicates very light amylopectin granule. Nu = Nucleus; Mn = Micronemes; Dg = Dense granules; Rh = Rhoptries; Am = Amylopectin granules. Bar = 2 μm

(B) Detail of a typical apicoplast in *Sarcocystis* sp. Note the homogeneous distribution of the proteins in the apicoplast lumen and the parasite cytoplasm. Ap = Apicoplast. Bar = 300 nm

large and extend deep into the parasite cytoplasm (Figures 2 and 4). Patches of lighter mass densities are bridging the two innermostmembranes. There are also patches of lighter mass densities located on the periplastid membrane (Figures 2A and 4A).

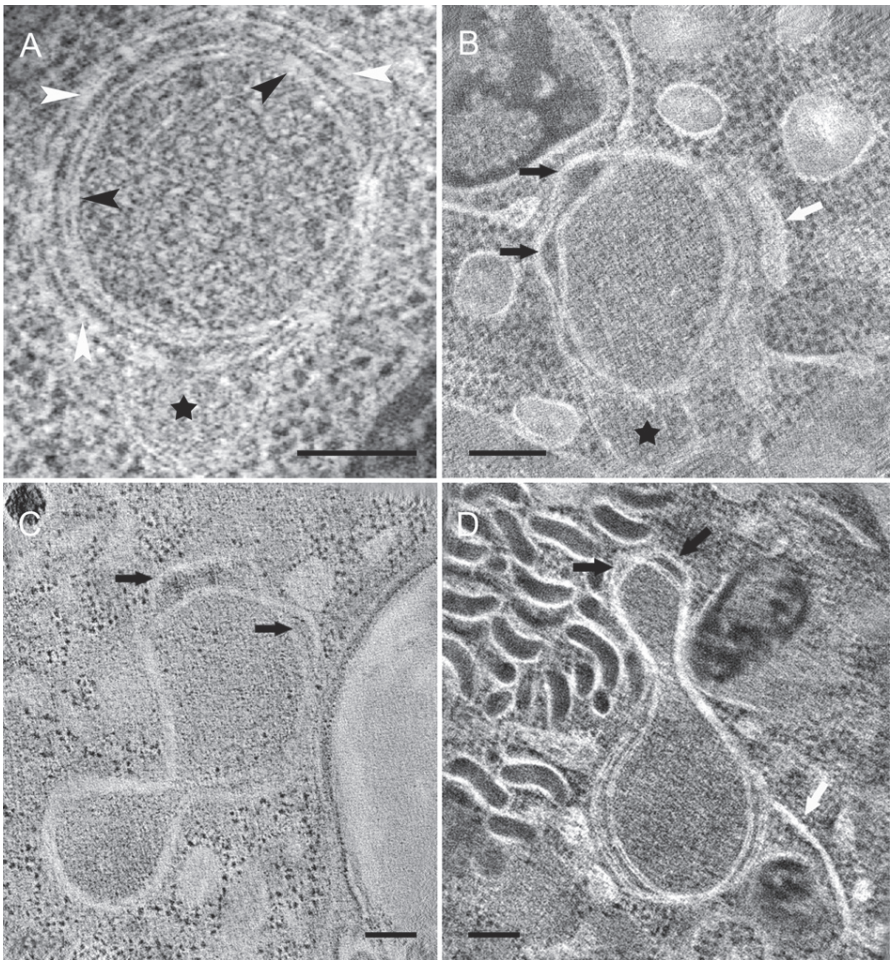

Figure 2 Structure of the apicoplast and variation in size and shape of the protuberances

(A–D) Representative tomographic slices, of a thickness of approx. 6 nm, of the three-dimensional double-tilt reconstruction of four different apicoplasts. The images elucidate most of the features of the apicoplast revealed by tomography: firstly, the four continuous membranes surrounding the apicoplast (A). Secondly, the protuberances (A, B, star) from the outermost membrane nto the parasite cytoplasm. Thirdly, the protein complexes spanning the two innermost membranes (black arrowhead) and in the periplastid membrane (white arrowhead). Fourthly, the variability of the periplastid space (black arrow). Fifthly, the close proximity of the apicoplast to the ER (white arrow), visible as tubules dotted with ribosomes. In (C, D), the apicoplasts have a bilobed appearance. This feature might indicate some dynamics of Sarocystis even in a so-called dormant state in the cyst, maybe a dividing apicoplast. Scale bar, 150 nm.

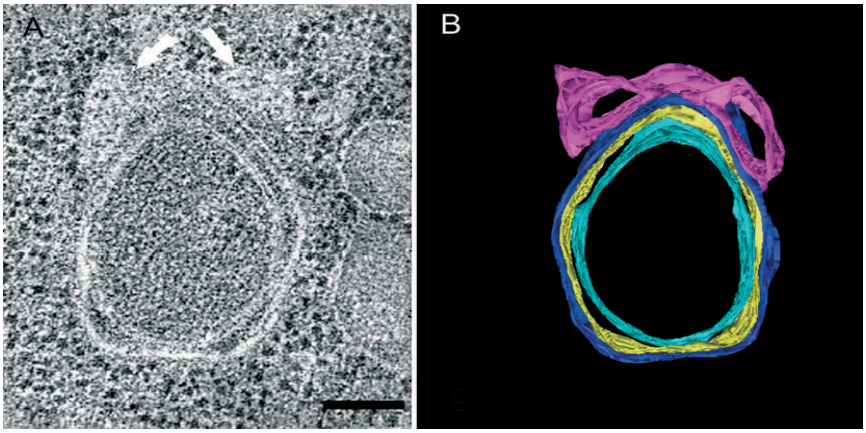

Figure 3 The ER is in close association with the apicoplast

(A) Tomogram reconstruction slide illustrating the close proximity of the ER (white arrows) to the outermost membrane of the apicoplast. Scale bar, 150 nm. (B) Model of a part of the ER (violet) showing the close proximity to the outer membrane (dark blue). The periplastid inner membrane (light blue) and the periplastid outer membrane (in yellow) enclose the periplastid space.

Discussion

To study the role of the apicoplast for the parasite–host cell interaction, it is important to have reliable morphological information. The time-consuming conventional chemical fixation procedures are known for their rather poor preservation of the cellular ultrastructure. Especially membranous continuities are vulnerable to fixation artefacts (Ebersold et al., 1981; Dubochet et al., 1983; Szczesny et al., 1996; Murk et al., 2003). It is generally accepted that cryofixation methods provide better ultrastructural preservation (Steinbrecht and Zierold, 1987; Dubochet et al., 1988; Müller, 1992). The most favourable follow-up method would be cryosectioning and imaging in the frozen-hydrated stage (Dubochet et al., 1988). Whereas cryosectioning is working well for thin sections of approx. 100 nm, adequate thick sections of approx. 300 nm needed for electron tomography cannot be made (Al-Amoudi et al., 2005).

Therefore the next best option is freeze substitution, which has proven to give a reliable view of the cellular ultrastructure (Van Harreveld et al., 1965; Steinbrecht, 1980; Ebersold et al., 1981; Humbel and Schwarz, 1989; Engfeldt et al., 1994; Kaneko and Walther, 1995). Furthermore, it could be shown by freeze substitution with acetone that only 5% of the lipids are extracted (Weibull et al., 1984). In addition, epoxy resins act as an additional fixative (Matsko and Müller, 2005). In summary, cryofixation followed by freeze substitution and embedding in Epon is the best compromise to preserve the cellular architecture with high fidelity and to be able to cut thick sections for electron tomography.

In combination with improved ultrastructural preservation by cryofixation methods,

transmission electron tomography can add valuable three-dimensional information. The laborious technique of serial thin sectioning (Hopkins et al., 1999) can be circumvented, thereby reducing material loss between individual sections and allowing the analysis of larger numbers and volumes of the apicoplast. The Z-resolution of transmission electron

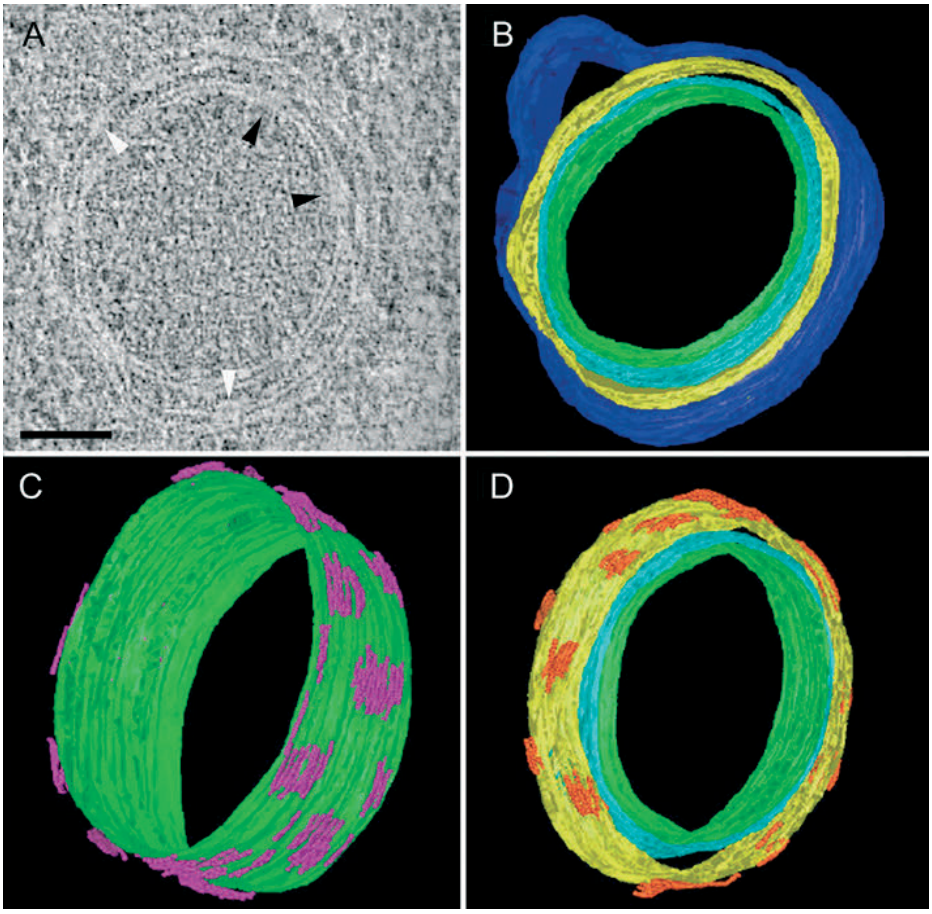

Figure 4 Three-dimensional models of the apicoplast membranes and the protein complexes in the different apicoplast membranes

(A) A median slice of the apicoplast in *Sarcocystis* generated from a double-tilt tomographic reconstruction. The image shows the four continuous membranes, the protein complexes in the inner membrane (black arrowheads), the protein complexes in the outer membrane (white arrowheads) and a protuberance of the outer membrane into the cytoplasm of the parasite (asterisk). Scale bar, 100 nm. (B) Three-dimensional model of the four membranes surrounding the apicoplast: in green the innermost membrane, in light blue the second membrane, in yellow the periplastid membrane and in dark blue the outermost membrane are shown. In the upper left part of the image, a clear protuberance of the outer membrane can be observed. (C) The model illustrates the distribution and size of the protein complexes (violet) between the two inner membranes. For clarity, only the innermost membrane (in green) is shown. Note that the model is not scaled correctly with respect to models (B, D). (D) Distribution of the protein complexes (orange) in the third periplastid membrane.

tomography is approx. 10 times higher (in the range of 5–8 nm) than in reconstructions of serial sections (50–80 nm section thickness). Combining two single-tilt tomograms into a double-tilt tomogram reduces the 540 C loss of information caused by the missing wedge (Mastronarde, 1997).

By combining and applying these state-of-the-art methods, the present study gives new insights concerning the morphology of the apicoplast and interpretation of already existing data.

Most of the proteins in the apicoplast are encoded in the nuclear genome of the parasite, synthesized on the cytoplasmic ribosomes and post-translationally imported into the apicoplast (Waller et al., 1998; Roos et al., 1999). In order to get a better understanding of the import mechanism, it is relevant to know how many membranes enclose the lumen of the plastid and whether they are continuous. The number of membranes is also indicative of the endosymbiotic origin of the apicoplast. In our cryofixed and freezesubstituted material, we now clearly show that four membranes surround the apicoplast. This is in agreement with the commonly accepted secondary endosymbiosis theory (Delwiche and Palmer, 1997; McFadden and Waller, 1997; Douglas, 1998; Cavalier-Smith, 1999). The four membranes are continuous without any visible tightly adjoined intervals or flattened structures in contrast with previous and most recent reports (Hopkins et al., 1999; Köhler, 2005). In *Plasmodium* (Hopkins et al., 1999), there were three membranes found to enclose the apicoplast and in *Toxoplasma* (Köhler, 2005) two. This difference might be a species-specific phenomenon or a metabolically dependent fact.On the other hand, this alteration in the numbers of membranes surrounding the apicoplast is in contradiction with the theory of a secondary symbiosis (Cavalier-Smith, 1999).

The two inner membranes are regularly shaped, almost circular membranes with a constant distance of 4–6 nm from each other. The third and the fourth membranes are less regularly shaped. The outer membrane displayed various outside-directed protuberances. The diverse shapes, sizes and number suggest that these protuberances might be involved in dynamic processes (Figure 2). This suggests that vesicular transport could be one of the ways for protein trafficking between cytosolic compartments and the apicoplast. Some experimental support for this notion comes from apicoplast-deficient cells of *Toxoplasma gondii*, in which apicoplast-targeted green fluorescent protein has been observed in vesicles located in the apical region of the cell (He et al., 2001b). The bilobed appearance of the apicoplast (Figures 2C and 2D) further substantiates the idea that the cyst of *Sarcocystis*, referred to also as a dormant state, is actually metabolically active. It is tempting to speculate that the apicoplast is dividing.

On the other hand, the clearly visible contact points between the ER and the outermost membrane suggest that ER–apicoplast protein transport could also occur directly. This suggestion takes into consideration that analogous contacts between the mitochondria and the ER were observed in rat liver cells (Mannella et al., 1998). Furthermore, physiological and structural interactions between mitochondria and the ER in terms of membrane and/

or protein flux have been described previously (Pitts et al., 1999; Simmen et al., 2005). Gibbs hypothesized that the outermost membrane of plastids, bound by four membranes like the apicoplast, is derived from the ER (Gibbs, 1981). Although we found the ER in close proximity and with contact points to the apicoplast, we found no unequivocal proof for the continuity of the ER into the outer apicoplast membrane. Additionally, no ribosomes were present on the outermost apicoplast membrane. Therefore our results do not confirm the hypothesis that the outer membrane is a part of the ER. The previously reported direct contact points between mitochondria and the apicoplast in *Plasmodium falciparum* (Van Dooren et al., 2005) could not be confirmed for *Sarcocystis* with our studies by electron microscopy.

The clearly visible mass densities, patches, between the two innermembranes and in the periplastid membrane most likely represent protein complexes. The regular distribution and the regular size of the patches favour the idea that these are real structures and not storage places or an accumulation of intermediates in transport. The exact nature and function of these protein complexes are not clear at the moment, but it is tempting to speculate that they might be involved in import of proteins and/or ions over the periplastid and the two inner membranes either by forming membrane pores or as transporter complexes. Our observations are in agreement with Cavalier-Smith's hypothesis (Cavalier-Smith, 1999), who favours the idea that transit peptide receptors are located in both the periplastid membrane and the second inner membrane of the apicoplast and that the same transit peptide is used serially to direct import across two successive membranes (the two inner membranes; see Figure 5). In neither of the tomograms recorded, however, any evidence for the postulated periplastid vesicles was found.

It is known that the apicoplast targeting sequences are rich in asparagine residue, lysine residue and basic amino acids. This positively charged transit peptide is suggested to be electrophoretically pulled into the apicoplast lumen by a series of negatively charged transmembrane pores (Van Dooren et al., 2001; Foth et al., 2003). So far there are no clear reports of translocator components in the apicomplexan genome except for the hypothetical *Plasmodium* protein (Gen- Bank® accession no. NP 705561; GI:23619599), which has some similarity to Toc 159 (translocon of the outer chloroplast envelope-159) (Schleiff et al., 2003; Soll and Schleiff, 2004) from pea with a leader sequence appropriate for plastid targeting (Nassoury and Morse, 2005). It is worthwhile to mention that the size of the published Toc 159 complex (height: 10–12.5 nm; diameter: 12–14 nm) is approximately one-fourth of the size of the mass densities observed in our tomograms (height: 15–20 nm; diameter: 60–80 nm).

Combining these observations (Figure 5), we hypothesize that apicoplast-specific proteins are transported into the space surrounded by the outermostmembrane, either by vesicular transport and/or by direct import via ER contact points. This hypothesis is also based on previously proposed models on protein import into plastids with three or four membranes by Cavalier-Smith (1999) and is also in agreement with the later refined version of the

same model by Van Dooren et al. (2001). It is suggested that protein complexes mediate translocation across the inner two membranes. This pore-like structure is proposed to be a specific protein complex, possibly a duplicate of the Toc apparatus (Van Dooren et al., 2000). A comparable import apparatus to the Tic–Toc system of plant chloroplasts is offered in the model for targeting host-encoded proteins into plastids of secondary endosymbiotic origin by McFadden (1999).

The protuberances are considered to indicate a dynamic process like vesicle formation. As already suggested by Van Dooren et al. (2001), secretory proteins lacking a transit peptide pass the apicoplast and are taken up by vesicles that bud from the outermost membrane, from where these vesicles carry proteins to another compartment of the secretory pathway (Van Dooren et al., 2001). It is also possible that these vesicles consist of cargo from the apicoplast itself. The validity of this suggestion has still to be proven by experimental data. In the model proposed here, it is hypothesized that there is a direct transport from the ER to the exoplastid space (Figure 5; 'E') via the contact sites (Figure 5; 'CS'). From there, they are directed into the apicoplast lumen passing through the pores formed by protein complexes in the periplastid membrane and in the two inner membranes. In the future, the hypothesis has to be tested with biochemical and molecular biological techniques in combinationwith specific immunolabelling studies.

Figure 5 Hypothetical model for the import of proteins encoded by the parasite nuclear genome into the lumen of the apicoplast

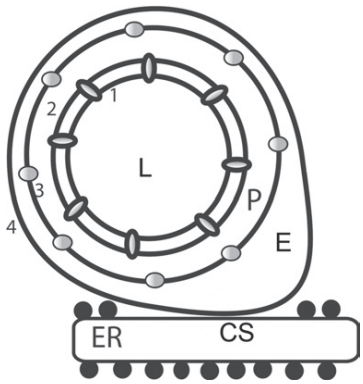

The schematic drawing represents a hypothetical model for the import of proteins encoded by the parasite nuclear genome into the lumen of the apicoplast. The model is based on the observed data in the present study and previously proposed models of protein import into plastids with three or four membranes (Cavalier-Smith, 1999; Van Dooren et al., 2001). It is hypothesized that there is a direct transport from the ER o the exoplastid space (E) via the contact sites (CS); from the exoplastid space (E), proteins could be translocated into the lumen via the protein complexes (patches), e.g. pores or transporters. 1, first inner membrane; 2, second inner membrane; 3, periplastid membrane; 4, outer membrane; L, lumen; P, periplastid space; E, exoplastid space; CS, contact site

Material and Methods

Sample preparation

Sarcocystis cysts were isolated from samples of tongue muscle from naturally infected roe deer (*Capreolus capreolus*). Cysts were kept in 1x PBS (pH = 7.4) at 4°C for two days before further processing for electron microscopic examination. The cysts were cryofixed by high-pressure freezing (EM PACT2+RTS, Leica Microsystems, Vienna) (Manninen et al., 2005) and freeze-substituted in a freeze-substitution medium consisting of anhydrous

acetone, 1% osmium tetroxide and 0.1% uranyl acetate (McDonald and Müller-Reichert, 2002). The samples were kept at -90°C for 36 hours, at -30°C for approximately 5 hours and finally brought to room temperature for 1 hour in a freeze-substitution unit (AFS, Leica Microsystems, Vienna). After removing osmium tetroxide and uranyl acetate with acetone the samples were gradually infiltrated with Epon/Araldite resin (Mollenhauer, 1964). Cysts were embedded in thin layers of resin on microscope slides (Müller-Reichert et al., 2003). Selected cysts were remounted on 'dummy' blocks for ultramicrotomy. Sections were cut using a Reichert Ultracut Microtome (Leica Microsystems, Vienna). Ultra-thin (ca. 80 nanometre) and semithin (250-300 nanometre) sections were collected on Formvar- carbon-coated copper hexagonal 50 mesh grids and post-stained with 20% (w/v) uranyl acetate in 70% (v/v) methanol/water followed by Reynolds's lead citrate staining (Reynolds, 1963).

Electron Tomography

Before recording EM projections of semi-thin sections (250-300 nm), 10-nm colloidal gold particles were applied on one surface of the sections to function as fiducial markers for subsequent image alignment. The specimens were placed in a high-tilt specimen holder (Fischione type 2020, Fischione Instruments, Pittsburgh, USA) and datasets were recorded at 200 kV (Tecnai 20 LaB_6, FEI Company, The Netherlands).

Angular tilt range was from -65° till +65° with an increment of 1 degree. Images (1024x1024 square pixels) were recorded using a CCD camera (Temcam F214, TVIPS GmbH, Germany). The sections were pre-irradiated to avoid shrinking effects during recording (Luther, 1992). Automated data acquisition of the tilt series was carried out using Xplore 3D (FEI Company, Eindhoven, The Netherlands). For dual axis tomography (Penczek et al., 1995), the grids were manually rotated over 90°, and a second tilt series was acquired over the same tilting range. For image alignment the colloidal gold particles were used as fiducial markers. Tomograms were computed for each tilt axis using the R-weighted back-projection algorithm and combined into one double tilt tomogram with the IMOD software package (Kremer et al., 1996). We recorded and reconstructed in total more than 20 double tilt series of the apicoplast.

Modelling and analysis of tomographic data

Double tilt tomograms were analyzed and modelled using the IMOD software package (Kremer et al., 1996). Features of interest were contoured manually in serial optical slices extracted from the tomogram. The 'image slicer' window in IMOD was used to facilitate the recognition of membranous structures. 3-D models were displayed and rotated to study its 3-D geometry.

Acknowledgements

We thank the European 3D EM Network of Excellence for financial support; Prof. G. Rödel for valuable discussions; Dr. P. Verkade for the use of the EM PACT2 + RTS High-Pressure Freezer and Dr. W. Voorhout, FEI Electron Optics for the S.I.R.T. reconstruction of one of the tomograms.

References

Al-Amoudi, A., Studer, D. and Dubochet, J. (2005) Cutting artefacts and cutting process in vitreous sections for cryo-electron microscopy. J. Struct. Biol. **150**, 109-121.

Cavalier-Smith, T. (1999) Principles of protein and lipid targeting in secondary symbiogenesis: euglenoid, dinoflagellate, and sporozoan plastid origins and the eukaryotic family tree. J. Eukaryot. Microbiol. **46**, 347-366.

Delwiche, C.F. and Palmer, J.D. (1997) The origin of plastids and their spread via secondary endosymbiosis. Plant Syst. Evol. **Suppl. 11**, 53-86.

Douglas, S.E. (1998) Plastid evolution: origins, diversity, trends. Curr. Opin. Genet. & Dev. **8**, 655-661.

Dubochet, J., Adrian, M., Chang, J.J., Homo, J.C., Lepault, J., McDowall, A.W. and Schultz, P. (1988) Cryo-electron microscopy of vitrified specimens. Q. Rev. Biophys. **21**, 129-228.

Dubochet, J., McDowall, A.W., Menge, B., Schmid, E.N. and Lickfeld, K.G. (1983) Electron microscopy of frozen-hydrated bacteria. J. Bacteriol. **155**, 381-390.

Ebersold, H.R., Cordier, J.L. and Lüthy, P. (1981) Bacterial mesosomes: method dependent artifacts. Arch Microbiol **130**, 19-22.

Engfeldt, B., Reinholt, F.P., Hultenby, K., Widholm, S.M. and Müller, M. (1994) Ultrastructure of hypertrophic cartilage: histochemical procedures compared with high pressure freezing and freeze substitution. Calcif. Tissue Int. **55**, 274-280.

Fichera, M.E., Bhopale, M.K. and Roos, D.S. (1995) In vitro assays elucidate peculiar kinetics of clindamycin action against *Toxoplasma gondii*. Antimicrob. Agents Ch. **39**, 1530–1537.

Fichera, M.E. and Roos, D.S. (1997) A plastid organelle as a drug target in apicomplexan parasites. Nature **390**, 407-409.

Foth, B.J., Ralph, S.A., Tonkin, C.J., Struck, N.S., Fraunholz, M., Roos, D.S., Cowman, A.F. and McFadden, G.I. (2003) Dissecting apicoplast targeting in the malaria parasite *Plasmodium falciparum*. Science **299**, 705-708.

Gibbs, S.P. (1978) The chloroplasts of Euglena may have evolved from symbiotic green algae. Can. J. Bot. **56**, 2882-2889.

Gibbs, S.P. (1981) The chloroplast endoplasmic reticulum, structure, function, and evolutionary significance. Int. Rev. Cytol. **72**, 49-99.

He, C.Y., Shaw, M.K., Pletcher, C.H., Striepen, B., Tilney, L.G. and Roos, D.S. (2001a) plastid segregation defect in the protozoan parasite *Toxoplasma gondii*. EMBO J. **20**, 330-339.

He, C.Y., Striepen, B., Pletcher, C.H., Murray, J.M. and Roos, D.S. (2001b) Targeting and processing of nuclear-encoded apicoplast proteins in plastid segregation mutants of *Toxoplasma gondii*. J. Biol. Chem. **276**, 28436-28442.

Hopkins, J., Fowler, R., Krishna, S., Wilson, I., Mitchell, G. and Bannister, L. (1999) The plastid in *Plasmodium falciparum* asexual blood stages: a three-dimensional ultrastructural analysis. Protist **150**, 283-295.

Humbel, B.M. and Schwarz, H. (1989) Freeze-substitution for immunochemistry. In Immuno-Gold Labeling in Cell Biology (A.J. Verkleij and J.L.M. Leunissen, eds.), pp. 115-134, (CRC Press, Boca Raton)

Jomaa, H., Wiesner, J., Sanderbrand, S., Altincicek, B., Weidemeyer, C., Hintz, M., Türbachova, I., Eberl, M., Zeidler, J., Lichtenthaler, H.K., Soldati, D. and Beck, E. (1999) Inhibitors of the nonmevalonate pathway of isoprenoid biosynthesis as antimalarial drugs. Science **285**, 1573-1576.

Kaneko, Y. and Walther, P. (1995) Comparison of ultrastructure of germinating pea leaves prepared by high-pressure freezing-freeze substitution and conventional chemical fixation. J. Electron Microsc. **44**, 104-109.

Köhler, S. (2005) Multi-membrane-bound structures of Apicomplexa: I. the architecture of the *Toxoplasma gondii* apicoplast. Parasitol. Res. **96**, 258-272.
Kremer, J.R., Mastronarde, D.N. and McIntosh, J.R. (1996) Computer visualization of three-dimensional image data using IMOD. J. Struct. Biol. **116**, 71-76.
Levine, N.D. (1973) Protozoan parasites of domestic animals and man (Burgess Publishing Co., Minneapolis)
Luther, P.K. (1992) Sample shrinkage and radiation damage. In Electron Tomography. Three-dimensional imaging with the transmission electron microscope (J. Frank, ed.), pp. 39-60, (Plenum Press, New York, London)
Mannella, C.A., Buttle, K., Rath, B.K. and Marko, M. (1998) Electron microscopic tomography of rat-liver mitochondria and their interaction with the endoplasmic reticulum. BioFactors **8**, 255-228.
Manninen, A., Verkade, P., Le Lay, S., Torkko, J., Kasper, M., Füllekrug, J. and Simons, K. (2005) Caveolin-1 is not essential for biosynthetic apical membrane transport. Mol. Cell. Biol. **25**, 10087-10096.
Mastronarde, D.N. (1997) Dual-axis tomography: an approach with alignment methods that preserve resolution. J. Struct. Biol. **120**, 343-352.
Matsko, N. and Müller, M. (2005) Epoxy resin as fixative during freeze-substitution. J. Struct. Biol. **152**, 92-103.
McDonald, K.L. and Müller-Reichert, T. (2002) Cryomethods for thin section electron microscopy. Methods Enzymol. **351**, 96-123.
McFadden, G.I. (1999) Plastids and protein targeting. J. Eukaryot. Microbiol. **46**, 339-346.
McFadden, G.I. (2001) Chloroplast origin and integration. Plant Physiol. **125**, 50-53.
McFadden, G.I., Reith, M.E., Munholland, J. and Lang-Unnasch, N. (1996) Plastid in human parasites. Nature **381**, 482.
McFadden, G.I. and Waller, R.F. (1997) Plastids in parasites of humans. Bioessays **19**, 1033-1040.
Medalia, O., Weber, I., Frangakis, A.S., Nicastro, D., Gerisch, G. and Baumeister, W. (2002) Macromolecular architecture in eukaryotic cells visualized by cryoelectron tomography. Science **298**, 1209-1213.
Mollenhauer, H.H. (1964) Plastic embedding mixtures for use in electron microscopy. Stain Technol. **39**, 111-114.
Müller, M. (1992) The integrating power of cryofixation-based electron microscopy in biology. Acta Microscopica **1**, 37-44.
Müller-Reichert, T., Hohenberg, H., O'Toole, E.T. and McDonald, K. (2003) Cryoimmobilization and three-dimensional visualization of C. elegans ultrastructure. J. Microsc. **212**, 71-80.
Murk, J.L.A.N., Posthuma, G., Koster, A.J., Geuze, H.J., Verkleij, A.J., Kleijmeer, M.J. and Humbel, B.M. (2003) Influence of aldehyde fixation on the morphology of endosomes and lysosomes: quatitative analysis and electron tomography. J. Microsc. **212**, 81-90.
Nassoury, N. and Morse, D. (2005) Protein targeting to the chloroplasts of photosynthetic eukaryotes: Getting there is half the fun. Biochim. Biophys. Acta **1743**, 5-19.
Nielsen, H., Engelbrecht, J., Brunak, S. and von Heijne, G. (1997) A neural network method for identification of prokaryotic and eukaryotic signal peptides and prediction of their cleavage sites. Int. J. Neural Syst. **8**, 581-599.
Penczek, P., Marko, M., Buttle, K. and Frank, J. (1995) Double-tilt electron tomography. Ultramicroscopy **60**, 393-410.
Pitts, K.R., Yoon, Y., Krueger, E.W. and McNiven, M.A. (1999) The dynamin-like protein DLP1 is essential for normal distribution and morphology of the endoplasmic reticulum and mitochondria in mammalian cells. Mol. Biol. Cell **10**, 4403-4417.

Reynolds, E.S. (1963) The use of lead citrate at high pH as an electron-opaque stain in electron microscopy. J. Cell Biol. **17**, 208-212.

Roos, D.S., Crawford, M.J., Donald, R.G., Kissinger, J.C., Klimczak, L.J. and Striepen, B. (1999) Origin, targeting, and function of the apicomplexan plastid. Curr. Opin. Microbiol. **2**, 426-432.

Schleiff, E., Soll, J., Küchler, M., Kühlbrandt, W. and Roswitha, H. (2003) Characterization of the translocon of the outer envelope of chloroplasts. J. Cell Biol. **160**, 541-551.

Simmen, T., Aslan, J.E., Blagoveshchenskaya, A.D., Thomas, L., Wan, L., Xiang, Y., Feliciangeli, S.F., Hung, C.-H., Crump, C.M. and Thomas, G. (2005) PACS-2 controls endoplasmic reticulum-mitochondria communication and Bid-mediated apoptosis. EMBO J. **24**, 717-729.

Soll, J. and Schleiff, E. (2004) Protein import into chloroplasts. Nature Review Molecular Cell Biology **5**, 198-208.

Steinbrecht, R.A. (1980) Cryofixation without cryoprotectants. Freeze substitution and freeze etching of an insect olfactory receptor. Tissue Cell **12**, 73-100.

Steinbrecht, R.A. and Zierold, K., eds. (1987) Cryotechniques in Biological Electron Microscopy (Springer-Verlag, Berlin, Heidelberg)

Van Dooren, G.G., Marti, M., Tonkin, C.J., Stimmler, L.M., Cowman, A.F. and McFadden, G.I. (2005) Development of the endoplasmic reticulum, mitochondrion and apicoplast during the asexual life cycle of *Plasmodium falciparum*. Mol. Microbiol. **57**, 405-419.

Van Dooren, G.G., Schwartzbach, S.D., Osafune, T. and McFadden, G.I. (2001) Translocation of proteins across the multiple membranes of complex plastids. Biochim. Biophys. Acta **1541**, 34-53.

Van Harreveld, A., J., C. and Malhotra, S.K. (1965) A study of extracellular space in central nervous tissue by freeze-substitution. J. Cell Biol. **25**, 117-137.

Verkleij, A.J., Humbel, B., Studer, D. and Müller, M. (1985) 'Lipidic particle' systems as visualized by thin-section electron microscopy. Biochim. Biophys. Acta **812**, 591-495.

Waller, R.F., Keeling, P.J., Donald, R.G.K., Striepen, B., Handman, E., Lang-Unnasch, N., Cowman, A.F., Besra, G.S., Roos, D.S. and McFadden, G.I. (1998) Nuclear-encoded proteins target to the plastid in *Toxoplasma gondii* and *Plasmodium falciparum*. Proc. Natl. Acad. Sci. USA **95**, 12352-12357.

Weibull, C. and Christiansson, A. (1986) Extraction of proteins and membrane lipids during low temperature embedding of biological material for electron microscopy. J. Microsc. **142**, 79 - 86.

Weibull, C., Villiger, W. and Carlemalm, E. (1984) Extraction of lipids during freeze-substitution of Acholeplasma laidlawii-cells for electron microscopy. J. Microsc. **134**, 213-216.

Wilson, R.J., Denny, P.W., Preiser, P.R., Rangachari, K., Roberts, K., Roy, A., Whyte, A., Strath, M., Moore, D.J., Moore, P.W. and Williamson, D.H. (1996) Complete gene map of the plastid-like DNA of the malaria parasite *Plasmodium falciparum*. J. Mol. Biol. **261**, 155-172.

Wilson, R.J.M. (2002) Progress with parasite plastids. J. Mol. Biol. **319**, 257-274.

Chapter 3

Membrane Contact Sites between the Apicoplast and the Endoplasmic Reticulum in *Toxoplasma gondii* Revealed by Electron Tomography

Cveta B. Tomova[1], Bruno M. Humbel[1], Willie J.C. Geerts[1], Rolf Entzeroth[3], Joost C.M. Holthuis[2] and Arie J. Verkleij[1]

[1] Electron Microscopy and Structural Analysis, Department of Biology, Faculty of Sciences, Utrecht University, The Netherlands.
[2] Membrane Enzymology, Department of Chemistry, Bijvoet Center and Institute of Biomembranes, The Netherlands
[3] Institut für Zoologie/Spezielle Zoologie, Technische Universität Dresden, Germany

Manuscript in preparation

Membrane Contact Sites between the Apicoplast and the Endoplasmic Reticulum in *Toxoplasma gondii* Revealed by Electron Tomography

Cveta B. Tomova, Bruno M. Humbel, Willie J.C. Geerts, Rolf Entzeroth, Joost C.M. Holthuis and Arie J. Verkleij

Abstract

Toxoplasma gondii is an obligate intracellular parasite from the phylum Apicomplexa. A hallmark of these protozoans is the presence of a unique apical complex of organelles that includes the apicoplast, a plastid acquired by secondary endosymbiosis. The apicoplast is indispensable for parasite viability. It harbours a fatty acid biosynthesis type II (FAS II) pathway and has a key part in the parasite lipid metabolism. Possibly the apicoplast provides components for the establishment and maturation of the parasitophorous vacuole, insuring the successful infection of the host cell. This fact implies the presence of a transport mechanism for the fast and accurate allocation of lipids between the apicoplast and other membrane-bound compartments in the parasite cell. Using a combination of high-pressure freezing, freeze-substitution and electron-tomography, we analyzed the ultra-structural organization of the apicoplast of *T. gondii* in relation with the endoplasmic reticulum (ER). This allowed us to clearly show the presence of four continuous membranes surrounding the apicoplast. In addition, we present, for the first time, the existence of membrane contact sites between the apicoplast outermost membrane and the ER. We describe the morphological characteristics of these structures and discuss their potential significance for the subcellular distribution of lipids in the parasite.

Introduction

Toxoplasma gondii is an obligate intracellular parasite from the phylum Apicomplexa, which includes important human and veterinary pathogens (1), responsible for life-threatening diseases in humans (malaria and toxoplasmosis) and livestock (coccidioses, theilerioses, babesioses etc.). *T. gondii* has a complex heteroxenous life cycle. Asexual replication can take place in virtually any vertebrate cell but the sexual differentiation is known to occur only in feline species (2). It is an important opportunistic pathogen of humans, causing severe encephalitis in immunocompromised individuals and congenital birth defects when primary infection occurs during pregnancy (3-5).

The apicoplast is a relic, non-photosynthetic, plastid-like organelle derived from secondary endosymbiosis (6;7). The apicoplast harbours key metabolic pathways such as fatty acid synthesis type II (FAS II), isoprenoid and haem synthesis (9) (10-12) that are essential for the viability and survival of the parasite (8;13). The prokaryotic nature of the apicoplast's biochemistry allows specific inhibition of the parasite's FAS II pathway without impairing the operation of the host-specific pathway FAS I, which is the basis in the development of a novel anti-malaria and anticoccidial medication (8;14;15).

The FAS II pathway in *T. gondii* synthesizes fatty acids de novo (16;17). The plastid fatty-acid synthesis requires acetyl-CoA, which can be generated from pyruvate by the pyruvate dehydrogenase complex (PDHC). Plastid PDHC comprises four distinct subunits, with cyanobacterial origin (18). This PDHC is the only one found in apicomplexans (19), which suggests that any other acetyl-CoA-related metabolic pathway in the parasite cell will dependent on acetyl-CoA exchange with the apicoplast. Localization studies showed that substrates for PDHC, the triose-phosphate-isomerase and lipoic acid cofactors, are synthesized and assembled within the apicoplast (20;21), which indicates an import of triose phosphates into the apicoplast. The products of the FAS II pathways mainly attribute to the apicoplast maintenance and biogenesis (17), but some compounds are very likely to be essential for the whole parasite cell. Fatty acids are probably exported to the ER (16;22), where they are likely to be incorporated into phospholipids, perhaps together with the fatty acids scavenged from the host cell. This, however, presupposes a specialized lipid trafficking system. Lipid transport between organelles must be specific to maintain their unique lipid compositions and in that way to ensure the specificity of the biochemical reactions they harbour. A common mechanism for lipid transport between many organelles is via routes independent of vesicle formation, migration and fusion. Evidently, the non-vesicular transport proved to be evolutionary more efficient and precise since it is retained as a default mechanism for the majority of phospholipid transport (23). A general model for such non-vesicular transport has emerged recently in which donor and acceptor membranes form transient zones of apposition and contact. It is suggested that in these contact sites lipid and protein binding domains on donor and/or acceptor membranes act as ligands to mediate the process precision (24-26) .

The presence of contact sites between specific domains of the ER and various other membrane-bound organelles (e.g. Golgi, mitochondria, chloroplast, endosomes, lysosomes etc.) have been described in a wide range of eukaryotic cell types (27-29) (24;26;30). It is believed that lipid trafficking between the ER and mitochondria in both, yeast (31;32) and animal cells (33-35) take place at such membrane contact sites. In plants, membrane contact sites (MCS) between ER and plastids are assumed to provide the plastids with membrane lipid precursors (36;37). In addition to mediating transport of acyl-lipids from the ER to plastids, such contact sites could also participate in lipid trafficking in the opposite direction (38).

Similar close associations of the apicoplast with the ER has been reported in *P. falciparum* (39-41) and *Sacrocystis sp*. (42). Unfortunately, the existence of the fourth outermost apicoplast membrane as a distinct continuous structure in *Plasmodium* species as well as in *Toxoplasma* is still obscure (43) (44) due to artefacts imposed by the chemical fixation

The chemical preparative procedures generally introduce artefacts into native cellular structures, notably in membrane systems (45-48), thus preventing the accurate interpretation of membranous continuities and/or interactions. The latter are of fundamental importance for understanding the functional complexity of the endomembrane system in cells.

In this study we employ the combination of high-pressure freezing (HPF), freeze-substitution (FS) and electron tomography (ET) as one of the most reliable approaches for studying membrane continuities and membrane-membrane interactions (49). This state-of-the-art method has proven to meet the requirements for obtaining a well-preserved cellular architecture at high resolution, which is essential in analyzing the structure of a biological specimen in its three dimensions.

Material and Methods

Sample preparation

Parasites, *Toxoplasma gondii* tachyzoites NTE strain (50), were propagated in Vero cells (Green Monkey kidney epithelial cells) in T25 plastic culture flasks. Vero cells were first grown to confluence in Dulbecco's Modified Eagles Medium (DMEM) supplemented with 10% foetal calf serum, followed by infection with *T. gondii* in DMEM as previously described (51), with high inoculum to ensure high infection rate.

To study intracellular parasites, in optimal physiological conditions, the infected host cells (at least 80% of infection) were trypsinized for 2 minutes, then resuspended in DMEM 10% and centrifuged for 10 minutes at 1500 g prior to cryofixation. For cryofixation of the free thachyzoites, freshly lysed cells were pelleted at 800 g for 5 minutes and subsequently the supernatant was centrifuged for 10 minutes at 1500 g to pellet the parasites.

The samples, infected Vero cells or free tachyzoites, were cryofixed by high-pressure freezing (Leica EM HPF; Leica Microsystems, Vienna, Austria; now M. Wohlwend,

Sennwald, Switzerland) and freeze-substituted in a freeze-substitution medium consisting of anhydrous acetone and 2% osmium tetroxide and alternatively 0.1% uranyl acetate. The samples were kept at -90°C for 46 hours; at -60°C for 8 hours and at -30°C for 8 hours (52) in a freeze-substitution unit (AFS, Leica Microsystems, Vienna) and finally rinsed 2 times (30 minutes) in acetone on ice. After rinsing the samples were infiltrated with gradually increasing concentrations of Epon (Fluka, Steinheim, Germany) : acetone (1 : 2, 1 : 1, 2 : 1, and finally pure Epon). Each infiltration step lasted for at least half a day. The final polymerization was performed at 60°C. The samples substituted with 0.1% uranyl acetate in acetone were infiltrated with gradually increasing concentrations of Lowicryl HM20 (EMS, Hatfield, USA) : acetone (1 : 3, 1 : 1, 3 : 1, and finally 3 times pure HM20 resin). The duration of each step was one hour. The infiltration was performed at -40°C, followed by 48 hours polymerization under UV light at the same temperature and subsequent curing at room temperature UV-light for approximately 10 hours. Sections (60 and 200-nm thick) were collected on Formvar-coated, carbon-stabilized one-slot and hexagonal 100 or 50 mesh copper grids. The osmium-Epon substituted samples were post-stained for 4 minutes with 20% (w/v) uranyl acetate in 70% (v/v) methanol/water followed by 2 minutes Reynolds's lead citrate staining (53). The uranyl-HM20 samples were examined directly without additional contrasting.

In this study we performed for the first time Electron Tomography on thick (200-250 nm), Lowicryl HM20 embedded sections without applying additional post-sectioning contrasting with uranyl acetate and lead citrate.

Electron tomography data acquisition

Fiducials of 5 or 10 nm protein A colloidal gold (Medical School, Utrecht University, The Netherlands) were applied to the top of the sections prior to image acquisition. In the samples embedded in Lowicryl HM20 the apicoplast was labeled with anti-ACP (McFadden); 10 nm PAG which was used also as fiducial markers for the image alignment. The specimens were placed in a high-tilt specimen holder (Fischione type 2020 or Fischione rotation holder type 2040, Fischione Instruments, Pittsburgh, USA) and datasets were recorded at 200 kV (Tecnai 20 LaB6, FEI Company, The Netherlands), with an increment of 1 degree and angular tilt range from -60 to +60 for both single and dual axis tomography (54). Images (1024x1024 square pixels) were recorded using a CCD camera (Temcam F214, TVIPS GmbH, Gauting, Germany). The sections were pre-irradiated to avoid shrinking effects during recording. Automated data acquisition of the tilt series was carried out using Xplore 3D (FEI Company, Eindhoven, The Netherlands). Tomograms were computed for each tilt axis using the R-weighted back-projection algorithm and combined into one double tilt tomogram with the IMOD software package (55) .

Modelling and analysis of tomographic data

Double tilt tomograms were analyzed and modelled using the IMOD software package (55). Features of interest were contoured manually in serial optical slices extracted from the tomogram.

The ‘image slicer’ window in IMOD was used to facilitate the recognition of membranous structures. 3-D models were displayed and rotated to study its 3-D geometry. For accurate interpretation of the data especially regarding the distance between the membranes the ‘graphic’ window in IMOD was used.

Results

Apicoplast morphology

We have studied the apicoplast morphology and its relation with the ER in free and intracellular tachyzoites of *T. gondii*. The parasites were cryofixed by HPF and subsequently freeze-substituted (FS) applying different substitution cocktails and resins to ensure the optimal preservation and visualization of the structure.

This study confirms the presence of four continuous membranes surrounding the apicoplast of *T. gondii*. The morphology of the plastid in *T. gondii* shows similarities with the one already described for *Sarcocystis sp*. (42).

The two innermost membranes (IMs), derived from the cyanobacteria ancestor, are always with a constant distance of 4-6 nm from each other and oval shaped (Fig.1,2). They show no variations in distance or form. Patches of lighter mass densities span the two inner membranes in a regular pattern, very similar to the IMs observed in *Sarcocystis* (Fig.1C, *arrow*). The patches seem to form membrane spanning disks of a regular size and shape of about 15-20 nm thick and 40-60 nm in diameter. These patches are visible predominantly in Epon samples.

The third ‘periplastid’ membrane (56) has generally an oval shape. This membrane seems to touch the second inner membrane at some points but they never fuse with each other. The periplastid membrane also contains patches similar to those in the inner membranes (Fig.1C, *arrow*). The space between the second and third membrane, the periplastid space, generally is 10-15 nm in thickness. It also can reach up to 30-40 nm at some parts leading to local asymmetric appearance of this plastid compartment (Fig. 2A-B *arrows*). The outermost membrane has no patches and is mostly equidistant to the periplastid membrane. Occasionally, the exoplastid space shows variously shaped protrusions towards the cytosol of the parasite (Fig.2 *asterisk*).

Apicoplast-ER membrane contact sites

An important finding in the tomograms is that the ER membrane does not fuse with the outermost membrane of the apicoplast. This confirms in an unambiguous manner the autonomous character of this membrane, although being derived from the endomembrane system of the ancestral protozoan parasite (57). The confirmation that the secondary plastid of Apicomplexa is not placed within the ER lumen is an indication for its evolutionary identity. As postulated by Cavalier-Smith, in his chromalveolate theory, the location of the plastid within the ER is the most essential point to separate chromists from the alveolates (56). It indicates that the putative phagosomal membrane never underwent fusion with the nuclear envelope of the ancestral parasite and places the Apicomplexa among the Alveolates

However, at some restricted areas the ER membrane aligns contiguously with the forth membrane forming narrow cytosolic gaps or 'membrane contact sites' (MCS) (Fig.1D and 4B *arrowheads*).

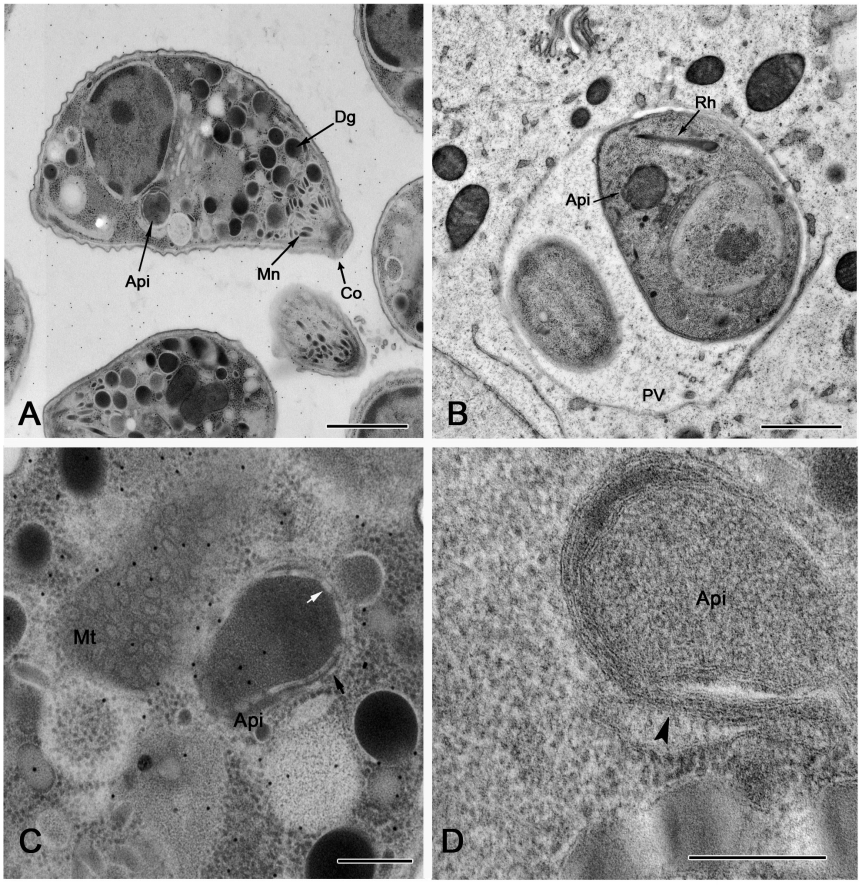

Figure 1 Micrographs (of 60-70 nm thick sections) illustrating the parasite *Toxoplasma gondii* with a focus on the apicoplast.
A) An overview of a sample of free tachyzoites substituted in 2% osmium and embedded in Epon. The typical features for the phylum are clearly distinguishable: the conoid (Co), dense granules (Dg), micronemes (Mn) and apicoplast (Api) **B)** An intracellular parasite substituted with 0.1% uranyl and embedded in Lowicryl HM20. Parasitophorous vacuole (PV), rhoptry (Rh) **C)** An apicoplast with its typical features: the four membranes; patches spanning the inner membranes (*white arrow*) and those on the periplastid (*black arrow*) are clearly visible. **D)** Another apicoplast, where the close association with the ER is indicated by an *arrowhead*. Note that the gold particles in images A and C are randomly applied fiducial markers used for image alignment. Epon embedded samples were post-stained with 20% uranyl acetate and lead citrate, as described. Lowicryl sections were examined without being post-stained. The scale bars in **A** and **B** are 500 nm and in **C** and **D** 100 nm.
Figure 1 is also an illustration of the differences in contrast, structure preservation and visualization depending on the sample preparation.

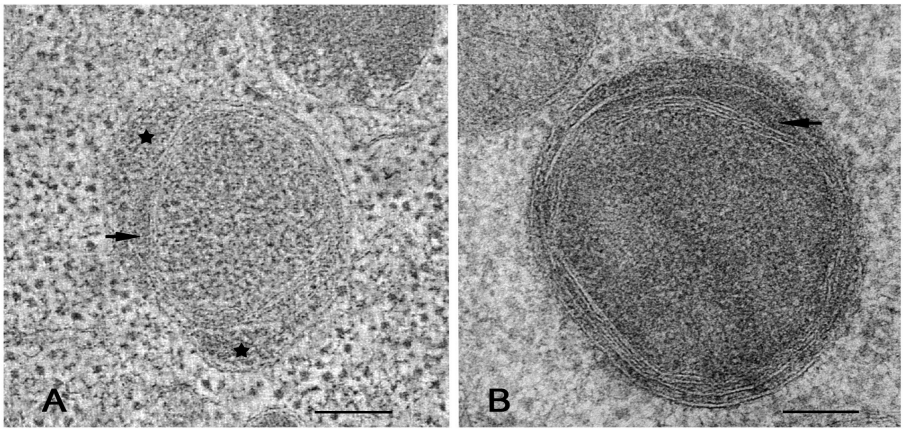

Figure 2 Different apicoplasts, showing the variability of the exoplastid compartment (EPC) and periplastid compartment (PPC).
A) A tomographic slice of a reconstruction from thick sections (200 nm) the EPS (*asterisk*) and the PPS (*arrow*) are indicated. **B)** Micrograph of 60-70 nm thick section, showing the same features. Both images are from samples substituted in 0.1% uranyl acetate and embedded in Lowicryl HM20. No additional contrasting was applied. Scale bars 50 nm.

3D dimensions features of apicoplast-ER MCSs

These ER-apicoplast MCS appeared to be limited within 40-50 nm in z direction of the sample volume and 30-40 nm parallel to the membranes, which makes them difficult to detect. These values are an average number from 15 reconstructed tomograms. The cytosolic gap between the two membranes in this particular membrane-membrane relation is between 6-10 nm (Fig.1B, 4). The measurements of the distance were performed in IMOD program. The pixel size in nanometers is automatically given for each tilt series acquisition by the FEI software (FEI, Eindhoven, The Netherlands). The contour displayed in the “Zap” window of the IMOD program (Fig.3C green line) connects two points one located on the outermost membrane of the apicoplast (red dot in Fig. 3C) and the other on the membrane of the ER, which is most closely apposing the plastid. These two points were chosen to overlap with the darkest (image inverted) pixel range to ensure they are within the hydrophobic part of the membrane. In that way the influence of the irregular stain distribution on the membrane surface is avoided. The distance between these two points is given in number of pixels, which can be directly seen in the x axis of the graphic (Fig.3A) or as a numerical value in Edit-Point-Dimension window (Fig.3B yellow highlight). The actual distance in nanometers is automatically calculated by the program using the image pixel size for the particular tomogram given in the text file of the tilt series (Fig. 3red highlight).

The same measurements were performed in tomograms of HM20 embedded samples. In these tomograms the lamellar structure of the membranes is easily distinguishable without any additional post-staining of the sections. The absence of any contrast alterations,

introduced by heavy metal stains, assured the precision of the measured distances between the apicoplast OM membrane and the ER.

The cytosolic gap distance of 6 to 10 nm is an average value based on 10 representative measurements from each tomogram of Epon and HM20 embedded samples, respectively. The distances selected to be measured accounts for the place of most closely appositional bilayers. The most commonly measured values were 8 to 10 nm.

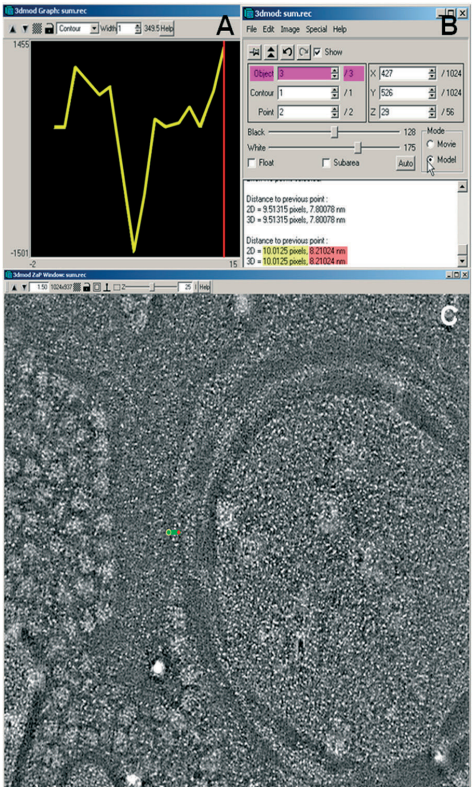

Figure 3 Illustration of the measurement and calculation of the cytosolic gap at the MCS.
Optical slice extracted from the reconstruction of an apicoplasts (**C**). The green contour illustrates the distance between the outermost membrane of the apicoplast (red dot) and the most closely situated membrane of the ER. The graphic (**A**) represents the number of pixels (*x* axis) along the green contour and the gray values of the pixels (*y* axis). The highest peaks in the graphic correspond to the darkest pixels (image is inverted) which are part of the two corresponding membranes. The distance between them indicates the cytosolic gap. The calculation of distance in nanometers was performed by multiplying the number of pixels in each contour by the image pixel size given for each data acquisition by the FEI software. In this particular case (**B**) the number of pixels is 10 (highlighted in yellow), the pixel size 0.82 nm which gives a distance of 8.2 nm (highlighted in red) between the two bilayers.

In the examined hundred of sections through different (at least three per section) apicoplasts in 30 per cent we identified associations between the ER and apicoplast OM membranes, which had the repetitive morphological features described above. Each section of 200 nm represents approximately 1/3 of the total surface of an apicoplast and each section of 60 nm approximately 1/10. This indicates the estimated average number of these specific MCS is one per plastid. When defining the frequency of such formations two important aspects have to be considered. First, the fact that we examined randomly selected areas of the apicoplast surface. Second, the dynamic character of these contacts sites. The MCSs are not static formations, with the two membranes permanently anchored together, but rather highly specialized points of molecule exchange based on metabolic demands.

The dynamic feature is nicely supported by the fact that we detected one apicoplast with three MCS while in others we did none. As a dynamic, time dependant event the evaluation of the MCS number in this particular case represents the occurrence of this event in one randomly selected time point. Taking this into account, the deduced number of one MCS per apicoplast indicates that this membrane-membrane association is of significant importance.

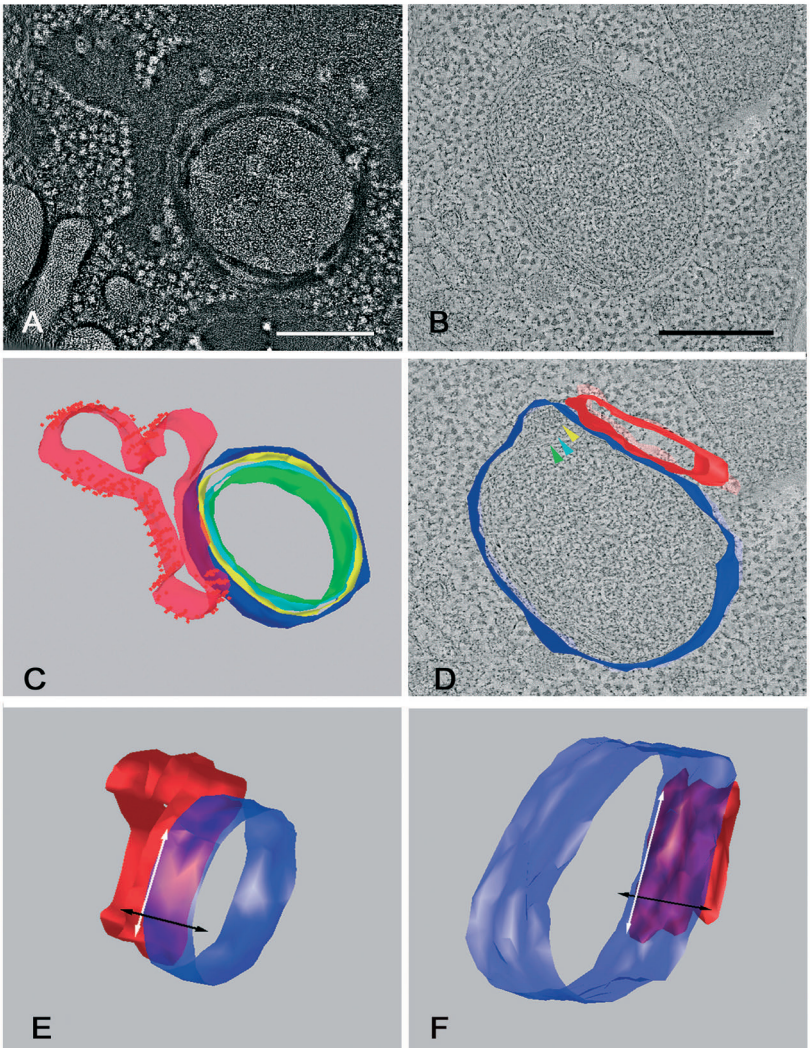

Figure 4 Images illustrating the relation between the ER and the apicoplast OM membrane.

A) Image of an apicoplast (inverted contrast) from a tomographic reconstruction of a thin section (60-70 nm) to enable better visualization of the exact relation between the membranes of the ER and the apicoplast. **B)** Tomographic slice of another apicoplast. This is a reconstruction of a thick section (200 nm). The lamellar structure of all the membranes is visible. No additional contrasting was applied. **C)** View of a model

generated by the tomographic reconstructions of the apicoplast in **A**. The ER sheet is made transparent so the OM membrane (dark blue) is being visible as an intact, continues membrane not fusing at any point with the membrane of the ER. **D)** View of a model generated by the tomographic reconstruction of the plastid shown in **B**. Only the OM membrane of the plastid and the closely apposed ER sheet are presented. **E)** and **F)** are the models of the two reconstructions, respectively **E** of the thin section and **F** of the thick section, presented only with the apicoplast OM membrane (transparent, dark blue). The models are oriented in a way to enable the visualization of the ER sheet through the inner side of the OM apicoplast membrane. The arrows indicate the *z* direction of the sample volume (black) and the direction parallel to the membranes (white). These images illustrate the actual dimensions of the MCS. The zones with highest intensity (very bright purple- resulting from the exact overlap of bright red –the ER membrane and the transparent blue-the OM apicoplast membrane) represent the place of closest apposition of the two membranes. In **E** such overlap- resulting in bright purple occupies the complete membrane in *z*, which is appr. 50 nm while in **F** it is clearly just one third of it and it also correspond to approximately 50 nm.

Discussion

In this study we provide the first experimental evidence for the existence of membrane contact sites (MCS) between the ER and the apicoplast in *Toxoplasma gondii*.

Based on the current knowledge of the putative function of the apicoplast and the emerging data on biomembrane dynamics we attempted to elucidate the nature of this MCS.

The significant role of the apicoplast in the lipid metabolism in the parasite cell (9-12;16;17) implies the existence of a reliable transport pathway for fast and accurate allocation of lipids. The statement that ER is a major lipid distribution system within the eukaryotic cell (24-26) suggests that the close associations between the apicoplast and the ER reported from *Sarcocystis* (42) and *Plasmodium* (40) are lipid trafficking points. It is, however, of crucial importance to establish the exact nature of such associations, whether they are 'membrane contact sites' –zones, in which the ER comes close to another membrane compartment without fusing with it; or 'fusion points'- points where the hydrophobic faces of the neighbouring bilayers are seen to be connected (58). This question is directly linked to the understanding of the evolutionary identity of the apicoplast and the transport of proteins and lipids to this complex organelle.

Such an entangled problem requires the study of the parasite in a sample with a reliable preservation of the membrane compounds in their three dimensions. A preservation that will guarantee that all constituents of the cell are immobilized before significant rearrangement can occur. Appropriate fixation is of curtail importance especially for an organelle such as the apicoplast where the pleomorphism of the four membranes (presumably due to differences in the lipid content as an indication for both different origin and function) makes the task of achieving optimal preservation and visualization of all four membranes extremely difficult.

The only method that could affix biological structure in its native state is cryofixation (45-47;59-63). Subsequent, direct examination of the frozen-hydrated sample with

cryo-tomography is currently the only chemical artefact-free, high-resolution method for obtaining three-dimensional structure of a biological material (64). However, the limited allocation and variable appearance of these 'contact sites' makes their identification more convoluted and comes as a major obstacle in applying cryo-ET in this particular case.
Alternatively, specimen prepared by HPF, followed by freeze-substitution (FS) and resin embedment ensures structural preservation as close as possible to the living state. It has been proven that the three-dimensional arrangement of membranes is retained and only few lipids are lost (65-71) and in addition giving the possibility to examine large sample areas. Combining the HPF/FS sample preparation with electron tomography had proven to reveal not only the morphology of cellular structures in its native context, but also the relationships they have at comparatively high resolution (72). Electron tomography (ET) had already changed our understanding of complex membranous structures and organelles in the cell, their spatial connections and functionality (29;32;73-76).
The combination of HPF and FS with ET in this study revealed areas of very close apposition of specialized, ribosome-free, domains of the ER to the outermost membrane of the apicoplast. This close association has a random spatial distribution. It appears to be restricted within the range of 40-60 nm in z direction of the sample volume and 30-40 nm parallel to the direction of the membranes (Fig. 4).
The morphological features of this membrane-membrane relation, being restricted within 40-50 nm in diameter and random distribution in addition to being a time-restricted event make the aim to analyze this MCS difficult. It is known that structures smaller than the thickness of a section may not be recognized and continuities with other structures missed (77). To ensure the relevance of our findings we recorded tilt series also of thin sections (60-70 nm), in which we can follow the approximation of the membrane in all three dimensions. This gives the opportunity to follow possible fusion points between the outermost apicoplast membrane and the ER membrane even if this would be an event with very rare occurrence.
Based on our observations it appears very unlikely that there is any continuity between the ER membrane and the OM membrane of the apicoplast. In all reconstructed tomograms (n=13) we did not observe any evidence for fusion between the ER membrane and the OM of the plastid. However, the approximation of these two membranes at some restricted areas is so repetitive in its morphological characteristic that it likely represents a functional feature. The distance of 8-10 nm between the associating membranes, measured in the tomograms (Fig. 3), could facilitate contact formation by protein bridges between the surfaces of both organelles. The structural organization of these membrane associations suggest that they are specialized MCSs for lipid transport.
The estimated number of MCS (one per apicoplast) indicates that such formations have an important role in the plastid-parasite relation. The FA that the parasite scavenge from its host cell, the FA being synthesized in the apicoplast and the FA elongation in the ER are three sites of a complex process which maintains the balance of lipid metabolism of

the parasite. Such complex system requires precise coordination, which also will account for the metabolic changes in the parasite cell dependant on the particular stage of its life cycle. Therefore, we can expect the number of MCS existing between the ER membrane and the apicoplast OM membrane will depend on the physiological need of the parasite. It should be noted the average number of MCS per apicoplast indicated in this study does not take into consideration the differences in the lipid metabolism of the parasite cell depending on its life cycle.

Although the precise mechanism by which lipids are moved across cellular membranes remains to be established, it is generally accepted that this process is protein-mediated (24;25).

Soluble fatty acid binding proteins (FABPs) are present within most eukaryotic cells and mediate the intracellular fatty acid transport. This process involves an interaction between a positively charged region of the binding protein and negative charges on the membrane surface, resulting in a conformational change that permits direct transfer of fatty acid between the protein binding site and the membrane (78).

Membrane-active binding proteins are most effective in catalyzing the inter-membrane flux when the membrane separation is sufficiently small (10 nm) so that the transport rate is limited by the rate of dissociation of the fatty acid from the donor membrane. Thus they would be expected in cells with large fatty acid fluxes across short membrane separations (79).

As suggested previously (24), in highly constricted cytosolic gaps lipid-transfer proteins (LTP) might simultaneously interact with the receptors on both sides of the membranes of an MCS. Such coinciding engagement of the donor-acceptor LTP domains will strongly amend the specificity and the efficiency of lipid exchange. This scenario of “bivalent binding” has the privilege of not only more accurate lipid targeting but also strongly reduced energy loss since the LTP remains connected to the donor –membrane.

Based on the expanding knowledge about lipid transport between membrane-bound organelles and the role of the ER as a highly efficient, lipid distribution system, we postulate that the MCS between the ER and the apicoplast we described are highly specialized units in a complex pathway for a rapid and accurate lipid trafficking in the parasite cell. This finding puts the challenge to be further investigated and to establish the precise functional mechanism of these MCS.

Acknowledgement:

European Network of Excellence ‘Three-Dimensional Electron Microscopy’, FP6 and the Dutch Cyttron consortium to CT and BMH

References

1 Levine, N.D., Protozoan parasites of domestic animals and man, Burgess Publishing Co., Minneapolis, 1973.

2 Frenkel, J.K. Toxoplasmosis. Parasite life cycle, pathology and immunology. Baltimore: University Park Press 1973;

3 Dubey, J.P. and Beattie, C.P. Toxoplasmosis of Animals and Man. Boca Raton, Florida: CRC Press 1988;61-114.

4 Luft, B.J., Hafner, R., Korzun, A. H., Leport, C., Antoniskis, D., Bosler, E. M., Bourland, D. D., Uttamchandani, R., Fuhrer, J., Jacobson, J., et al. Toxoplasmic encephalitis in patients with the acquired immunodeficiency syndrome. N. Engl. J. Med 1993;329: 995-1000.

5 Wong, S.Y. and Remington, J.S. Toxoplasmosis in pregnancy. Clin. Infect. Dis. 1994;18: 853–862.

6 Wilson, R.J.M., Williamson, D.H. and Preiser, P. Malaria and other apicomplexans: the 'plant' connection. Infectious Agents Diseases 1994;3: 29-37.

7 McFadden, G.I., Reith, M.E., Munholland, J. and Lang-Unnasch, N. Plastid in human parasites. Nature 1996;381: 482.

8 Waller, R.F., Keeling, P.J., Donald, R.G.K., Striepen, B., Handman, E., Lang-Unnasch, N., Cowman, A.F., Besra, G.S., Roos, D.S. and McFadden, G.I. Nuclear-encoded proteins target to the plastid in *Toxoplasma gondii* and *Plasmodium falciparum*. Proceedings of the National Academy of Science USA 1998;95: 12352-12357.

9 Jomaa, H., Wiesner, J., Sanderbrand, S., Altincicek, B., Weidemeyer, C., Hintz, M., Türbachova, I., Eberl, M., Zeidler, J., Lichtenthaler, H.K., Soldati, D. and Beck, E. Inhibitors of the nonmevalonate pathway of isoprenoid biosynthesis as antimalarial drugs. Science 1999;285: 1573-1576.

10 Roos, D.S., Crawford, M.J., Donald, R.G., Kissinger, J.C., Klimczak, L.J. and Striepen, B. Origin, targeting, and function of the apicomplexan plastid. Current Opinion in Microbiology 1999;2: 426-432.

11 Ralph, S.A., van Dooren, G.G., Waller, R.F., Crawford, M.J., Fraunholz, M.J., Foth, B.J., Tonkin, C.J., Roos, D.S. and McFadden, G.I. Methabolic Maps and Functions of the *Plasmodium falciparum* Apicoplast. Nature Reviews | Microbiology 2004;2: 204-216.

12 Fichera, M.E. and Roos, D.S. A plastid organelle as a drug target in apicomplexan parasites. Nature 1997;390: 407-409.

13 Wilson, R.J.M. Progress with parasite plastids. Journal of Molecular Biology 2002;319: 257-274.

14 Waller, R.F.e.a. A type II pathway for fatty acid biosynthesis presents drug targets in *Plasmodium falciparum*. Antimicrobial Agents Chemotherapy 2003;47: 297–301.

15 Wiesner, J. and Seeber, F. The plastid-derived organelle of protozoan human parasites as a target of established and emerging drugs. Expert Opin.Ther. Targets 2005;9: 23-44.

16 Bisanz, C., Bastien, O., Grando, D., Jouhet, J., Marechal, E. and Cesbron-Delauw, M.F. *Toxoplasma gondii* acyl-lipid metabolism: de novo synthesis from apicoplast-generated fatty acids versus scavenging of host cell precursors. J.Biochem 2006;394: 197-205.

17 Mazumdar, J., Wilson, E.H., Masek, K., Hunter, C.A. and Striepen, B. Apicoplast fatty acid synthesis is essential for organelle biogenesis and parasite survival in *Toxoplasma gondii*. Proceedings of the National Academy of Science of the Unated States of America 2006;103: 13192–13197.

18 Schnarrenberger, C. and Martin, W. Evolution of the enzymes of the citric acid cycle

and the glyoxylate cycle of higher plants. A case study of endosymbiotic gene transfer. European Journal of Biochemistry 2002;269: 868–883.
19 Foth, B.J., Stimmler, L.M., Handman, E., Crabb, B.S., Hodder, A.N. and McFadden, G.I. The malaria parasite *Plasmodium falciparum* has only one pyruvate dehydrogenase complex, which is located in the apicoplast. Molecular Microbiology 2005;55: 39–53.
20 Crawford, M.J., Zhu, G. and Roos, D.S. in Molecular Parasitology Meeting XIV 2003.
21 Fleige, T., Fischer, K., Ferguson, D.J., Gross, U. and Bohne, W. Carbohydrate metabolism in the *Toxoplasma gondii* apicoplast: localization of three glycolytic isoenzymes, the single pyruvate dehydrogenase complex, and a plastid phosphate translocator. Eukaryotic Cell 2007;6: 984–996.
22 Mazumdar, J. and Striepen, B. Make It or Take It: Fatty Acid Metabolism of Apicomplexan Parasites. Eukaryotic Cell 2007;6: 1727–1735.
23 Voelker, D.R. Bridging gaps in phospholipid transport. Trends in Biochemical Sciences 2005;30: 396-404.
24 Holthuis, J.C.M. and Levine, T.P. Lipid Traffic: Floppy Drives and a Superhighway. Nature Reviews Molecular Cell Biology 2005;6: 209-220.
25 van Meer, G., Voelker, D.R. and Feigenson, G.W. Membrane lipids: where they are and how they behave. Nature Reviewsws | molecular cell biology 2008;9: 112-124.
26 Levine, T. and Loewen, C. Inter-organelle membrane contact sites: Through a glass, darkly. Current Opinion in Cell Biology 2006;18: 371–378.
27 Craig, S. and Staehelin, L.A. High pressure freezing of intact plant tissues. Evaluation and characterization of novel features of the endoplasmic reticulum and associated membrane systems. Eur J Cell Biol 1988;46: 81-93.
28 Achleitner, G., Gaigg, B., Krasser, A., Kainersdorfer, E., Kohlwein, S., Perktold, A., Zellnig, G. and Daum, G. Association between the endoplasmic reticulum and mitochondria of yeast facilitates interorganelle transport of phospholipids through membrane contact. European Journal of Biochemistry 1999;264: 545–553.
29 Marsh, B.J., Mastronarde, D.N., Buttle, K.F., Howell, K.E. and McIntosh, J.R. Organellar relationships in the Golgi region of the pancreatic beta cell line, HIT-T15, visualized by high resolution electron tomography. Proceedings of the National Academy of Science USA 2001;98: 2399-2406.
30 Voelker, D.R. New perspectives on the regulation of intermembrane glycerophospholipid traffic. Journal of Lipid Research 2003;44: 441-449.
31 Gaigg, B., Simbeni, R., Hrastnik, C., Paltauf, F. and Daum, G. Characterization of a microsomal subfraction associated with mitochondria of the yeast, Saccharomyces cerevisiae. Involvement in synthesis and import of phospholipids into mitochondria. Biochimica et Biophysica Acta 1995;1234: 214-220.
32 Perktold, A., Zechmann, B., Daum, G. and Zellnig, G. Organelle association visualized by three-dimensional ultrastructural imaging of the yeast cell. FEMS Yeast Res 2007;7: 629-638.
33 Vance, J.E. Phospholipid synthesis in a membrane fraction associated with mitochondria. Journal of Biological Chemistry 1990;265: 7248-7256.
34 Shiao, Y.J., Lupo, G. and Vance, J.E. Evidence that phosphatidylserine is imported into mitochondria via a mitochondria associated membrane and that the majority of phosphatidylethanolamine is derived from decarboxylation of phosphatidylserine. Journal of Biological Chemistry 1995;270: 11190-11198.
35 Perkins, G.A., Renken, C.W., Frey, T.G. and Ellisman, M.H. Membrane Architecture of Mitochondria in Neurons of the Central Nervous System. Journal of Neuroscience Research 2001;66: 857-865.

36 Kunst, L. and Samuels, A.L. Biosynthesis and secretion of plant cuticular wax. Progress in Lipid Research 2003;42: 51–80.
37 Hanson, M.R. and Köhler, R.H. GFP imaging: methodology and application to investigate cellular compartmentation in plants. Journal of Experimental Botany 2001;52: 529-539.
38 Andersson, M.X., Goksor, M. and Sandelius, A.S. Optical Manipulation Reveals Strong Attracting Forces at Membrane Contact Sites between Endoplasmic Reticulum and Chloroplasts. Journal of Biological Chemistry 2007;282: 1170–1174.
39 Aikawa, M. The fine structure of the erythrocytic stages of three avian malarial parasites, *Plasmodium fallax*, *Plasmodium lophurae* and *Plasmodium cathemerium*. American Journal of Tropical Medicine and Hygiene 1966;15: 449–471.
40 Tonkin, C.J., Struck, N.S., Mullin, K.A., Stimmler, L.M. and McFadden, G.I. Evidence for Golgi-independent transport from the early secretory pathway to the plastid in malaria parasites. Molecular Microbiology 2006;61: 614–630.
41 van Dooren, G.G., Marti, M., Tonkin, C.J., Stimmler, L.M., Cowman, A.F. and McFadden, G.I. Development of the endoplasmic reticulum, mitochondrion and apicoplast during the asexual life cycle of *Plasmodium falciparum*. Molecular Microbiology 2005;57: 405-419.
42 Tomova, C., Geerts, W.J.C., Müller-Reichert, T., Entzeroth, R. and Humbel, B.M. New comprehension of the apicoplast of *Sarcocystis* by transmission electron tomography. Biology of the Cell 2006;98: 535–545.
43 Hopkins, J., Fowler, R., Krishna, S., Wilson, I., Mitchell, G. and Bannister, L. The plastid in *Plasmodium falciparum* asexual blood stages: a three-dimensional ultrastructural analysis. Protist 1999;150: 283-295.
44 Köhler, S. Multi-membrane-bound structures of Apicomplexa: I. the architecture of the *Toxoplasma gondii* apicoplast. Parasitology Research 2005;96: 258-272.
45 Ebersold, H.R., Cordier, J.L. and Lüthy, P. Bacterial mesosomes: method dependent artifacts. Archives of Microbiology 1981;130: 19-22.
46 Dubochet, J., McDowall, A.W., Menge, B., Schmid, E.N. and Lickfeld, K.G. Electron microscopy of frozen-hydrated bacteria. Journal of Bacteriology 1983;155: 381-390.
47 Murk, J.L.A.N., Posthuma, G., Koster, A.J., Geuze, H.J., Verkleij, A.J., Kleijmeer, M.J. and Humbel, B.M. Influence of aldehyde fixation on the morphology of endosomes and lysosomes: Quatitative analysis and electron tomography. Journal of Microscopy 2003;212: 81-90.
48 Matsko, N. and Mueller, M. Epoxy resin as fixative during freeze-substitution. Journal of Structural Biology 2005;152: 92–103.
49 Geerts, W.J.C., Koster, A.J., Verkleij, A.J. and Humbel, B.M. in (Golemis, E.A. and Adams, P.D., eds.) Protein-Protein Interactions. A molecular cloning manual, Cold Spring Harbor Laboratories Press, New York 2005, pp. in press.
50 Gross, U., Muller, W.A., Knapp, S. and Heesemann, J. Identification of a Virulence-Associated Antigen of *Toxoplasma gondii* by Use of a Mouse Monoclonal Antibody. Infection and Immunity 1991;59: 4511-4516.
51 Roos, D., S., Donald, R.G., Morrissette, N.S. and Moulton, A.L. Molecular tools for genetic dissection of the protozoan parasite *Toxoplasma gondii*. Methods Cell Biol. 1994;45: 27-63.
52 Müller, M., Marti, T. and Kriz, S. Improved structural preservation by freeze substitution. In: Proceedings of the 7th European Congress on Electron Microscopy. P. Brederoo and W. de Priester, editors 1980;720-721.
53 Reynolds, E.S. The use of lead citrate at high pH as an electron-opaque stain in electron microscopy. Journal of Cell Biology 1963;17: 208-212.
54 Penczek, P., Marko, M., Buttle, K. and Frank, J. Double-tilt electron tomography. Ul-

tramicroscopy 1995;60: 393-410.
55 Kremer, J.R., Mastronarde, D.N. and McIntosh, J.R. Computer visualization of three-dimensional image data using IMOD. Journal of Structural Biology 1996;116: 71-76.
56 Cavalier-Smith, T. Principles of protein and lipid targeting in secondary symbiogenesis: euglenoid, dinoflagellate, and sporozoan plastid origins and the eukaryotic family tree. Journal of Eukaryotic Microbiology 1999;46: 347-366.
57 Douglas, S.E. Plastid evolution: origins, diversity, trends. Current Opinion in Genetics & Development 1998;8: 655-661.
58 Burger, K.N.J. and Verkleij, A.J. Membrane fusion. Experientia 1990;46: 631-644.
59 Fernández-Morán, H. Low-temperature preparation techniques for electron microscopy of biological specimens based on rapid freezing with liquid Helium II. Annals of the New York Academy of Sciences 1960;85: 689-713.
60 van Harreveld, A. and Crowell, J. Electron microscopy after rapid freezing on a metal surface and substitution fixation. Anatomical Record 1964;149: 381-386.
61 Müller, M., Moor, Hans. in (Revel, J.P., Barnard, T. and Haggis, G.H., eds.) Science of Biological Specimen Preparation 1983, SEM Inc., AMF O'Hare 1984, pp. 131-138.
62 McDonald, K. and Morphew, M.K. Improved preservation of ultrastructure in difficult-to-fix organisms by high pressure freezing and freeze substitution: I. Drosophila melanogaster and Strongylocentrotus purpuratus embryos. Microsc. Res. Tech 1993;24: 465-473.
63 Dubochet, J. High-pressure freezing for cryoelectron microscopy. Trends in Cell Biology 1995;5: 366-368.
64 Lucic, V., Forster, F. and Baumeister, W. Structural studies by electron tomography: from cells to molecules. Ann Rev. Biochem 2005;74: 833-865.
65 Steinbrecht, R.A. and Müller, M. Cryotechniques in Biological Electron Micoscopy, Springer-Verlag, Berlin, Heidelberg 1987, pp. 149-172.
66 Szczesny, P.J., Walther, P. and Müller, M. Light damage in rod outer segments: the effects of fixation on ultrastructural alterations. Current Eye Research 1996;15: 807-814.
67 Studer, D., Hennecke, H. and Müller, M. High-pressure freezing of soyabean nodules leads to an improved preservation of ultrastructure. Planta 1992;188: 155-163.
68 Verkleij, A.J., Humbel, B., Studer, D. and Müller, M. 'Lipidic particle' systems as visualized by thin-section electron microscopy. Biochimica et Biophysica Acta 1985;812: 591-495.
69 Weibull, C. and Christiansson, A. Extraction of proteins and membrane lipids during low temperature embedding of biological material for electron microscopy. J. Microsc. 1986;142: 79 - 86.
70 Knoll, G., Burger, K.N.J., Bron, R., van Meer, G. and Verkleij, A.J. Fusion of Liposomes with the Plasma Membrane of Epithelial Cells: Fate of Incorporated Lipids as Followed by Freeze Fracture and Autoradiography of Plastic Sections. J. Cell Biol 1988;107: 2511-2521.
71 Humbel, B.M. and Schwarz, H. in (Verkleij, A.J. and Leunissen, J.L.M., eds.) Immuno-Gold Labeling in Cell Biology, CRC Press, Boca Raton 1989, pp. 115-134.
72 McIntosh, J., Richard Electron Microscopy of Cells: A New Beginning for a New Century. The Journal of Cell Biology 2001;153: F25–F32.
73 Mannella, C.A., Pfeiffer, D.R., Bradshaw, P.C., Moraru, I.I., Slepchenko, B., Loew, L.M., Hsieh, C.-e., Buttle, K. and Marko, M. Topology of the Mitochondrial Inner Membrane: Dynamics and Bioenergetic Implications. IUBMB Life 2001;52: 93–100.
74 Ladinsky, M.S., Mastronarde, D.N., McIntosh, J.R., Howell, K.E. and Staehelin, L.A. Golgi structure in three dimensions: functional insights from the normal rat kidney cell. Journal of Cell Biology 1999;144: 1135-1149.

75 Murk, J.L.A.N., 3-D Analysis of Endosomes, Lysosomes and Peroxisomes, Ph. D. Thesis, Utrecht, 2004.
76 Mogelsvang, S., Gomez-Ospina, N., J., S., Glick, B.S. and Staehelin, L.A. Tomographic evidence for continuous turnover of Golgi cisternae in Pichia pastoris. Molecular Biology of the Cell 2003;14: 2277–2291.
77 Griffiths, G. Fine Structure Immunocytochemistry. Springer-Verlag, Berlin, Heidelberg. 1993;
78 Hsu, K.-T. and Storch, J. Fatty Acid Transfer from Liver and Intestinal Fatty Acid-binding Proteins to Membranes Occurs by Different Mechanisms. Journal of Biological Chemistry 1996;271: 13317–13323.
79 Weisiger, R.A. and Zucker, S.D. Transfer of fatty acids between intracellular membranes: roles of soluble binding proteins, distance, and time. Journal of Gastrointestinal and Liver Physiology 2002;282: G105–G115.

Chapter 4

Toxoplasma gondii Tic20 is essential for apicoplast protein import

Giel G. van Dooren[2], Cveta Tomova[1], Swati Agrawal[2],

Bruno M. Humbel[1] and Boris Striepen[2,3]

[1] Electron Microscopy and Structural Analysis, Department of Biology, Faculty of Sciences, Utrecht University, The Netherlands
[2] Centre for Tropical and Emerging Global Diseases and [3] Department of Cellular Biology, University of Georgia, Athens, USA

PNAS (2008) Vol. 105 Nr 36 pp. 13574 - 13579

Toxoplasma gondii Tic20 is essential for apicoplast protein import

Giel G. van Dooren, Cveta Tomova, Swati Agrawal,
Bruno M. Humbel and Boris Striepen

Abstract

Apicomplexan parasites harbor a secondary plastid that has lost the ability to photosynthesise yet is essential for the parasite to multiply and cause disease. Bioinformatic analyses predict that 5-10% of all proteins encoded in the parasite genome function within this organelle. However, the mechanisms and molecules that mediate import of such large numbers of cargo proteins across the four membranes surrounding the plastid remain elusive. In this study, we identify a highly diverged member of the Tic20 protein family in Apicomplexa. We demonstrate that Tic20 of *Toxoplasma gondii* is an integral protein of the innermost plastid membrane. We engineer a conditional null-mutant and show that *Tg*Tic20 is essential for parasite growth. To functionally characterize this mutant we develop several independent biochemical import assays that reveal that loss of *Tg*Tic20 leads to severe impairment of plastid protein import. *Tg*Tic20 is the first experimentally validated protein import factor identified in apicoplasts and in secondary plastids generally.

Introduction

Organelle acquisitions through endosymbiotic events have been major drivers of eukaryotic evolution. The incorporation of a cyanobacterium into a heterotrophic eukaryote led to the formation of plastids (e.g. chloroplasts), enabling eukaryotes to become autotrophic. It is thought that a single, so-called “primary”, endosymbiotic event led to the acquisition of chloroplasts in a lineage that later evolved into eukaryotic phyla such as red algae, green algae and plants (1). An alternative means by which eukaryotes have obtained plastids is through a process of “secondary” endosymbiosis. Here, a eukaryote containing a primary plastid is incorporated into a heterotrophic eukaryote. Secondarily-derived plastids are found in numerous lineages of ecologically, economically and medically important organisms, including diatoms, dinoflagellates and Apicomplexa. Apicomplexa are a phylum of obligate intracellular parasites that include *Plasmodium* species, the causative agents of malaria, and *Toxoplasma gondii*, which causes severe encephalitis upon congenital infection and in immunocompromized patients. The plastids of apicomplexans are known as apicoplasts, and are thought to function in a range of biosynthetic pathways, such as fatty acid, haem and isoprenoid biosynthesis (2, 3).

A key step in the conversion of an endosymbiont into a fully-fledged plastid is the transfer of endosymbiont genes to the nucleus of the host. This affords the host cell control over its endosymbiont, but requires the evolution of molecular machinery to enable the import of proteins encoded in the nuclear genome back into the organelle to carry out their role. This targeting process has been well studied in plants, where plastids are bound by two membranes. To enable proteins to traverse these membranes, plant plastids contain multi-subunit protein complexes in both the outer and inner membranes, called the translocons of the outer chloroplast membrane (Toc) and inner chloroplast membrane (Tic), respectively (4). Plastids derived by secondary endosymbiosis differ significantly from their primary counterparts. Secondary plastids are typically surrounded by three or four membranes and protein targeting to the organelle occurs via the secretory pathway. While the protein motifs required to direct proteins into secondary plasids are reasonably well characterised (5), little is known of the molecular mechanisms involved in import.

Four membranes surround the apicoplast of *T. gondii*. To characterise proteins involved in protein import across each of these membranes, we performed comparative genomic analyses to identify proteins with possible roles in apicoplast protein import. In this study we identify a divergent *T. gondii* homologue of the plant Tic20 protein (*Tg*Tic20). By generating a conditional null mutant of *Tg*Tic20, we demonstrate that *Tg*Tic20 is essential for parasite viability, and is required for import of proteins into the apicoplast. We develop several assays that establish *T. gondii* as a rigorous model system to genetically dissect the protein machinery required for import into secondary plastids.

Results and Discussion

A Tic20 homologue in Apicomplexa

We performed iterative BLAST searches to identify homologues of the plant inner membrane translocase component Tic20 in apicomplexan parasites. We identified Tic20 homologues from all the available genomes of apicomplexans containing a plastid. Alignments of apicomplexan Tic20 homologues with plant, red algal, diatom and cyanobacterial counterparts (supporting information (SI) Fig. S1) reveal the presence of an N-terminal extension with characteristics of a bipartite apicoplast targeting sequence. Similarity to plant and algal Tic20 homologues resides in the C-terminal portion of the protein, although very few residues are conserved between all homologues depicted (Fig. S1).

*Tg*Tic20 is an integral protein of the inner apicoplast membrane

Cloning of the full open reading frame of *Tg*Tic20 revealed the presence of three introns, and a predicted protein size of 43.4 kDa. We generated a transgenic parasite line expressing *Tg*Tic20 fused to a C-terminal HA tag and monitored its localisation by immunofluorescence assay (Fig. 1*A*). *Tg*Tic20-HA (green) localised to a small, apical organelle that overlapped with acyl carrier protein (ACP; red), a marker for the apicoplast stroma. A Western blot of cells expressing the *Tg*Tic20-HA transgene revealed a major protein species of approximately 23 kDa, and a less abundant species of around 45 kDa (Fig. 1*B*). This suggests that the N-terminal portion of the protein is cleaved to yield the mature protein of around 20 kDa, consistent with the N-terminus of the protein functioning as an apicoplast-targeting domain that is processed upon import into the apicoplast (6, 7). *In silico* modelling of the protein structure of *Tg*Tic20 suggests the presence of four transmembrane domains in *Tg*Tic20, found in close succession at the C-terminus of the protein (Fig. S1). To determine whether *Tg*Tic20 is an integral membrane protein, we performed sodium carbonate extractions and Triton X-114 (TX-114) phase partitioning. Sodium carbonate extractions resulted in *Tg*Tic20 localising to the membrane fraction, much like the previously characterised apicoplast phosphate transporter (APT1; (8)) and unlike the soluble ACP (Fig. 1*C*). Much, but not all, *Tg*Tic20 localised to the detergent (i.e. membrane) phase during TX-114 phase partitioning, again consistent with a membrane localisation for *Tg*Tic20.

To further characterise the subcellular localisation of *Tg*Tic20 we performed transmission immuno-electron microscopy on parasites expressing *Tg*Tic20-HA, labelling with anti-HA and anti-ACP antibodies. This revealed the localisation of *Tg*Tic20-HA to membrane-bound organelles that also contained ACP (Fig. 1*D*), consistent with the apicoplast localisation of this protein. Localisation of *Tg*Tic20-HA within the apicoplast was generally confined to the membranes of the organelle, consistent with the membrane localisation of *Tg*Tic20, while ACP was distributed throughout the entire organelle.

Four membranes surround the apicoplast, and until now it has been difficult to determine to which membrane a given apicoplast membrane protein localises. To determine the

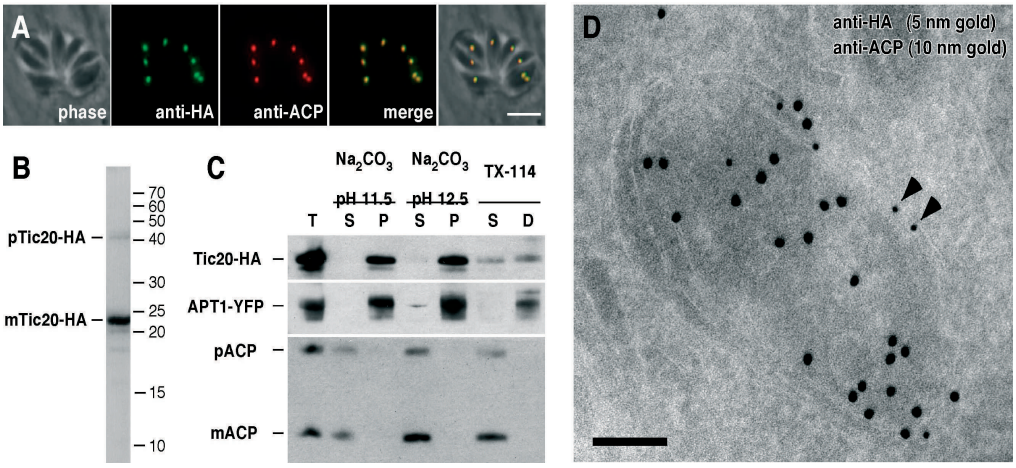

Figure1 *Tg*Tic20 is an apicoplast integral membrane protein.

(A) Immuofluorescence assay depicting an eight-cell *T. gondii* vacuole. *Tg*Tic20-HA (green) co-localises with the apicoplast marker ACP (red). Scale bar is 5 mm. ***(B)*** A Western blot of protein extracts from the *Tg*Tic20-HA line with anti-HA antibodies. A mature *Tg*Tic20 protein species is labelled at around 23 kDa, while a weaker precursor band is labelled at around 40 kDa. ***(C)*** Proteins were extracted from the *Tg*Tic20-HA/APT1-YFP line and fractionated into soluble (S) and membrane pellet (P) fractions by sodium carbonate treatment, or into soluble (S) and detergent (D) phases by TX-114 phase partitioning. Total protein extracts (T) are shown in the first lane.
(D) Transmission electron micrograph of the *Tg*Tic20-HA cell line, where *Tg*Tic20-HA is labelled with 10 nm gold beads and ACP with 15 nm gold beads. Arrowheads show *Tg*Tic20-HA labelling at the membranes of the organelle. Scale bar 100 nm.

membrane to which *Tg*Tic20 localises, we developed a novel green fluorescent protein (GFP) assay, making use of a previously established self-assembling split GFP (9). In this system, the C-terminal β-strand of GFP (GFP-11) was removed from the remaining 10 β-strands (GFP 1-10) of the molecule. This GFP-11 was engineered with the ability to self-assemble with GFP 1-10 if both molecules localise to the same compartment (9). As a proof of principle, we first targeted GFP 1-10 to the apicoplast stroma by adding the N-terminal apicoplast-targeting domain of ferredoxin-NADP+ reductase (FNR). By itself, this protein was unable to fluoresce (not shown). We next fused GFP-11 to the C-terminus of ACP and transfected this into the FNR-GFP 1-10 line. The resultant parasites revealed GFP fluorescence in the apicoplast (Fig. 2*A*). This indicated that when both components of the split GFP are targeted to the apicoplast stroma, we observe apicoplast fluorescence. We were concerned that the two GFP domains may interact in the secretory pathway before entry into the apicoplast, thus limiting the predictive value of the assay. To test this, we generated constructs where we fused both GFP 1-10 and GFP-11 to the C-terminus of P30, a previously established secretory marker protein for *T. gondii* (10). Expressed together, secreted GFP 1-10 and GFP-11 result in fluorescence in the parasitophorous

vacuole that surrounds *T. gondii* parasites (Fig. 2*C*), indicating that the split GFP domains are capable of interacting when targeted to the same compartment in the secretory system. However, when we express the P30-GFP-11 construct in the FNR-GFP 1-10 line, we see no fluorescence (not shown), suggesting that any interaction of the split GFP components in the secretory pathway does not result in mis-targeting of the component proteins.

Having established the split GFP assay for determining whether proteins are localised to the apicoplast stroma, we sought to establish whether *Tg*Tic20 localises to the inner membrane. We fused GFP-11 to the C-terminus of *Tg*Tic20 and transfected this into the FNR-GFP 1-10 cell line. The resultant line revealed fluorescence that co-localised with an apicoplast red fluorescent protein (RFP) marker (Fig. 2*B*), consistent with the C-terminus of *Tg*Tic20 residing in the apicoplast stroma. Flow cytometric analyses of the various cell lines described above supported the results obtained by microscopic analysis (Fig. S2*A*). One concern was that the observed apicoplast fluorescence might result from retention of FNR-GFP 1-10 in an outer membrane. To control for this, we monitored cleavage of the apicoplast-targeting leader of FNR-GFP 1-10, a measure for whether proteins are accessible to the stromal processing peptidase enzyme that likely resides in the apicoplast stroma (7). We found no difference in processing of FNR-GFP 1-10 whether expressed by itself or with interacting components (Fig. S2*B*), indicating that most of FNR-GFP 1-10 protein resides in the stroma, and consequently that *Tg*Tic20-GFP-11 does not prevent targeting of FNR-GFP 1-10 to the stroma.

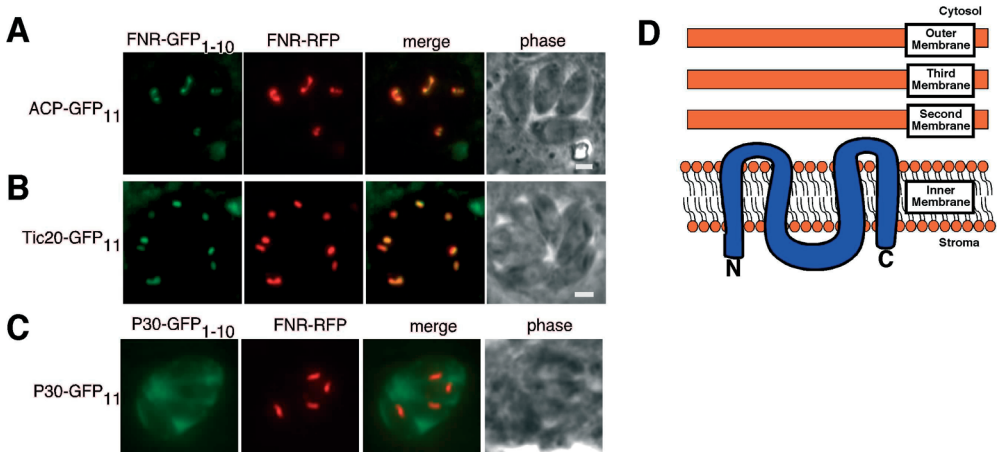

Figure 2 *Tg*Tic20 localises to the inner apicoplast membrane.

(A-B) Live images of *T. gondii* cells expressing FNR leader fused to GFP 1-10, where GFP-11 was fused to the C-terminus of either ACP (A) or *Tg*Tic20 (B). In both cell lines, green fluorescence co-localises with the apicoplast stromal marker FNR-RFP. Scale bar is 2 mm. ***(C)*** Live image of *T. gondii* parasites expressing the secretory marker protein P30 fused to both GFP 1-10 and GFP-11. Green fluorescence localises to the parasitophorous vacuole. ***(D)*** Model for localisation of *Tg*Tic20. We predict that *Tg*Tic20 localises to the inner membrane of the apicoplast, with the C-terminus in the stroma. *In silico* predictions suggest the presence of four transmembrane domains (Fig. S1).

We conclude that *Tg*Tic20 is an integral protein of the inner apicoplast membrane, with its C-terminus residing in the apicoplast stroma. Assuming that the predictions of four transmembrane domains is correct, the N-terminus would also be in the stroma, resulting in the model for *Tg*Tic20 topology presented in Fig. 2*D*. Recently, candidate proteins that likely localise to outer membranes of the apicoplast have been identified (8, 11), and the split GFP assay may help to pinpoint the residence of these and other proteins to a specific membrane or apicoplast compartment.

***Tg*Tic20 is essential for parasite viability**

To characterise the function of *Tg*Tic20, we generated a conditional *Tg*Tic20 mutant parasite cell line using a previously described tetracycline-based system (2, 12). We generated a parental cell line (iTic20/eTic20) that contains both endogenous (eTic20) and inducible (iTic20) copies of the *Tg*Tic20 gene (Fig. S3*A*), where transcription of inducible genes can be down-regulated by the addition of the tetracycline analogue anhydrotetracycline (ATc) to the growth medium. We generated a conditional *Tg*Tic20 mutant cell line (iTic20/DTic20) by disrupting the endogenous gene through homologous replacement of native *Tg*Tic20 with a selectable marker, verifying successful disruption of the native locus through polymerase chain reaction-based screening and Southern blotting (Figs. S3*B*-*C*).

We wanted to establish whether *Tg*Tic20 was essential for parasite growth and viability. To do this, we performed plaque assays, adding 400 parasites to a flask containing a confluent monolayer of human foreskin fibroblast cells. We grew parasites for 9 days in the absence or presence of ATc. During this period, parasites will go through several replication cycles, and form zones of clearance (plaques) in the host cell monolayer. We observed a severe growth defect in the presence of ATc in knockout cell line (Fig. 3*B*, double arrowhead), but not in the parental line (Fig. 3*A*). To confirm that this defect was specifically due to disruption of *Tg*Tic20, we complemented the conditional mutant by ectopically expressing *Tg*Tic20 from a constitutive promoter (iTic20/DTic20/cTic20). This restored parasite growth in the presence of ATc (Fig. 3*C*). These data indicate that *Tg*Tic20 is essential for parasite growth.

***Tg*Tic20 is essential for apicoplast protein import**

Having established that *Tg*Tic20 is an essential protein of the inner apicoplast membrane, we sought to determine its function. First, we measured the time frame for down-regulating *Tg*Tic20 expression in the mutant cell line. We harvested parasites after growing them for 0 to 4 days in ATc and monitored protein levels by Western blot. Growth on ATc resulted in swift down-regulation of expression of the inducible *Tg*Tic20 protein (Fig. 4*A*, top). As a more sensitive measure for *Tg*Tic20 abundance, we immunoprecipitated *Tg*Tic20 protein from approximately 10^7 parasites grown for 0 to 4 days on ATc. We measured immunopurified protein levels by Western blot, and found that after 2 days growth on ATc, we could no longer detect *Tg*Tic20 protein in the mutant cell line (Fig. 4*A*, bottom).

We hypothesised that *Tg*Tic20 may function in protein import into the apicoplast. To test this, we established several assays for successful protein import into apicoplasts (Fig. 4*B*). First we examined processing of the N-terminal targeting domain of apicoplast proteins, a process that likely occurs subsequent to import into the organelle stroma. Apicoplast-targeted proteins typically reveal two differently sized molecular species: a slow migrating band corresponding to the precursor protein (with its N-terminal targeting leader still attached), and a faster migrating mature protein (where the leader has been cleaved; (6, 7)). We asked whether leader processing was affected following incubation of the conditional *Tg*Tic20 mutant cell line on ATc. To facilitate these studies, we generated a cell line in the conditional *Tg*Tic20 mutant background that expressed a "synthetic" apicoplast-targeted protein, consisting of the apicoplast-targeting leader of *Tg*FNR fused to mouse dihydrofolate reductase (a reporter protein typically used for organellar import assays in other systems; (13)) and a C-terminal HA tag for detection. To gain a dynamic measure for the timing of defects on protein import in the *Tg*Tic20 mutant we conducted pulse-chase labelling experiments. We incubated mutant parasites growing in host cells for 0, 2, 3, 4 and 5 days on ATc, and radiolabeled proteins with ^{35}S-amino acids for one

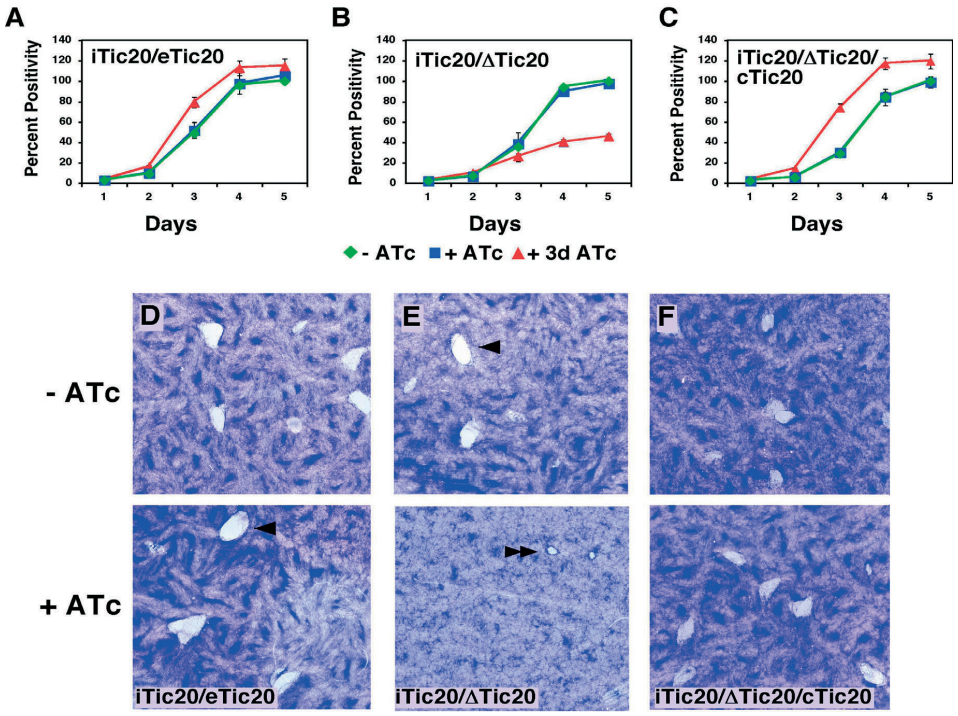

Figure 3 *Tg*Tic20 is essential for growth of *T. gondii* parasites.

(A-C) We performed plaque assays on parental parasites (A), knockout parasites (B) and knockout parasites complemented with ectopically expressed *Tg*Tic20 (C) in the absence (top) or presence (bottom) of ATc. Arrowheads and double arrowheads depict large and small plaques, respectively.

hour (pulse). We then washed out the radiolabel and incubated in medium containing an excess of unlabeled amino acids for an additional 2 hours (chase). We purified proteins of interest by immuno- or affinity-purification, separated them by SDS-PAGE and detected by autoradiography. After 5 days growth on ATc, precursor FNR-DHFR-HA protein was made at similar levels to that formed in cells grown in the absence of ATc, indicating that knockdown of *Tg*Tic20 does not affect synthesis of apicoplast-targeted proteins (Fig. 4*C*). However, after two days growth in ATc there is a 35% reduction in formation of mature, processed FNR-DHFR-HA, which decreases further after three days growth on ATc (Fig. 4*C*; Fig. 4*D*, green diamonds).

We also monitored processing of the native apicoplast protein ACP in the *Tg*Tic20 mutant. Mature ACP contains only one sulfur-containing amino acid, making detection difficult. The experiment shown in Fig. 4*C* suggests that ACP is processed at day 2 on ATc and not beyond, but detection levels are too low to draw a definitive conclusion. As a control, we monitored processing of MIC5, which occurs in a post-Golgi compartment of the secretory pathway (14). Even after 5 days incubation on ATc, MIC5 is processed (Fig. 4*C*), suggesting that *Tg*Tic20 knockdown does not affect other parts of the secretory pathway.

Although we suspect that precursor protein cleavage is a solid marker for whether proteins are able to traffic into the apicoplast stroma, it has not been formally shown that the processing event occurs here. Therefore, we sought to establish independent measures for successful protein targeting to the apicoplast. Several apicoplast enzymes are post-translationally modified by co-factors after import into the stroma. One such modification is the biotinylation of acetyl-CoA carboxylase (ACC; (15); Fig. 4*B*), a protein involved in biosynthesis of fatty acids. We purified biotinylated proteins using an immobilised streptavidin column. Radiolabeled biotinylated ACC is not yet detectable after the 1 hour pulse. In the absence of ATc, we observe robust biotinylation of ACC during the 2 hour chase (Fig. 4*C*). Biotinylated ACC is reduced after 2 days incubation in ATc, and severely reduced after 3 days (Fig. 4*C*; Fig. 4*D*, red triangles), consistent with the results of the leader-processing assay. *T. gondii* contains a second major biotinylated protein, the mitochondrial pyruvate carboxylase (PC) enzyme (15). Levels of biotinylated PC remain unchanged after incubation in ATc.

A second post-import modification is lipoylation of the E2 subunit of pyruvate dehydrogenase (PDH-E2). Lipoylation of PDH-E2 is solely mediated by apicoplast-targeted LipA and LipB and requires a substrate synthesized *de novo* within the apicoplast stroma (octanoyl-ACP; (2, 16), Fig. 4*B*).

We purified lipoylated proteins using an antibody against lipoic acid. *T. gondii* contains numerous lipoylated proteins; in addition to PDH-E2, the mitochondrion is thought to harbour the lipoylated E2 subunits of several 2-oxo-acid dehydrogenases (mito-E2; (2, 16)). The mitochondrion contains a specific protein (LplA) that functions in the addition of the lipoyl-moiety to the E2 enzymes (16), suggesting that, much like the apicoplast, lipoylation can only occur after successful import into the organelle. After the 1 hour

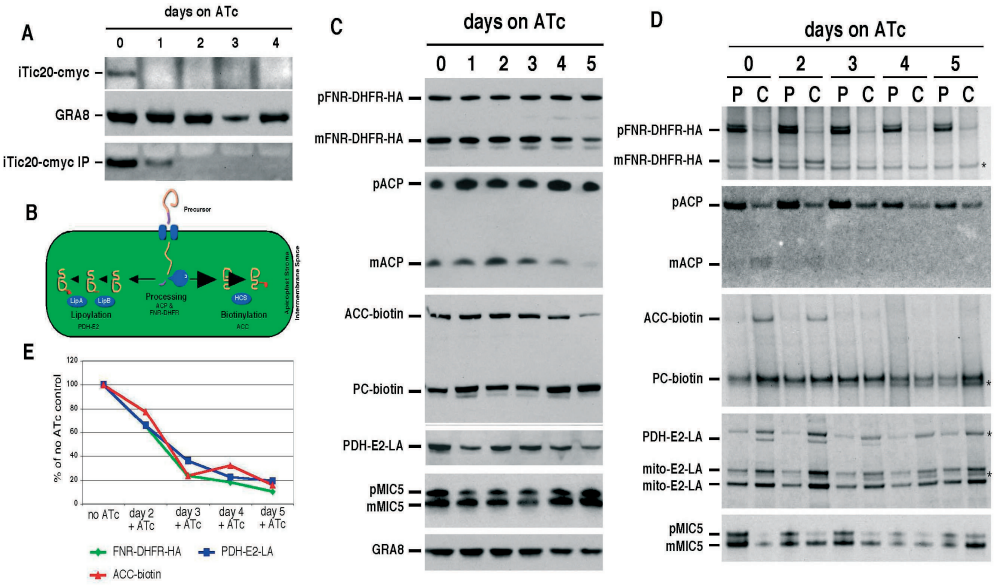

Figure 4 *Tg*Tic20 is essential for apicoplast protein import.

(A) Regulation of the inducible *Tg*Tic20-c-myc protein. iTic20/DTic20 parasites were grown for 0 to 4 days on ATc. Proteins were extracted and subjected to Western blotting with either anti-c-myc or anti-GRA8 antibodies (as a loading control), or subjected to immunoprecipitation of the inducible *Tg*Tic20-c-myc protein followed by Western blotting with anti-c-myc antibodies (bottom lane).
(B) Schematic depiction of the three protein import assays used in this study. We measured cleavage of preprotein leader sequences, a process probably mediated by the stromal processing peptidase (SPP) in the apicoplast stroma. Additionally we measured the biotinylation of ACC, a process probably mediated in the apicoplast by a holocarboxylase synthetase (HCS), and lipoylation of PDH-E2, a process mediated by the apicoplast enzymes LipB and LipA.
(C) Pulse-chase analysis of proteins from the *Tg*Tic20 knockout line grown for 0, 2, 3, 4 or 5 days on ATc. Infected host cells were incubated in medium containing ^{35}S-amino acids for one hour and either harvested (P) or further incubated in non-radioactive medium for two hours (C). After detergent solubilization, proteins were purified by immunoprecipitation or affinity purification and separated by SDS-PAGE before detection by autoradiography. Protein bands marked by an asterisk in lanes containing biotinylated and lipoylated proteins represent contaminating host cell proteins. The band marked by an asterisk in HA pulldown lanes possibly results from the use of an alternative internal start codon representing a shorter cytosolic version of FNR-DHFR-HA. ***(D)*** Quantification of bands in Fig. 4*C*. FNR-DHFR-HA values (green diamonds) were quantified as the percentage of mature protein in the chase compared to the precursor protein after the pulse. ACC-biotin values (red triangles) were quantified as a percentage of the intensity of PC in the same lane. PDH-E2-LA values (blue squares) were quantified as a percentage of the intensity of the lower-most mito-E2 band in the same lane. To enable all three assays to be plotted on the same graph, values for each day are expressed as a percentage of the no ATc value. ***(E)*** Pulse-chase analysis of proteins from the *Tg*Tic20 parental (iTic20/eTic20) line grown for 0, 2, 3, 4 or 5 days on ATc, performed in an identical manner to Fig. 4*C*.

pulse, mito-E2 enzymes are labelled, consistent with rapid import into mitochondria (Fig. 4*C*). As with biotinylated ACC, lipoylated PDH-E2 is not observed until the 2 hour chase. Lipoylation of the apicoplast PDH-E2 is reduced after 2 days growth on ATc and severely reduced after 3 days, while modification of mitochondrial enzymes was not affected, even after 5 days incubation on ATc (Fig. 4*C*; Fig. 4*D*, blue squares).

Together, these data indicate that knockdown of *Tg*Tic20 impairs import of apicoplast-targeted proteins into the stroma of the organelle, but does not impair targeting of proteins to other destinations of the secretory pathway or to the mitochondrion. To rule out the possibility that defects in apicoplast protein import resulted from non-specific effects of ATc, we performed pulse-chase analysis on the parental strain containing both inducible and endogenous *Tg*Tic20 genes, grown on ATc for 5 days. These results indicate that neither processing of the FNR-DHFR-HA leader nor biotinylation of ACC are affected by ATc alone (Fig. 4*E*).

Our results indicate that *Tg*Tic20 is required for apicoplast protein import. What, then, is the function of *Tg*Tic20 in this process? The precise role of Tic20 in chloroplast import in plants has been elusive. Knockdown of plant Tic20 by antisense RNA results in a reduced efficiency of chloroplast protein import (17). Based on its integral membrane localisation, it has been postulated that plant Tic20 forms part of the protein import channel of the inner chloroplast membrane (18), although no direct experimental evidence supports this. Our results suggest that knockdown of *Tg*Tic20 protein expression does not immediately ablate import. Two days after the addition of ATc, the amount of *Tg*Tic20 is below our limits of detection, although we cannot rule out basal levels of *Tg*Tic20 expression. At this time point, apicoplast protein import is clearly affected (as measured by three independent assays), yet still occurs at between 65 and 77% the level of wild-type cells (Fig. 4*D*). This argues against *Tg*Tic20 functioning directly in an inner membrane import channel, since the lack of an import channel would likely result in immediate ablation of import into the apicoplast. It might be that *T. gondii* harbours proteins that can partly complement the function of *Tg*Tic20. Plants contain multiple Tic20 paralogues and may also have additional non-related proteins with similar functions to Tic20 (19, 20). However, we did not identify *Tg*Tic20 paralogues in the *T. gondii* genome. Another possibility is that *Tg*Tic20 is an accessory or regulatory component of a putative import complex in the inner membrane. In such a scenario, *Tg*Tic20 may influence the efficiency of protein import through the Tic complex, assembly of the Tic complex, or be involved in a separate process that is essential for functioning of the inner membrane import complex. Identifying and characterising additional inner membrane import components should allow us to address these questions.

Preliminary experiments revealed that *Tg*Tic20 knockdown results in defects in apicoplast segregation or biogenesis. This raised the possibility that the inhibition of apicoplast protein import may be a consequence of the loss of apicoplasts from significant numbers of parasites rather than a specific effect on apicoplast import. Alternatively, lack of protein

import could lead to biogenesis defects. To visualise the apicoplast and allow us to establish the sequence of events, we targeted RFP to the apicoplast of *Tg*Tic20 mutant parasites. After prolonged incubation in ATc, we observed vacuoles where not all plastids contained visible apicoplasts (Fig. 5*A*). Quantification revealed that major defects in apicoplast biogenesis occurred after 5 days of incubation in ATc, subsequent to the observed defects in apicoplast protein targeting (Fig. 5*B-C*).

We were able to identify a sequential series of phenotypes in the *Tg*Tic20 mutant. Two days after initiation of the mutant phenotype, *Tg*Tic20 protein is no longer detectable. Coincident with *Tg*Tic20 knockdown is a reduced efficiency of apicoplast protein import, which increases to essentially complete inhibition four days after the addition of ATc. Five days after initiation, we observe major defects in apicoplast biogenesis, with arrest of parasite growth approximately 6 or 7 days after the addition of ATc. It is likely that death of the parasites results from the loss of apicoplasts and impairment of apicoplast functions. Apicoplasts are thought to perform several essential functions, such as the biosynthesis of fatty acids and isoprenoids (2, 3). It is likely that the failure to correctly target biosynthetic proteins (such as ACP, ACC and PDH-E2, Fig. 4*C*) leads to ablation of these pathways, resulting in inhibition of parasite growth. Indeed, the apparent universal defects seen in apicoplast protein import in the *Tg*Tic20 mutant suggest that we are simultaneously impairing all apicoplast proteins, making this mutant an attractive candidate to identify novel apicoplast functions (e.g. through proteomic and metabolomic approaches).

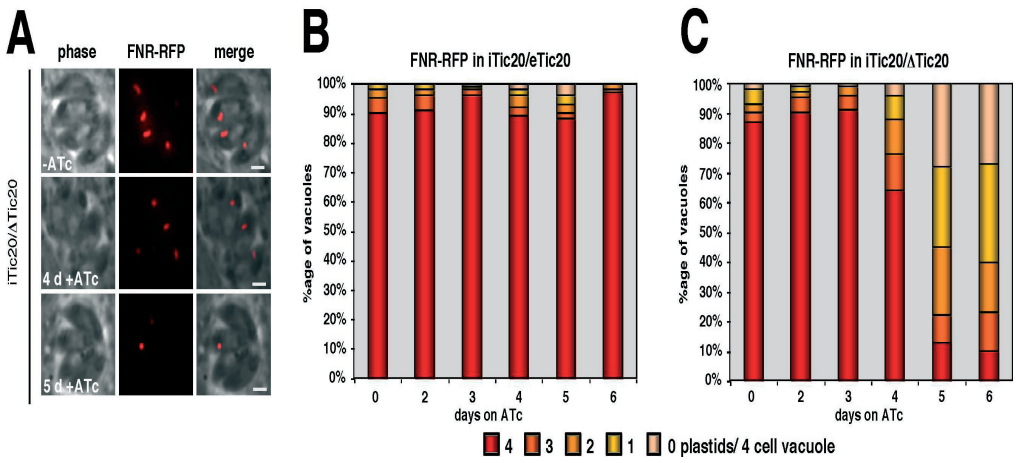

Figure 5 *Tg*Tic20 is essential for apicoplast biogenesis.

(A) *Tg*Tic20 knockout parasites containing apicoplast-targeted RFP (FNR-RFP) were grown for 0, 4 or 5 days on ATc and subjected to live cell imaging. Scale bar is 2 μm. ***(B-C)*** *Tg*Tic20 parental (B) or knockout (C) parasites containing apicoplast-targeted RFP were grown for 0 to 6 days on ATc. 100 four-cell vacuoles were imaged at each time point. The number of apicoplasts in those four cell vacuoles at each time point were counted and graphed.

Concluding Remarks

During their intracellular development, apicomplexan parasites such as *T. gondii* must target large numbers of proteins to their apicoplast. Protein targeting occurs via the secretory pathway, and requires proteins to cross 4 membranes before reaching the organelle stroma (5). There has been considerable speculation about how protein targeting across these four membranes is mediated (e.g. (5, 21)), but there has been a distinct lack of functional evidence for the various models. In this study we have examined the effects of *Tg*Tic20 knockdown on apicoplast protein import, and conclude that *Tg*Tic20 is essential for protein import across the inner apicoplast membrane. As such, *Tg*Tic20 is the first functionally characterised apicoplast import protein identified in Apicomplexa, and, more generally, in organisms containing secondary plastids.

Emerging evidence suggests that *T. gondii* and other Apicomplexa belong to a eukaryotic "supergroup" known as the Chromalveolata (22, 23). Chromalveolates include other major eukaryotic groups such as dinoflagellates and heterokonts (including diatoms and brown algae). A distinguishing feature of chromalveolates is the presence of a plastid that was derived by secondary endosymbiosis from a red alga. Chromalveolate plastids, then, represent a cellular *ménage a trois* of three 'founder' organisms: a cyanobacterium, a red alga and a heterotrophic eukaryote. An early requirement in the acquisition of plastids is the evolution of protein import machinery. An intriguing evolutionary question is which of these founders 'donated' the import machinery and whether the origin of individual translocons is tied to the origin of the membrane they cross. In this study we show that the innermost membrane is likely crossed using machinery derived from the Tic complex of the red algal chloroplast (which itself is partially derived from cyanobacterial components (19)). We establish *T. gondii* as a robust genetic system to identify and analyse proteins involved in protein import into apicoplasts. We have developed several assays that should allow us to determine whether a candidate protein is required for apicoplast protein import, and to which compartment of the plastid it localises. We hypothesise that apicoplast import proteins in *T. gondii* are conserved among the chromalveolates, and we anticipate that such approaches will provide important clues to the mechanisms and evolution of protein import systems in chromalveolate plastids, and the establishment of organelles by secondary endosymbiosis.

Materials and Methods

Parasite culture and manipulation

Parasites were passaged in human foreskin fibroblasts and genetically manipulated as described previously (24). GenBank accession number for *Tg*Tic20 is EU427503. Plasmid construction and flow cytometry techniques are described in detail in SI Material and Methods. All parasite strains described in this paper were cloned by either limiting dilution or flow cytometry. Where applicable, parasites were grown in anhydrotetracycline (IBA, St Louis, MO) at a final concentration of 0.5 mg/ml.

Immunoprecipitation, SDS-PAGE and Immunoblotting

For pulse-chase analyses, infected host cells were radiolabelled with 100 mCi/ml of ^{35}S methionine and cysteine (GE Healthcare) for one hour. Cells were either harvested (pulse) or washed twice with 10 ml of parasite growth medium, and incubated in 10 ml parasite growth medium lacking radioactive amino acids for 2 (chase) before harvesting. Proteins of interest were purified by immunoprecipitation or affinity purification and separated by SDS-PAGE using standard procedures (7), and detected by autoradiography or PhosphorImaging (GE Healthcare). Immunoblotting, sodium carbonate extractions and Triton X-114 phase partitioning were performed by standard procedures. Detailed protocols are listed in *SI Material and Methods*.

Microscopy

Immunofluorescence assays and light microscope imaging were performed essentially as previously described (24). Detailed methods for electron microscopy are included in *SI Material and Methods*.

Acknowledgements

We thank Geoff Waldo, David Sibley, Manami Nishi, Marc-Jan Gubbels and Markus Meissner for plasmids, Jörn Lakowski for mouse cDNA, and Vern Carruthers, Gary Ward and Geoff McFadden for antibodies. We are grateful to Carrie Brooks, Lisa Sharling, Kylie Mullin and Geoff Waldo for technical advice and discussions, and especially to Julie Nelson of the Center for Tropical and Emerging Global Diseases Flow Cytometry Facility at the University of Georgia for performing cell sorting and flow cytometry analyses. This work was supported by a C.J. Martin Overseas Fellowship (400489) from the Australian National Health and Medical Research Council to GvD, funding from the European Network of Excellence 'Three-Dimensional Electron Microscopy', FP6 and the Dutch Cyttron consortium to CT and BMH, and a grant from the National Institutes of Health to BS (AI 64671).

References

1. Rodriguez-Ezpeleta, N.*, et al.* (2005) Monophyly of primary photosynthetic eukaryotes: green plants, red algae, and glaucophytes *Curr Biol* 15: 1325-30.
2. Mazumdar, J., Wilson, E. H., Masek, K., Hunter, C. A. & Striepen, B. (2006) Apicoplast fatty acid synthesis is essential for organelle biogenesis and parasite survival in *Toxoplasma gondii Proc Natl Acad Sci U S A* 103: 13192-7.
3. Ralph, S. A.*, et al.* (2004) Tropical infectious diseases: Metabolic maps and functions of the *Plasmodium falciparum* apicoplast *Nat Rev Microbiol* 2: 203-16.
4. Soll, J. & Schleiff, E. (2004) Protein import into chloroplasts *Nat Rev Mol Cell Biol* 5: 198-208.
5. Hempel, F.*, et al.* (2007) Transport of nuclear-encoded proteins into secondarily evolved plastids *Biol Chem* 388: 899-906.
6. Waller, R. F.*, et al.* (1998) Nuclear-encoded proteins target to the plastid in T*oxoplasma gondii* and *Plasmodium falciparum Proc Natl Acad Sci U S A* 95: 12352-12357.
7. van Dooren, G. G., Su, V., D'Ombrain, M. C. & McFadden, G. I. (2002) Processing of an apicoplast leader sequence in *Plasmodium falciparum* and the identification of a putative leader cleavage enzyme *J Biol Chem* 277: 23612-9.
8. Karnataki, A.*, et al.* (2007) Cell cycle-regulated vesicular trafficking of *Toxoplasma* APT1, a protein localized to multiple apicoplast membranes *Mol Microbiol* 63: 1653-68.
9. Cabantous, S., Terwilliger, T. C. & Waldo, G. S. (2005) Protein tagging and detection with engineered self-assembling fragments of green fluorescent protein *Nat Biotechnol* 23: 102-7.
10. Striepen, B., He, C. Y., Matrajt, M., Soldati, D. & Roos, D. S. (1998) Expression, selection, and organellar targeting of the green fluorescent protein in *Toxoplasma gondii Mol Biochem Parasitol* 92: 325-38.
11. Sommer, M. S.*, et al.* (2007) Der1-mediated preprotein import into the periplastid compartment of chromalveolates? *Mol Biol Evol* 24: 918-28.
12. Meissner, M., Schluter, D. & Soldati, D. (2002) Role of *Toxoplasma gondii* myosin A in powering parasite gliding and host cell invasion *Science* 298: 837-40.
13. Eilers, M. & Schatz, G. (1986) Binding of a specific ligand inhibits import of a purified precursor protein into mitochondria *Nature* 322: 228-32.
14. Brydges, S. D., Harper, J. M., Parussini, F., Coppens, I. & Carruthers, V. B. (2008) A transient forward targeting element for microneme regulated secretion in *Toxoplasma gondii Biol Cell* 100: 253-265.
15. Jelenska, J.*, et al.* (2001) Subcellular localization of acetyl-CoA carboxylase in the apicomplexan parasite *Toxoplasma gondii Proc Natl Acad Sci U S A* 98: 2723-2728.
16. Crawford, M. J.*, et al.* (2006) *Toxoplasma gondii* scavenges host-derived lipoic acid despite its de novo synthesis in the apicoplast *EMBO J* 25: 3214-22.
17. Chen, X., Smith, M. D., Fitzpatrick, L. & Schnell, D. J. (2002) In vivo analysis of the role of atTic20 in protein import into chloroplasts *Plant Cell* 14: 641-54.
18. Kouranov, A., Chen, X., Fuks, B. & Schnell, D. J. (1998) Tic20 and Tic22 are new components of the protein import apparatus at the chloroplast inner envelope membrane *J Cell Biol* 143: 991-1002.
19. Reumann, S., Inoue, K. & Keegstra, K. (2005) Evolution of the general protein import pathway of plastids *Mol Membr Biol* 22: 73-86.
20. Teng, Y. S.*, et al.* (2006) Tic21 is an essential translocon component for protein translocation across the chloroplast inner envelope membrane *Plant Cell* 18: 2247-57.
21. McFadden, G. I. & van Dooren, G. G. (2004) Evolution: red algal genome affirms a common origin of all plastids *Curr Biol* 14: R514-6.

22. Fast, N. M., Kissinger, J. C., Roos, D. S. & Keeling, P. J. (2001) Nuclear-encoded, plastid-targeted genes suggest a single common origin for apicomplexan and dinoflagellate plastids *Mol Biol Evol* 18: 418-26.
23. Moore, R. B*., et al.* (2008) A photosynthetic alveolate closely related to apicomplexan parasites *Nature* 451: 959-63.
24. Striepen, B. & Soldati, D. (2007) in *Toxoplasma gondii. The Model Apicomplexan - Perspectives and Methods*, eds. Weiss, L. D. & Kim, K. (Elsevier, London), pp. 391-415.

Supplemental Experimental Procedures

Gene cloning and sequence analyses

We used sequence from a Tic20 homologue from the red alga *Cyanidioschyzon merolae* (CMS050C; [1]) as a query for an iterative PSI-BLAST search [2] against a non-redundant protein sequence database (ncbi.nlm.nih.gov/blast/Blast.cgi). After two iterations using default parameters, we identified a hit to genes from *Theileria* species and used these as query sequences to identify Tic20 homologues in other Apicomplexa. We identified one predicted gene in *T. gondii* with homology to the *Theileria* genes. An EST covered the 3' end of this gene. To identify the 5' end, we performed 5' RACE using the SMART RACE cDNA amplification kit (BD Biosciences), using the initial primer 5'-TTGAGATATATCATGCTCA and the nested primer 5'-AGCATAGACAGTAGCAAA. Sequencing of the entire *Tg*Tic20 gene revealed the presence of three introns, and an open reading frame of 1170 bp. GenBank accession number for *Tg*Tic20 is EU427503. To compare *Tg*Tic20 with other known Tic20 homologues we generated a multi-sequence alignment as previously described [3]. Other sequences included in the alignment were identified from publicly available databases.

Plasmid construction, parasite transfection and parasite culture

The open reading of *Tg*Tic20 was amplified by PCR using the primers: 5'-AGATCTAAAATGGGG TTCCCTTCAGCTCTCT and 5'-CCTAGGGTACGAGTCTGAC GGCTTCTCGCCGAT.

The resultant PCR product was subcloned into pCR2.1 (Invitrogen) and verified by sequencing. The resulting vector was digested with *Bgl*II and *Avr*II and cloned into the equivalent sites of the pCTH vector (GvD and R. Opperman, unpublished) to generate pCTH(Tic20). This vector contains the Tic20 open reading frame downstream of the *T. gondii* alpha-tubulin promoter, with a 3' HA-tag fusion, and a chloramphenicol-resistance marker for selection in *T. gondii*. This was transfected into RH strain *T. gondii* parasites as previously described [4]. Stable lines expressing the tub-*Tg*Tic20-HA construct were generated by chloramphenicol selection [5]

To generate a conditional knockout of *Tg*Tic20, we first generated a parental strain that expressed inducible copies of *Tg*Tic20. To do this, we placed the *Tg*Tic20 open reading frame into the *Bgl*II and *Avr*II cut sites of pDt7s4M vector (GvD, unpublished), which contains a mutant form of DHFR that encodes resistance to pyrimethamine, an inducible teto7/sag4 promoter, and a c-myc tag at the 3' end of the gene-of-interest. We transfected the resulting construct into TATi strain *T. gondii* parasites, containing the transactivating tetracycline repressor protein to enable inducible repression of *Tg*Tic20-c-myc gene expression [6]. We then proceeded to knockout endogenous *Tg*Tic20 through double homologous recombination. We amplified approximately 2 kb downstream of the *Tg*Tic20 protein coding sequences with the primers 5'-AAGCTTACAAGTTGCAGTAGGTGTTCCA and 5'-CTCGAGAAGCAGTGTGGTCGAAAGATA and placed this into the *Hin*dIII

and *Xho*I cut sites of the vector pTCY (GvD, unpublished). pTCY is a modified version of the ptubCAT vector (a kind gift from Markus Meissner, U. Heidelberg), containing a chloramphenicol resistance marker driven by the tubulin promoter and containing multi-cloning sites flanking both sides of the expression cassette. This vector also contains a YFP marker for negative selection of successful homologous recombinants [7]. We amplified approximately 2 kb upstream of the *Tg*Tic20 protein coding sequence with the primers 5'-ACTAGTAACAGCGCTGTCTCCCCCATAA and 5'-AGATCTTTTCCTCGAGGCAGTAGTATA and ligated this into the *Spe*I and *Bgl*II cut sites of the pTCY(Tic20 3') vector. This generated the vector pTCY(Tic20 KO). We linearised this plasmid with *Not*I and transfected it into the parental strain and selected on chloramphenicol. After obtaining chloramphenicol-resistant parasites, we cloned YFP negative parasites by cell sorting as described previously [7]. We isolated 16 clones and performed diagnostic PCR and Southern blotting (see below) to identify successful targeting of the *Tg*Tic20 locus.

To complement the *Tg*Tic20 knockout, we expressed a tub-*Tg*Tic20-HA plasmid containing a phleomycin-resistance cassette in the knockout parasite line. We generated this vector by digesting the phleomycin-resistance cassette of the pBSSK+ SAG1/Ble/SAG1 (a kind gift from David Sibley, Washington U.) with *Hin*dIII and *Spe*I and ligated this into the equivalent sites of pCTH(Tic20) to generate the vector pBTH(Tic20). We transfected this into the *Tg*Tic20 knockout cell line and selected for parasites stably expressing the complemented *Tg*Tic20-HA construct by phleomycin selection as previously described [8].

To generate *Tg*Tic20 parental, mutant and complemented cell lines expressing tandem Tomato RFP parasites, we amplified tandem dimeric tomato sequence [9] using the primers 5'-AGTCCCTAGGGTGAGCAAGGGCGAGGAG and 5'-AGTCCCCGGGCTTGTACAGCTCGTCCATGC.

We digested the resulting PCR product with *Avr*II and *Xma*I and ligated it into the equivalent sites of pCTG (GvD and R. Opperman, unpublished). This generated the vector $pCTR_{2T}$, containing the tandem dimeric Tomato RFP expressed from the tubulin promoter. We transfected this construct into the various cell lines, and subjected parasites to three or four rounds of cell sorting before cloning. Cell sorting was performed using a MoFlo sorter (Dako, Ft. Collins, CO), with an Enterprise 621 laser tuned to 488 nm. We sorted cells expressing Tomato parasites using a 570/40 nm BP filter.

To generate vectors for the split GFP system [10], we amplified GFP 1-10 with the primers 5'-AGTCCCTAGGAGCAAAGGAGAAGAACTTTT and 5'-AGTCC CCGGGTTAGGTACCCTTTTCGTTGGGATCT and GFP-11 with the primers 5'-AGTCCCTAGGGGTTCCGATGGAGGGTCTGGTG and 5'-AGTCCCCGGGT TATGTAATCCCAGCAGCATT

(parent vectors were kind gifts from Geoff Waldo, Los Alamos National Research Laboratory). We digested the resultant PCR products with *Avr*II and *Xma*I and ligated these into the equivalent sites of the pCTG vector to make the vectors $pCTG_{1-10}$ and

pCTG$_{11}$. We digested the FNR leader sequence from the ptubFNR-RFP/sagCAT vector [11] and the P30 sequence from the ptubP30-GFP/sag-CAT vector [12] with *Bgl*II and *Avr*II, ligated these into equivalent sites in the pCTG$_{1-10}$ vector and transfected RH strain *T. gondii* parasites. Parasites stably expressing FNR-GFP 1-10 and P30-GFP 1-10 were obtained through chloramphenicol selection. The entire *T. gondii* ACP coding region was digested from the vector ptubACPfull-GFP/sag-CAT [13] with *Bgl*II and *Avr*II and ligated into equivalent sites of pCTG$_{11}$. The result vector was transfected into the cell line stably expressing FNR-GFP 1-10 and fluorescent parasites obtained through several rounds of cell sorting using a MoFlo flow cytometer (Dako, Ft. Collins, CO) as described above but using a 530/40 nm BP filter. P30 and the complete Tic20 open reading frame were digested from the ptubP30-GFP/sag-CAT and pCTH (Tic20) vectors with *Bgl*II and *Avr*II, and ligated into the equivalent sites of pCTG$_{11}$. The chloramphenicol-resistance cassette of pCTG$_{11}$(P30) was replaced with a DHFR cassette encoding resistance to pyrimethamine by digestion of the pKOsagDHFR vector (a kind gift from Marc-Jan Gubbels, Boston College) with *Hin*dIII and *Spe*I and ligation into the equivalent sites of pCTG$_{11}$(P30). The resultant construct was transfected into the FNR-GFP 1-10 cell line and selected on pyrimethamine as previously described [14] and cloned by limiting dilution. The chloramphenicol-resistance cassette of pCTG$_{11}$(Tic20) was replaced with a BLE cassette encoding resistance to phleomycin by digestion of the pBSSK+ SAG1/Ble/SAG1 vector with *Hin*dIII and *Spe*I and ligation into equivalent sites of pCTG$_{11}$(Tic20). The resultant pBTG$_{11}$(Tic20) vector was transfected into the parasite line expressing FNR-GFP 1-10, selected on phleomycin and cloned by limiting dilution. Fluorescence intensities were quantified by flow cytometry using a MoFlo cytometer as described above, and results were analysed and graphed used FlowJo software (Tree Star, Inc., Ashland, OR).

To generate a cell line expressing both tub-*Tg*Tic20-HA and APT1-YFP, we made a plasmid expressing APT1-YFP containing a phleomycin selectable marker. We digested pBTH(Tic20) and a tubAPT1-YFP vector (a kind gift from Manami Nishi and David Roos, U. Pennsylvania) with *Bgl*II and *Not*I, and ligated APT1-YFP into the equivalent sites of the pBT vector. We transfected this construct into the cell line expressing tub-*Tg*Tic20-HA and generated parasites stably expression APT1-YFP by phleomycin selection

To generate a construct that targeted mouse DHFR fused to a C-terminal HA-tag to the apicoplast, we digested the FNR leader sequence from the ptubFNR-RFP/sagCAT vector [11] with *Bgl*II and *Avr*II and ligated this into the equivalent sites of pCTH. We then amplified mouse DHFR from cDNA (a kind gift from Jorn Lakowski, U. Georgia) with the primers 5'-CCTAGGGGTGGAAGCATGGTTCGACCATTGAACTGC and 5'-ACTAGTGTCTTTC-TTCTCGTAGACTT. Mouse DHFR was digested with *Avr*II and *Spe*I and ligated into the *Avr*II site of pCTH(FNR). We replaced the chloramphenicol resistance cassette with a phleomycin-resistance cassette and transfected the resultant pBTH(FNR-mDHFR) vector into the *Tg*Tic20 knockout and parental lines. Stable parasites expressing this construct were obtained through phleomycin selection.

To generate *Tg*Tic20 knockout and parental cell lines expressing apicoplast-targeted RFP, we digested the ptubFNR-RFP/sagCAT vector with *Bgl*II and *Not*I and ligated this into the equivalent sites of pBTH(Tic20). We transfected the resultant pBTR(FNR) construct into the *Tg*Tic20 knockout and parental lines and obtained stable expressors through phleomycin selection. We quantified fluorescence intensities of cells expression apicoplast-targeted RFP by flow cytometry using a FACSCalibur cytometer (Becton Dickinson, San Jose, CA). Samples were excited at 488 nm using an argon laser, and detected by emission through a 585/42 BP filter. Results were analysed and graphed using FlowJo software.

Parasite growth assays

To measure parasite growth we performed plaque assays by adding 400 parasites to a T25 flask containing a confluent monolayer of human foreskin fibroblasts. We grew parasites undisturbed for 9 days, washed once with phosphate-buffered saline (PBS; 0.8% w/v NaCl, 0.02% w/v KCl, 0.14% w/v Na_2HPO_4, 0.02% KH_2PO_4, pH 7.4), fixed the monolayer with ethanol, and stained with 2% (w/v) crystal violet in a solution of 20% (v/v) ethanol and 0.8% (w/v) ammonium oxalate. Tandem tomato RFP fluorescence plate assays were performed essentially as previously described [15]. Human foreskin fibroblast cells were grown to confluency in 96-well Costar optical bottom plates (Corning Incorporated, Corning, NY). We seeded 4000 parasites per well, and measured Tomato fluorescence daily using a SpectraMax M2^e microplate reader (Molecular Devices, Sunnyvale, CA). Readings were taken from the bottom, using a 544 nm excitation and a 590 nm emission wavelength with a 570 nm cutoff. Percent positivity values were derived as previously described [15].

Western blotting and detection of membrane proteins

Protein samples (typically to a cell equivalent of 5 x 10^6 parasites) were loaded onto precast 12 % Bis-Tris and 3-8% Tris-Acetate NuPAGE gels (Invitrogen). After separation by electrophoresis, proteins were transferred to nitrocellulose membrane. Blots were probed with antibodies against ACP (1:1000 to 1:2000 dilution; a kind gift from Geoff McFadden, U. Melbourne, [13]), GRA8 (1:200 000; a kind gift from Gary Ward, U. Vermont, [16]), MIC5 (1:1000; a kind gift from Vern Carruthers, U. Michigan, [17]), lipoylated E2-subunit (1:1000; clone 3H-2H4; a kind gift from Eric Gershwin, U. California, San Diego, [18]), HA (1:100 to 1:500; clone 3F10, Roche Applied Science), c-myc (1:50 to 1:100; clone 9E10, Roche Applied Science) and GFP (1:1000; Torry Pines Biolabs). HRP-conjugated anti-rat and anti-rabbit antibodies (Pierce) were used at 1:5000 to 1:10000 dilutions, while HRP-conjugated anti-mouse antibodies (TrueBlot, eBioscience) were used at 1:1000 dilution. To detect biotinylated proteins, we blocked membranes with 1% anti-His-HRP Blocking Reagent (Qiagen) and probed with ImmunoPure horse-radish peroxidase-conjugated streptavidin (1:25 000; Pierce).

Membrane proteins were identified by alkaline (sodium carbonate) extractions and by Triton X-114 phase partitioning. For alkaline extractions [19], parasite pellets were washed once in PBS then incubated in 100 mM sodium carbonate (pH 11.5 to 12.5) for 30 minutues

on ice. Samples were centrifuged at 150 000 g at 4°C for 45 minutes. Pellets (containing integral membrane proteins) were resuspended in sample buffer, while supernatant proteins were precipitated by trichloroacetic acid before resuspension in sample buffer. Triton X-114 partitioning was performed as described previously [20, 21]. Briefly, parasite pellets were resuspended in PBS containing 1 % (v/v) Triton X-114, 2 mM EDTA and supplemented with protease inhibitors (Complete protease inhibitor cocktail, Roche). Cells were incubated on ice for 30 minutes and centrifuged to remove insoluble material. The supernatant was layered onto a sucrose cushion (6% sucrose, 0.06% Triton X-114 in PBS) and incubated at 37°C for three minutes. The sample was centrifuged for 2 minutes at room temperature, and the layer above the cushion (containing soluble phase proteins) subjected to trichloroacetic acid precipitation before resuspension in sample buffer. The detergent micelles below the sucrose cushion (containing membrane proteins) were also extracted, resuspended in cold PBS and subjected to trichloracetic acid precipitation before resuspension in sample buffer. Proteins were separated by SDS-PAGE and detected by Western blotting (see above).

Pulse-chase and immunoprecipitation

Confluent T25 flasks were infected with approximately 2 x 10^6 parasites and allowed to grow for two days. Infected host cells were starved for one hour in cysteine and methionine-free Dulbecco's Modified Eagles medium supplemented with 1% dialysed foetal bovine serum and antibiotics. Infected host cells were radiolabelled with 100 mCi/mL of ^{35}S methionine and cysteine (GE Healthcare) for one hour. Cells were either harvested (pulse) or washed twice with 10 mL of parasite growth medium, and incubated in 10 mL parasite growth medium for 2 to 8 hours (chase) before harvesting. Proteins of interest were purified by immunoprecipitation or affinity purification (see below) and separated by SDS-PAGE as described above. Gels were dried and bands were visualised by autoradiography or using a Storm 860 PhosphorImager (GE Healthcare). Band intensities were quantified using ImageQuant TL software (GE Healthcare).

For immunoprecipitations, parasites were lysed from host cells by passage through a 26 gauge needle, and pelleted by centrifugation at 1500 g for 10 minutes. Pellets were washed in PBS then lysed for 30 minutes on ice in immunoprecipitation lysis buffer (50 mM Tris-HCl, pH 8.0, 150 mM NaCl, 1 % (v/v) noniodet P-40 substitute (Fluka), 0.5 % (w/v) sodium deoxycholate, 0.1 % (w/v) sodium dodecyl sulphate, 2 mM EDTA) supplemented with protease inhibitors. Samples were centrifuged to remove insoluble material. Proteins-of-interest were purified by immunoprecipitation using either anti-HA conjugated agarose beads (Roche Applied Science), anti-c-myc-conjugated agarose beads (Santa Cruz Biotechnology) or with antibodies bound specifically to protein A-sepharose CL-4B beads (GE Healthcare). For the latter application, samples were pre-cleared by incubation in 30 to 40 mL of a 50 % slurry of Protein A-Sepharose CL-4B beads. Antibodies including anti-MIC5, anti-lipoic acid (Calbiochem) and anti-ACP were bound to protein A-sepharose CL-4B beads for one hour at 4°C before addition to pre-cleared lysates. All samples were

incubated overnight at 4°C then washed 4 times in immunoprecipitation wash buffer (50 mM Tris-HCl, pH 8.0, 150 mM NaCl, 1 % (v/v) noniodet P-40 substitute, 0.5 % (w/v) sodium deoxycholate, 0.25 % w/v bovine serum albumin, 2 mM EDTA) and twice in PBS. Samples were eluted by boiling in reducing or non-reducing sample buffer then separated by SDS-PAGE as described above. For affinity purification of biotinylated proteins, lysates were incubated overnight with immobilised streptavidin-agarose beads (Pierce). Samples were washed 4 times in Streptavidin wash buffer (50 mM Tris-HCl, pH 8.0, 150 mM NaCl, 1 % (v/v) noniodet P-40 substitute, 0.5 % (w/v) sodium deoxycholate, 0.1 % w/v sodium dodecyl sulfate, 2 mM EDTA) and twice in PBS, before elution by boiling in reducing sample buffer.

Southern blotting

Genomic DNA was extracted from parasite strains using the DNeasy kit (Qiagen). 2 mg was digested overnight with KpnI and separated by electrophoresis on a 0.8 % agarose gel. Gels were treated with 0.2 M HCl for 15 minutes, denatured in 1.5 M NaCl/0.5 M NaOH for 30 minutes and neutralised for 40 minutes in 1.5 M NaCl/1 M Tris base (pH 8.0). DNA was capillary transferred onto Nytran SuPerCarge nylon membrane (Schleicher and Schuell BioScience, Keene, NH) overnight in 20X SSPE buffer (3 M NaCl, 20 mM EDTA, 0.2 M sodium phosphate, pH 7.4), then crosslinked using a CL-1000 UV crosslinker (UVP, Upland, CA). The membrane was prehybridised for four hours at 42°C in 40 % (v/v) formamide, 1.25 X SSPE, 0.625 % (w/v) sodium docecyl sulfate, Denhardt's solution (0.02 % w/v Ficoll, 0.02 % w/v polyvinylpyrrolidone, 0.02 % w/v bovine serum albumin) and 10 % (w/v) dextran sulfate. A probe against *Tg*Tic20 was amplified from genomic DNA using the same primers as for amplifying the entire open reading frame (above). The probe was radiolabeled with ^{32}P-dATP using the Random Primers DNA Labelling System (Invitrogen) as per the manufacturer's instructions, and hybridised to the nylon membrane overnight at 42°C. The membrane was washed three times in 2X SSPE for 15 minutes at room temperature, three times in 2X SSPE containing 1 % (w/v) sodium docecyl sulfate for 15 minutes at 42°C, and rinsed a further two times in 2X SSPE. Bands were detected by exposure to autoradiography film.

Microscopy

Light microscope images were taken with a DM IRBE inverted epifluorescence microscope (Leica) fitted with a 100X oil immersion objective lens (PL APO 1.40 NA). Images were recorded using a Hamamatsu C4742-95 digital camera, and adjusted for brightness and contrast using Openlab software (Improvision). Live imaging was performed on infected coverslips in a sealed chamber at room temperature. For immunofluorescence, we fixed infected coverslips in 3 % paraformaldehyde for 15 minutes, permeabilised in 0.25 % Triton X-100 for 10 minutes, then blocked in 2 % (w/v) bovine serum albumin for 30 minutes. Samples were labelled with primary antibody for 1 hour, washed 3 times in PBS, incubated in secondary antibody for a further hour and washed 3 times in PBS. Primary

antibodies used were rabbit anti-ACP (1:1000 to 1:2000 dilution) and rat anti-HA (1:100 to 1:500). Secondary antibodies used were goat anti-rabbit Alexa Fluor 546 (1:500) and goat anti-rat Alexa Fluor 488 (1:200; Molecular Probes, Eugene, OR).

For electron microscopy, flasks containing confluent human foreskin fibroblast cells were infected with the tub*Tg*Tic20-HA strain of *T. gondii*. Cryosectioning was done according to [22-24]. Cells were fixed for 24 hours in 2 % formaldehyde and 0.2% glutaraldehyde in 0.1 M phosphate buffer, and subsequently embedded in 12% gelatin in phosphate buffer. The gelatin embedded cells were cut in cubes and infiltrated with 2.3 M sucrose for 10 to 20 hours at 4oC. Samples were mounted on a sample holder, frozen in liquid nitrogen and cryo-sectioned using cryo-ultramicrotome UCT/ FCS (Leica Microsystems, Vienna, Austria). The cryo-sections were picked up with a drop of 1% methyl cellulose and 1.5 M sucrose in PBS [25] and transferred to Formvar-carbon-coated hexagonal 200 mesh grids. The grids with ultra-thin sections were washed for 30 min at 37 oC in phosphate buffer (pH 7.4) and blocked for 15 minutes on drops of PBS containing 1% BSA and 0.05% cold water fish skin gelatin (Sigma). The grids were incubated for 60 minutes with anti-HA antibody (12CA5, Roche), rinsed in PBS containing 0.1% BSA and 0.005% cold water fish skin gelatin, and incubated for 20 minutes with a bridging rabbit anti-mouse antibody (DakoCytomation). After the second washing step, the grids were incubated for 20 minutes with protein A coupled to gold (PAG, 10 nm; Medical School, Utrecht University, the Netherlands). The label was fixed onto the cryo-sections with 1% glutaraldehyde in PBS for 5 minutes. For double labelling, the cryo-sections were subsequently blocked as described above, then incubated for 60 minutes with anti-ACP antibody, rinsed and incubated for 20 minutes with PAG 15 nm. The grids were fixed for 5 minutes in 1% glutaraldehyde in PBS and rinsed in distilled water for 10 minutes. Cryosections were poststained with 2% uranyl acetate in 0.15 M oxalic acid (pH 7.4; [23]) and embedded in 1.8% methyl cellulose containing 0.4% aqueous uranyl acetate. Grids were examined in a transmission electron microscope (Tecnai 12, FEI Company, Eindhoven, the Netherlands) at 120 kV. Images were recorded using a CCD camera (MegaView II, Soft Imaging Systems GmbH, Münster, Germany). Image processing was done with Analysis 3.2 (Soft Imaging Systems GmbH, Münster, Germany).

Supplemental Figure Legends

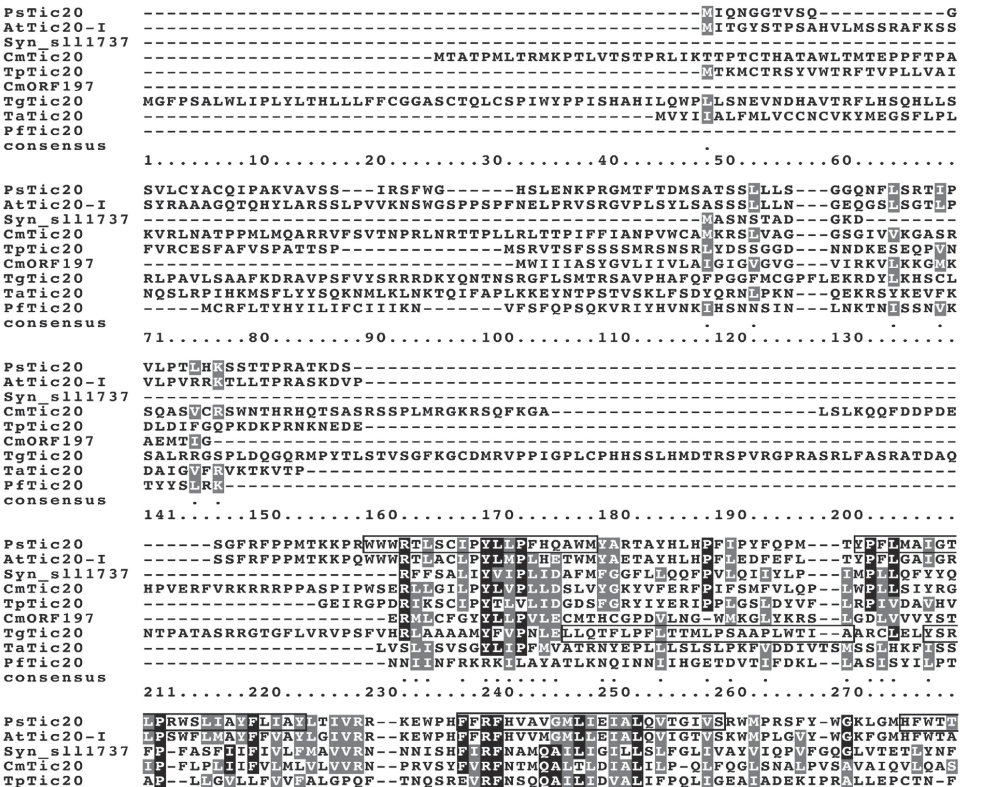

Figure S1 Multiple sequence alignment of Tic20 protein homologues.

The alignment includes Tic20 homologues from *Pisum sativum* (PsTic20; GenBank accession number AAC64607), *Arabidopsis thaliana* (AtTic20-I; NP_171986), *Synechocystis* species PCC 6803 (Syn_sll1737; NP_440747), *Cyanidioschyzon merolae* nuclear-encoded (CmTic20; genome accession number CMS050C, http://merolae.biol.s.u-tokyo.ac.jp/; [1]), *C. merolae* plastid-encoded (CmORF197; CMV078C), *Thalassiosira pseudonana* (TpTic20; gene model predicted by authors based on sequence available at genome website: http://genome.jgi-psf.org/Thaps3/Thaps3.home.html; [26]), *Toxoplasma gondii* (TgTic20; this study; EU427503), *Theileria annulata* (TaTic20; XP_951914) and *Plasmodium falciparum* (PfTic20; AAN36039). Conserved and similar residues with an identity threshold of 0.60 are shaded and marked by asterisks and dots on the consensus line. The boxed regions in the *Ps*Tic20 and *Tg*Tic20 sequences represent predicted transmembrane domains (based on TMHMM Server predictions; http://www.cbs.dtu.dk/services/TMHMM/).

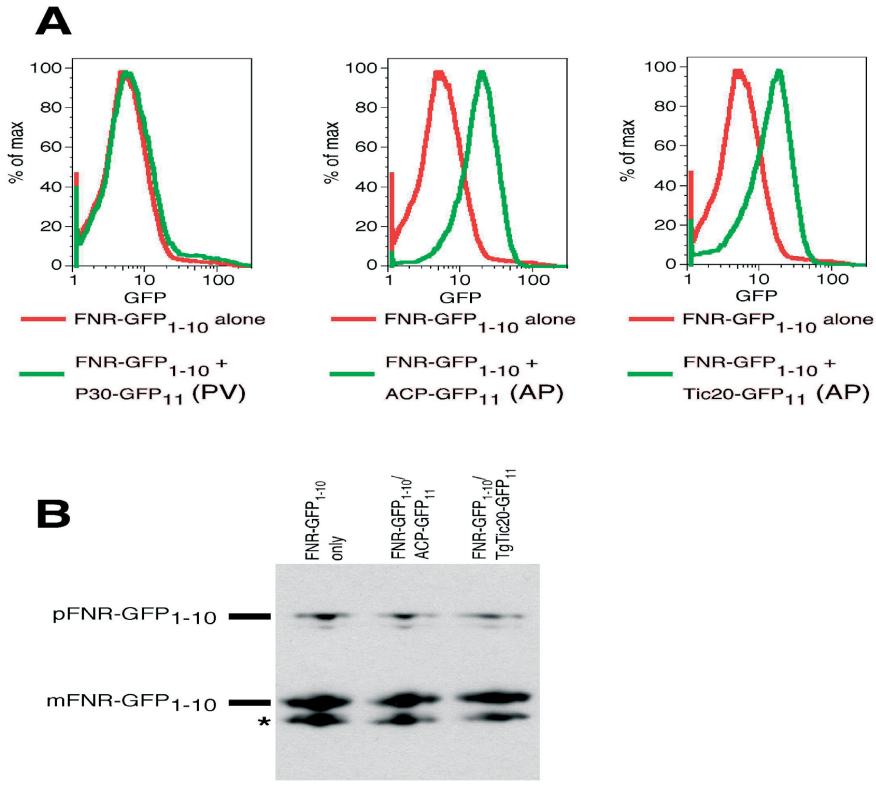

Figure S2 Quantification of split GFP experiments.

(**A**) To quantify fluorescence levels, cell lines depicted in Figure 3, in addition to a cell line expressing FNR-GFP 1-10 alone and FNR-GFP 1-10 with P30-GFP-11 were analysed by flow cytometry. When the split GFP molecules are targeted to separate compartments of the secretory pathway (left, green line), fluorescence intensity equates to that of FNR-GFP 1-10 alone (red line on all graphs). Fluorescence in lines co-expressing FNR-GFP 1-10 with either ACP-GFP-11 (centre, green line) or *Tg*Tic20-GFP-11 (right, green line) have considerably greater fluorescence intensities than FNR-GFP 1-10 alone.
(**B**) Western blot of parasite cell lines containing either FNR-GFP 1-10 alone, or co-expressed with ACP GFP-11 or *Tg*Tic20 GFP-11. The anti-GFP antibody labels GFP 1-10 alone. Each cell line contains low levels of precursor FNR-GFP 1-10, with most GFP 1-10 existing in the mature, processed form, suggesting that in each cell line, most GFP 1-10 reaches the apicoplast stroma. Asterisk labels a possible GFP 1-10 degradation product, similar to those previously observed for apicoplast-targeted GFP molecules (Waller et al., 1998).

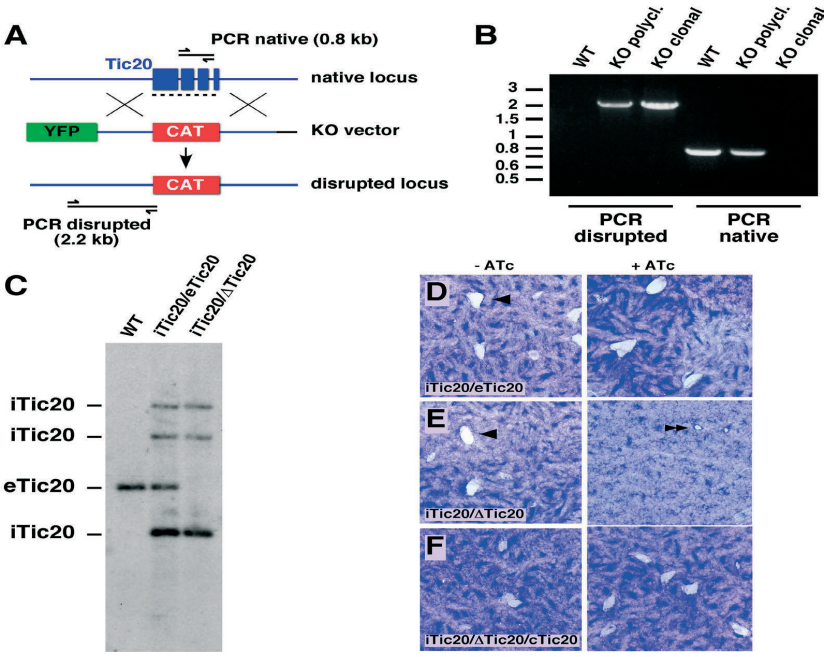

Figure S3 Genetic disruption of *Tg*Tic20.

(**A**) A schematic depicting genetic disruption of the native *Tg*Tic20 locus. We generated a knockout construct (KO vector) containing a chloramphenicol acetyl transferase (CAT) gene flanked by 2 kb sequences homologous to the 5' and 3' flanks of the native *Tg*Tic20 locus. A YFP marker for negative selection is located outside this knockout cassette. We transfected the knockout vector into a parasite cell line expressing inducible copies of *Tg*Tic20, selected for chloramphenicol-resistant parasites, and then further selected for homologous integrants through fluorescence sorting of parasites not expressing YFP.
(**B**) We performed diagnostic PCR analysis to verify disruption of the *Tg*Tic20 locus. One set of PCR primers was specific for the disrupted *Tg*Tic20 locus (PCR disrupted) and a second set was designed within introns of the *Tg*Tic20 gene and is thus specific to the native locus (PCR native).
(**C**) We performed Southern blotting on RH strain wild-type (WT), parental (iTic20/eTic20) and knockout (iTic20/DTic20) parasites using a probe against the entire *Tg*Tic20 gene. Endogenous *Tg*Tic20 (eTic20) is present in wild-type and parental strains but absent in knockout parasites.
(**D-F**) We performed plaque assays on parental parasites (iTic20/eTic20; D), knockout parasites (iTic20/DTic20; E) and knockout parasites complemented with ectopically expressed *Tg*Tic20 (iTic20/DTic20/cTic20; F) in the absence (left) or presence (right) of ATc. To do this, we added 400 parasites to a flask containing a confluent monolayer of human foreskin fibroblast cells. We grew parasites for 9 days in the absence or presence of ATc. During this period, parasites will go through several replication cycles, and form zones of clearance (plaques) in the host cell monolayer. In both the absence and presence of ATc, the parental cell line (iTic20/eTic20) formed large plaques (arrowhead). The *Tg*Tic20 conditional mutant cell line (iTic20/DTic20) formed large plaques in the absence of ATc (arrowhead), but much smaller plaques in the presence of ATc (double arrowhead), indicating a severe growth defect in the absence of *Tg*Tic20. When we complemented the *Tg*Tic20 conditional mutant line by adding back *Tg*Tic20 (iTic20/DTic20/cTic20) the formation of large plaques in the presence of ATc was restored.

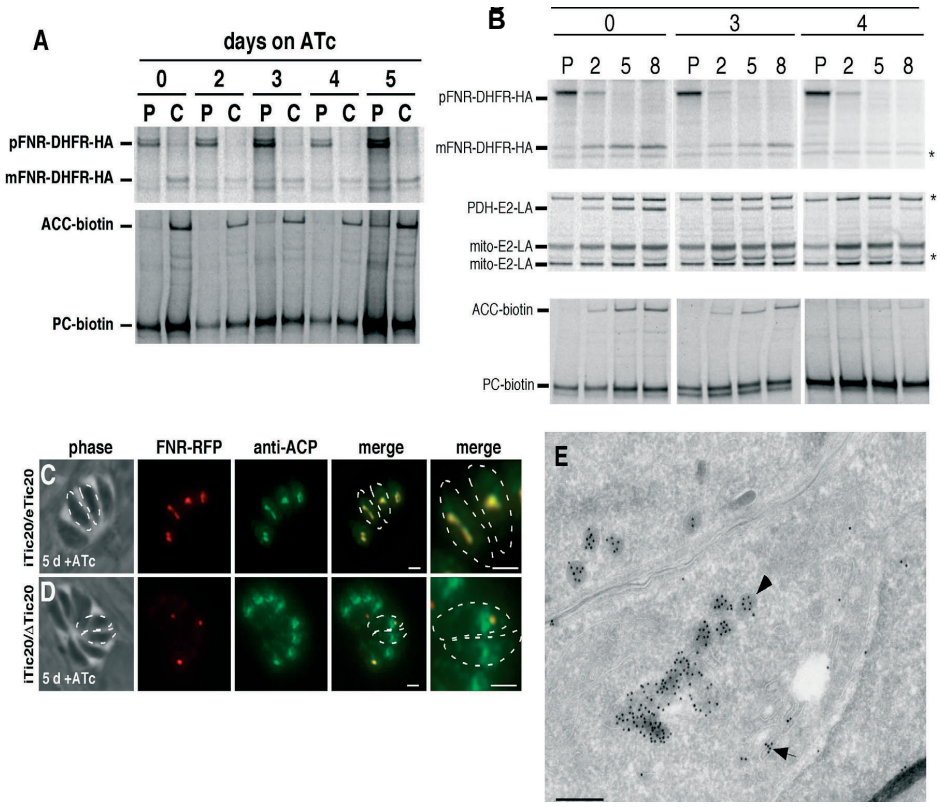

Figure S4 Knockdown of *Tg*Tic20 results in reduced efficiency of apicoplast protein import and mislocalisation of apicoplast targeted proteins.

(**A**) Pulse-chase analysis of proteins from the *Tg*Tic20 parental line grown for 0, 2, 3, 4 or 5 days on ATc, performed in an identical manner to Figure 4D.
(**B**) Pulse-chase analysis of proteins from the *Tg*Tic20 knockout line grown for 0, 3 or 4 days on ATc. Infected host cells were incubated in medium containing ^{35}S-amino acids for one hour (P) and either harvested or further incubated in non-radioactive medium for two (2), five (5) or eight (8) hours. After solubilization in detergents, proteins were purified by immunoprecipitation or affinity purification and separated by SDS-PAGE before detection by autoradiography or PhosphorImaging. Protein bands marked by an asterisk in lanes containing lipoylated proteins represent contaminating host cell proteins. The band marked by an asterisk in HA pulldown lanes possibly results from the use of an alternative internal start codon representing a shorter cytosolic version of FNR-DHFR-HA.
(**C-D**) *Tg*Tic20 parental or *Tg*Tic20 knockout parasites were grown for 5 days on ATc. Localisation of FNR-RFP and ACP was determined by immunofluorescence. In the parental strain (**C**), ACP co-localises with FNR-RFP in the presence of ATc. In the knockout cell line (**D**), however, ACP localises to tubule-or vesicle-like structures in cells lacking an apicoplast (as determined by FNR-RFP labelling). Scale bar 2 mm. (**E**) A transmission electron micrograph depicting *Tg*Tic20 knockout parasites expressing FNR-DHFR-HA grown for 5 days on ATc. FNR-DHFR-HA was labelled with 10 nm gold particles. Labelling is observed in the endoplasmic reticulum (arrow) as well as in electron dense vesicles or tubules (arrowhead). Scale bar 100 nm.

Supplemental References

1. Matsuzaki, M., Misumi, O., Shin, I.T., Maruyama, S., Takahara, M., Miyagishima, S.Y., Mori, T., Nishida, K., Yagisawa, F., Yoshida, Y., Nishimura, Y., Nakao, S., Kobayashi, T., Momoyama, Y., Higashiyama, T., Minoda, A., Sano, M., Nomoto, H., Oishi, K., Hayashi, H., Ohta, F., Nishizaka, S., Haga, S., Miura, S., Morishita, T., Kabeya, Y., Terasawa, K., Suzuki, Y., Ishii, Y., Asakawa, S., Takano, H., Ohta, N., Kuroiwa, H., Tanaka, K., Shimizu, N., Sugano, S., Sato, N., Nozaki, H., Ogasawara, N., Kohara, Y., and Kuroiwa, T. (2004). Genome sequence of the ultrasmall unicellular red alga *Cyanidioschyzon merolae* 10D. Nature *428*, 653-657.
2. Altschul, S.F., Madden, T.L., Schaffer, A.A., Zhang, J., Zhang, Z., Miller, W., and Lipman, D.J. (1997). Gapped BLAST and PSI-BLAST: a new generation of protein database search programs. Nucleic Acids Res *25*, 3389-3402.
3. Gubbels, M.J., Vaishnava, S., Boot, N., Dubremetz, J.F., and Striepen, B. (2006). A MORN-repeat protein is a dynamic component of the *Toxoplasma gondii* cell division apparatus. J Cell Sci *119*, 2236-2245.
4. Striepen, B., and Soldati, D. (2007). Genetic manipulation of *Toxoplasma gondii*. In *Toxoplasma gondii.* The Model Apicomplexan - Perspectives and Methods, L.D. Weiss and K. Kim, eds. (London: Elsevier), pp. 391-415.
5. Kim, K., Soldati, D., and Boothroyd, J.C. (1993). Gene replacement in *Toxoplasma gondii* with chloramphenicol acetyltransferase as selectable marker. Science *262*, 911-914.
6. Meissner, M., Schluter, D., and Soldati, D. (2002). Role of *Toxoplasma gondii* myosin A in powering parasite gliding and host cell invasion. Science *298*, 837-840.
7. Mazumdar, J., E, H.W., Masek, K., C, A.H., and Striepen, B. (2006). Apicoplast fatty acid synthesis is essential for organelle biogenesis and parasite survival in *Toxoplasma gondii*. Proc Natl Acad Sci U S A *103*, 13192-13197.
8. Messina, M., Niesman, I., Mercier, C., and Sibley, L.D. (1995). Stable DNA transformation of *Toxoplasma gondii* using phleomycin selection. Gene *165*, 213-217.
9. Shaner, N.C., Campbell, R.E., Steinbach, P.A., Giepmans, B.N., Palmer, A.E., and Tsien, R.Y. (2004). Improved monomeric red, orange and yellow fluorescent proteins derived from *Discosoma* sp. red fluorescent protein. Nat Biotechnol *22*, 1567-1572.
10. Cabantous, S., Terwilliger, T.C., and Waldo, G.S. (2005). Protein tagging and detection with engineered self-assembling fragments of green fluorescent protein. Nat Biotechnol *23*, 102-107.
11. Striepen, B., Crawford, M.J., Shaw, M.K., Tilney, L.G., Seeber, F., and Roos, D.S. (2000). The plastid of *Toxoplasma gondii* is divided by association with the centrosomes. J Cell Biol *151*, 1423-1434.
12. Striepen, B., He, C.Y., Matrajt, M., Soldati, D., and Roos, D.S. (1998). Expression, selection, and organellar targeting of the green fluorescent protein in *Toxoplasma gondii*. Mol Biochem Parasitol *92*, 325-338.
13. Waller, R.F., Keeling, P.J., Donald, R.G.K., Striepen, B., Handman, E., Lang-Unnasch, N., Cowman, A.F., Besra, G.S., Roos, D.S., and McFadden, G.I. (1998). Nuclear-encoded proteins target to the plastid in *Toxoplasma gondii* and *Plasmodium falciparum*. Proc Natl Acad Sci U S A *95*, 12352-12357.
14. Donald, R.G., and Roos, D.S. (1993). Stable molecular transformation of *Toxoplasma gondii*: a selectable dihydrofolate reductase-thymidylate synthase marker based on drug-resistance mutations in malaria. Proc Natl Acad Sci U S A *90*, 11703-11707.
15. Gubbels, M.J., Li, C., and Striepen, B. (2003). High-throughput growth assay for *Toxoplasma gondii* using yellow fluorescent protein. Antimicrob Agents Chemother *47*, 309-316.
16. Carey, K.L., Donahue, C.G., and Ward, G.E. (2000). Identification and molecular characterization of GRA8, a novel, proline-rich, dense granule protein of *Toxoplasma*

gondii. Mol Biochem Parasitol *105*, 25-37.
17. Brydges, S.D., Sherman, G.D., Nockemann, S., Loyens, A., Daubener, W., Dubremetz, J.F., and Carruthers, V.B. (2000). Molecular characterization of TgMIC5, a proteolytically processed antigen secreted from the micronemes of *Toxoplasma gondii*. Mol Biochem Parasitol *111*, 51-66.
18. Migliaccio, C., Nishio, A., Van de Water, J., Ansari, A.A., Leung, P.S., Nakanuma, Y., Coppel, R.L., and Gershwin, M.E. (1998). Monoclonal antibodies to mitochondrial E2 components define autoepitopes in primary biliary cirrhosis. J Immunol *161*, 5157-5163.
19. Fujiki, Y., Hubbard, A.L., Fowler, S., and Lazarow, P.B. (1982). Isolation of intracellular membranes by means of sodium carbonate treatment: application to endoplasmic reticulum. J Cell Biol *93*, 97-102.
20. Bordier, C. (1981). Phase separation of integral membrane proteins in Triton X-114 solution. J Biol Chem *256*, 1604-1607.
21. Mullin, K.A., Lim, L., Ralph, S.A., Spurck, T.P., Handman, E., and McFadden, G.I. (2006). Membrane transporters in the relict plastid of malaria parasites. Proc Natl Acad Sci U S A *103*, 9572-9577.
22. Tokuyasu, K.T. (1973). A technique for ultracryotomy of cell suspensions and tissues. J Cell Biol *57*, 551-565.
23. Tokuyasu, K.T. (1978). A study of positive staining of ultrathin frozen sections. J Ultrastruct Res *63*, 287-307.
24. Tokuyasu, K.T. (1980). Immunochemistry on ultrathin frozen sections. Histochem J *12*, 381-403.
25. Liou, W., Geuze, H.J., and Slot, J.W. (1996). Improving structural integrity of cryosections for immunogold labeling. Histochem Cell Biol *106*, 41-58.
26. Armbrust, E.V., Berges, J.A., Bowler, C., Green, B.R., Martinez, D., Putnam, N.H., Zhou, S., Allen, A.E., Apt, K.E., Bechner, M., Brzezinski, M.A., Chaal, B.K., Chiovitti, A., Davis, A.K., Demarest, M.S., Detter, J.C., Glavina, T., Goodstein, D., Hadi, M.Z., Hellsten, U., Hildebrand, M., Jenkins, B.D., Jurka, J., Kapitonov, V.V., Kroger, N., Lau, W.W., Lane, T.W., Larimer, F.W., Lippmeier, J.C., Lucas, S., Medina, M., Montsant, A., Obornik, M., Parker, M.S., Palenik, B., Pazour, G.J., Richardson, P.M., Rynearson, T.A., Saito, M.A., Schwartz, D.C., Thamatrakoln, K., Valentin, K., Vardi, A., Wilkerson, F.P., and Rokhsar, D.S. (2004). The genome of the diatom *Thalassiosira pseudonana*: ecology, evolution, and metabolism. Science *306*, 79-86.

Chapter 5

Vesicular trafficking of proteins to the apicoplast of *Toxoplasma gondii*

The first step for stromal proteins to cross multiple bilayers.

C. Tomova[1], G. G. van Dooren[2], B. Striepen[2,3], E. G. van Donselaar[1], W. H. Müller[1], B. M. Humbel[1] and A. J. Verkleij[1]

[1] Electron Microscopy and Structural Analysis, Department of Biology, Faculty of Sciences, Utrecht University, The Netherlands
[2] Centre for Tropical and Emerging Global Diseases and [3] Department of Cellular Biology, University of Georgia, Athens, USA

Manuscript in preparation

Vesicular trafficking of proteins to the apicoplast of *Toxoplasma gondii*

The first step for stromal proteins to cross multiple bilayers.

C. Tomova, G. G. van Dooren, B. Striepen, E. G. van Donselaar,
W. H. Müller, B. M. Humbel and A. J. Verkleij

Abstract

The apicoplast is a relict plastid found in many apicomplexans, including the pathogens *Toxoplasma gondii* and *Plasmodium falciparum*. The apicoplast biochemicals pathways are absent from the human host and represent novel therapeutic targets. The apicoplast is a plastid of secondary endosymbiotic origin. It is surrounded by four membranes. Most apicoplast proteins are nuclear encoded and post-translationally targeted into the organelle courtesy of a bipartite N-terminal extension consisting of a typical endomembrane signal peptide and a plant-like transit peptide.

We explored the possible mechanisms for translocation of the nuclear encoded apicoplast proteins across the four membranes. We provide strong evidence that vesicle targeting is required to convey proteins to the apicoplast and that fusion of cargo vesicles with the outermost membrane is the first step of protein translocation into the apicoplast. We further characterize the recent insights in the role of *Tg*Tic20 for protein import through the inner membrane of the apicoplast. We demonstrate not only its importance in mediating protein transport but also identify the potential this protein has as a target for therapeutics by regulation of the trafficking events it mediates.

Introduction

Every eukaryotic cell consists of membrane-enclosed compartments with a specialized function, the most remarkable of which are plastids. These organelles are bound by two or more membranes, which is a remnant of their endosymbiotic origin.

During the process of symbiont integration a major per cent of genetic material was transferred to the host cell nucleus (Martin and Herrmann, 1998). As a consequence, a complex mechanism has evolved to enable the transport of already nuclear encoded products back to the organelle. How this mechanism of protein targeting and translocation across membranes functions is a fundamental question in cell biology. Understanding this mechanism is the key to regulation of the fragile balance between life and death in each cell.

The question of how plastid-targeted proteins are distinguished from other proteins and how they are transported through multiple membrane bilayers is still an entangled issue, especially for complex (secondary) plastids. These plastids are surrounded by either three or four membranes, acquired through a secondary endosymbiosis (McFadden and Gilson, 1995; Palmer and Delwiche, 1996). These plastids have different strategies to import proteins across their multiple membranes, but they all have similar bipartite targeting sequences. The first component of this sequence directs protein entry into the endoplasmic reticulum, while the second component directs subsequent trafficking to the plastid (Hempel et al., 2007; Nassoury and Morse, 2005).

The plastid of apicomplexan parasites (the apicoplast) is of secondary endosymbiotic origin and is often referred to as a relict plastid because it contains no photosynthetic apparatus. The inner two membranes are presumably derived from the chloroplast inner and outer membranes (McFadden, 1999a), the third from the endosymbiont plasma membrane, and the outer membrane from the phagocytic vacuole of the ancestral apicomplexan. The 35 kb apicoplast genome is the smallest plastid genome (encoding only 30 proteins) described so far (Köhler et al., 1997). Thus, most apicoplast proteins are encoded in the nucleus. A few unclear encoded plastid proteins of *T. gondii* have been identified and they contain an N-terminal extension with bipartite targeting peptide (Waller et al., 1998).

In apicomplexans, trafficking of luminal proteins occurs via the secretory pathway, and appears to bypass the Golgi (DeRocher, 2005; Tonkin et al., 2006b). The targeting of soluble proteins from the ER to the apicoplast is mediated by the transit region (DeRocher et al., 2000; Waller et al., 2000; Yung et al., 2001). In both *Plasmodium falciparum* (Foth et al., 2003) and *Toxoplasma gondii* (Tonkin et al., 2006a), the positive charges near the N-terminus of the transit peptide are essential for directing the proteins accurately. Still, apicoplast stromal-proteins have to cross four membranes. Although there are various models (e.g. (van Dooren et al., 2001; Foth and McFadden, 2003; Parsons et al., 2007; Tonkin et al., 2008) the question how proteins tackle this challenge remains unanswered.

In this study, we combine the molecular approach and 3D Electron Microscopy to bring

the understanding of protein transport to the apicoplast a step forward. We present data that strongly implies vesicular trafficking as the way how proteins encoded by the nucleus and synthesized externally of the plastid are routed back to their functional site. We analyzed the distribution of stroma-targeted proteins in the conditional *Tg*Tic20KO FNR-DHFR mutant line, which further supported the vesicular hypothesis and confirmed the significant role of the *Tg*Tic20 for the biogonesis of the apicoplast. We propose a model, which represents most accurately the present knowledge of protein transport to the apicoplast.

Materials and Methods

Parasites, *T. gondii* NTE strain (Gross et al., 1991) and the conditional *Tg*Tic20 knockout line expressing iTic20-myc and FNR-DHFR-HA (van Dooren et al., 2008), were propagated in Vero cells (Green Monkey kidney epithelial cells) in 25-cm^2 plastic culture flasks. Vero cells were first grown to confluency in Dulbecco's Modified Eagles Medium (DMEM) supplemented with 10% fetal calf serum, followed by infection with *T. gondii* in DMEM (Roos et al., 1994), with high inoculum to ensure high infection rate. To induce the knock-out anhydrous tetracycline (ATc) was added to the growth medium in a final concentration of 0.5 µg/ml and parasites were cultured for another 3 and respectively 5 days before being cryofixed.

The infected host cells (at least 80% of infection) were trypsinized for 2 minutes, then resuspended in DMEM 10% and centrifuged for 10 minutes at 1500 g prior to cryofixation.

The samples were cryofixed by high-pressure freezing (Leica EM HPF; Leica Microsystems, Vienna, Austria; now M. Wohlwend, Sennwald, Switzerland) and freeze-substituted. The samples presented in this study were processed in two alternative ways. The first was in freeze-substitution medium consisting of anhydrous acetone and 2% osmium tetroxide. The samples were kept at -90°C for 46 hours; at -60°C for 8 hours and at -30°C for 8 hours (Müller et al., 1980) in a freeze-substitution unit (AFS, Leica Microsystems Vienna, Austria) and finally rinsed (2 x 30 minutes) in acetone on ice. After rinsing, the samples were infiltrated with gradually increasing concentrations of Epon (Fluka, Steinheim, Germany) : acetone (1:2, 1:1, 2:1 and finally pure Epon). Each infiltration step lasted for at least half a day. The final polymerization was performed at 60°C. The alternative way was in freeze-substitution medium consisting of anhydrous acetone and 0.1% uranyl acetate. The samples were kept at -90°C for 42 to46 hours; at -60°C for 8 hours and warmed to -40°C. At this temperature, the samples were rinsed in acetone and infiltrated with gradually increasing concentrations of Lowicryl HM20 (EMS, Hatfield, USA) : acetone (1:3, 1:1, 3:1, and finally 3 times pure HM20 resin,). The duration of each step was one hour. The infiltration was performed at -40°C, followed by 48 hours polymerization under UV light at the same temperature and subsequent curing at room temperature UV-light for approximately 10 hours.

Sections (60 and 200-nm thick) were collected on Formvar-coated, carbon-stabilized one-slot and hexagonal 100 or 50 mesh copper grids. The osmium-substituted and Epon-embedded samples were post-stained for 4 minutes with 20% (w/v) uranyl acetate in 70% (v/v) methanol/water followed by 2 minutes Reynolds's lead citrate staining (Reynolds, 1963). The uranyl-substituted and HM20-embedded samples were examined directly without any additional contrasting.

Immunolabelling

The cells prepared for cryosectioning were fixed for 24 hours in 2 % formaldehyde and 0.2% glutaraldehyde in 0.1 M phosphate buffer, and further processed according to Tokuyasu (Tokuyasu, 1973; Tokuyasu, 1980). Samples were cryo-sectioned using a cryo-ultramicrotome UCT/FCS (Leica Microsystems, Vienna, Austria) and picked up as previously described (Liou et al., 1996). The labelling was performed according to (Slot and Geuze, 2007). The grids with ultra-thin and thick sections were blocked for 10 minutes with BSA-C 0.1%. The incubation time with the primary antibodies anti-HA (12CA5, Roche); anti-myc (10E9, Roche) and anti-ACP (McFadden) was 60 minutes. Incubation time with secondary antibody rabbit anti-mouse antibody (Dako Cytomation) and with protein A coupled to gold (PAG, 5, 10 and 15 nm; Medical School, Utrecht University, the Netherlands) was 20 minutes.

The labelling of the HPF-FS, HM20 embedded samples was performed almost identically as described for the cryo-sections. In this case instead of PBS buffer we used PHEM buffer pH 7.4 (modified (Schliwa and van Blerkom, 1981)). After the last step of 1% glutaraldehyde fixation sections were examined directly without any additional contrasting.

Grids were examined in a transmission electron microscope (Tecnai 12, FEI Company, Eindhoven, the Netherlands) at 120 kV. Images were recorded using a CCD camera (MegaView II, Olympus Soft Imaging Solutions GmbH, Münster, Germany). Image processing was done with Analysis 3.2 (Olympus Soft Imaging Solutions GmbH, Münster, Germany).

Electron tomography data acquisition

Fiducials of 5 or 10 nm protein A colloidal gold (PAG) (Medical School, Utrecht University, The Netherlands) were applied on top of the sections prior to image acquisition. In the case of HPF-FS and HM20 embedded samples we did not apply fiducial markers. The PAG (5 or/and 10 nm) indicating the specific localization of the two stromal proteins, was used also as referent points for the alignment of the tilt series.

The specimens were placed in a high-tilt specimen holder (Fischione type 2020 or Fischione rotation holder type 2040, Fischione Instruments, Pittsburgh, USA) and data sets were recorded at 200 kV (Tecnai 20 LaB_6, FEI Company, Eindhoven, The Netherlands), with an increment of 1 degree and angular tilt range from -60 to +60 for both single and dual axis tomography (Penczek et al., 1995). Images (1024x1024 square pixels) were recorded using a CCD camera (Temcam F214, TVIPS GmbH, Gauting, Germany). The sections were pre-irradiated to avoid shrinking effects during recording. Automated data

acquisition of the tilt series was carried out using Xplore 3D (FEI Company, Eindhoven, The Netherlands). Tomograms were computed for each tilt axis using the R-weighted back-projection algorithm and combined into one double tilt tomogram with the IMOD software package (Kremer et al., 1996).

Modelling and analysis of tomographic data

Double and single tilt tomograms were analyzed and modelled using the IMOD software package (Kremer et al., 1996). Features of interest were contoured manually in serial optical slices extracted from the tomogram.

Results

The aim of this work was to trace the import of the nuclear-encoded proteins acyl carrier protein (ACP) and ferrodoxin NADP reductase (FNR-DHFR) to the stroma of the apicoplast of *T. gondii*. The apicoplast is surrounded by four distinct membranes, and by following the transport of these stromal-targeted proteins we investigated the mechanisms of protein translocation through multiple biological barriers.

We performed immunocytochemical studies on high pressure frozen (HPF) samples to obtain the most reliable information regarding the exact distribution of the apicoplast stromal-targeted proteins within the parasite cell and the plastid sub-compartments. We examined the localization of the two stromal proteins in *Tg*Tic20-myc FNR-DHFR knockout mutant line and in the *T. gondii* NTE strain.

The immunocytochemical studies revealed co-localization of the two stromal-targeted proteins (ACP and FNR-DHFR) in the nuclear envelope, cytosolic vesicles and the apicoplast. We detected these proteins in vesicles closely positioned to the apicoplast and in the protrusions of the exoplastid compartment (Fig.1A, *arrows*). Both proteins (ACP and FNR) have been localized in three compartments of the plastid: the exoplastid space (Fig.1 A *arrows*), the periplastid spaces (Fig.2 C, D, E, F *arrows*) and the stroma. The localization of the two proteins in the exoplastid space is mainly concentrated in specific protrusions that this compartment forms. Although these protrusions have variable size in the most profound cases they reach 40 to 50 nm, very similar to the size of the cargo-vesicles in the vicinity of the apicoplast (50-60 nm). To avoid any misleading interpretation of the observations the labelling for ACP in the parasite *T. gondii* strain NTE was used as a control for specificity and quantification of the ACP detection in the knockout line TgTic20-myc FNR-DHFR-HA. The labelling in both cases was identical (e.g. Fig.1 B and Fig.2 D). This fact, and the previously mentioned co-localization of the two stroma-targeted proteins, is a confirmation that the localization results for the FNR-DHFR are a reliable indication for the distribution of this protein within the parasite cell and the apicoplast compartments.

To validate the results and to obtain information regarding membrane continuities in their three dimensions, as well as the precise distribution of proteins in the examined volume, we performed electron tomography.

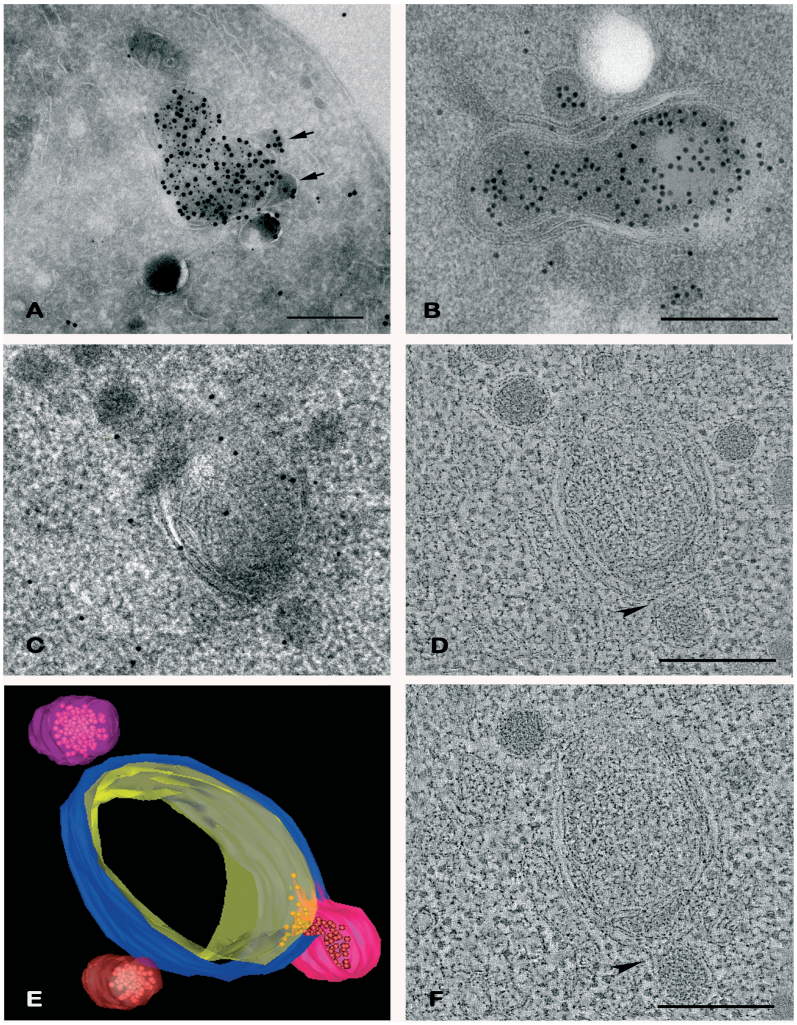

Figure 1 A) Chemically fixed and further processed for cryo-sectioning parasites from the *Tg*Tic 20 KO line cultured under normal conditions. Sections were labelled for ACP (PAG 5 nm) and FNR (PAG 15 nm). These two proteins co-localize not only in the stroma of the plastid but also in vesicles, and in the protrusions of the EPC (*arrows*). **B)** Micrograph of 60 nm thick sections. Parasites (wild type) HPF, FS in acetone with 0.1% uranyl acetate and embedded in HM20. The apicoplast and the vesicle adjacent to the OMM are labelled for ACP (PAG 10 nm). **C)** Image extracted from the raw-tilt stuck acquired of 200 nm thick section of a HPF and FS with 0.1% uranyl acetate and embedded in HM20 sample. The gold particles (10 nm) used as fiducials are specific labelling for ACP, localized in the plastid and the closely situated vesicular structures. **D)** and **F)** Optical slices from a tomographic reconstruction of an apicoplast. The OMM and a closely situated vesicle shown as separate structures (**D** arrows) at some point, further in the reconstructed volume, fuse with each other and become one continuous structure (**F** arrow). **E)** View of a model generated by the tomographic reconstructions of the same apicoplast. The OM membrane of the plastid is presented in dark blue and the PPM in yellow. The PPM is made transparent to enable better visualization of probable the fusion point between the OMM with one of the vesicles (violet).

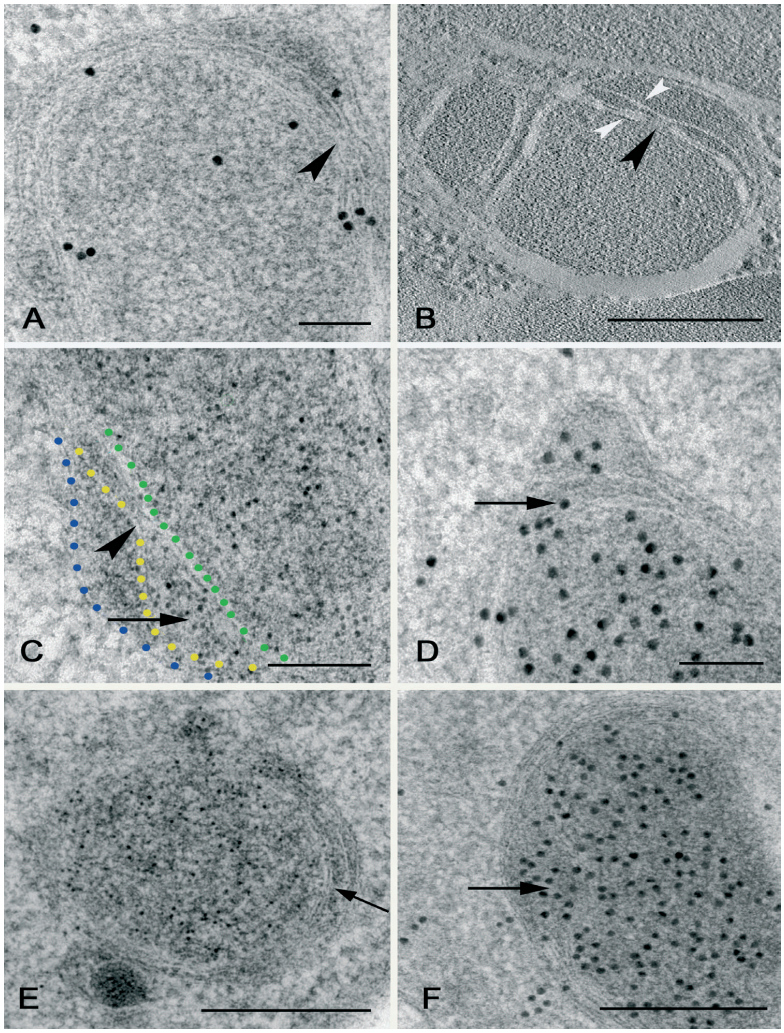

Figure 2 Micrographs of 60 nm thick sections.

All samples with the exception of the plastid on panel **B** are HPF and FS with 0.1% uranyl acetate and embedded in HM20. The sections are not post-stained. **A)** Apicoplast from the TgTic20 KO line labelled with anti-myc 9E10 antibody, depicting the localization of the Tic20. **B)** Optical slice from a reconstruction of an apicoplast HPF, FS with 2% osmium tetroxide and Epon embedded. The four membranes; patches spanning the inner membranes and those on the periplastid membrane (*arrowheads white*) are visible. In panels **C)** and **E)** the labelling represents the distribution of FNR in the plastid (PAG 5 nm) and in **D)** and **F)** depicts the localization of ACP (PAG 10 nm). The apicoplasts in panel **C**, **E** and **F** are from the TgTic20 KO mutant line grown under permissive conditions and in **D** from *T. gondii* NTE.
The *arrows* show the accumulation of these stromal proteins also in the PPC.
The locations where the PPM and the second inner membrane come into close contact are indicated (*arrowhead black*).
For clarity in panel **C** the innermost membrane, the PPM and the outermost membrane are indicated with colours green, yellow and blue, respectively.
Scale bars in **A)**, **C)** and **D)** are 50 nm and in **B)**, **E)** and **F)** are 200 nm

In the reconstructed tomograms, the vesicles closely situated to the outermost apicoplast membrane and the protrusions of this membrane were specifically labelled for the two stroma-targeted proteins. In some of these tomograms, the specific shape and dimensions of the observed protrusions are indications of the moment shortly after the cargo vesicle had fused with the outermost membrane (Fig.1D and F *arrowheads*). These results attest vesicular trafficking for these two nuclear-encoded proteins and strongly support the hypothesis of vesicular protein transport to the apicoplast. This observation affiliates with the finding that the apicoplast outermost membrane (OMM) in *T. gondii* is a distinct, continues membrane, not in direct connection with the ER of the parasite (Tomova, 2008, unpublished data).

To further confirm our observations and the vesicular trafficking pathway we investigated where stromal-targeted proteins accumulate when protein import is impaired. Recently, it was demonstrated that, in the conditional *Tg*Tic20 knockout mutant, ablation of *Tg*Tic20 (the *T. gondii* homologue of the plant chloroplast import protein Tic20) results in an impairment of apicoplast proteins (van Dooren et al., 2008). We were interested in observing the fate of apicoplast-targeted proteins in the mutant at ultra-structural level. We identified the precise protein localization in each apicoplast compartment, and followed the morphological changes imposed by the ablation of the hypothetical channel-forming import protein *Tg*Tic20.

The distribution of the two stromal-targeted proteins in the conditional *Tg*Tic20-KO mutant parasites, grown under permissive conditions, appears to be in the stroma of the plastid, but also in vesicles and in the protrusions of the EPC, as described above. However, when these parasites are grown in the presence of anhydrotetracycline (ATc) to turn off *Tg*Tic20 function, there is a significant change in the localization pattern, accompanied with changes in the morphology of the plastid itself. In the parasites harvested after three days growth in ATc the apicoplast is recognizable, with four membranes still present, but showing extensive protuberances of the exoplastid space (Fig. 3A, *arrowhead*). This is accompanied by increased labelling of the two proteins in the nuclear envelope and in cytosolic vesicles. After five days growth in ATc, the apicoplast is hardly recognizable, if present at all. In 80 per cent of the parasites (appr. in 12 of every 15 parasites) at this stage no apicoplast could be observed and the stroma-targeted proteins are localised in different-sized vesicles, the nuclear envelope, and in different cytosolic sub-compartments (Fig.3 D). The apicoplast morphology has changed dramatically. It is possible to distinguish only two or three membranes without the certainty that they are separate continuous structures. The general appearance of the presumed plastid is a lobed structure (Fig.3 B, C). This finding clearly shows that disruption of the *Tg*Tic20 results in defects in apicoplast biogenesis. It is not clear from our data whether disruption of *Tg*Tic20 directly impairs the import to the stroma or whether defects in protein targeting are a consequence of the gradual desintegration and final loss of the apicoplast. Our results demonstrate that *Tg*Tic20 is is indispensible for the apicoplast function and biogenesis.

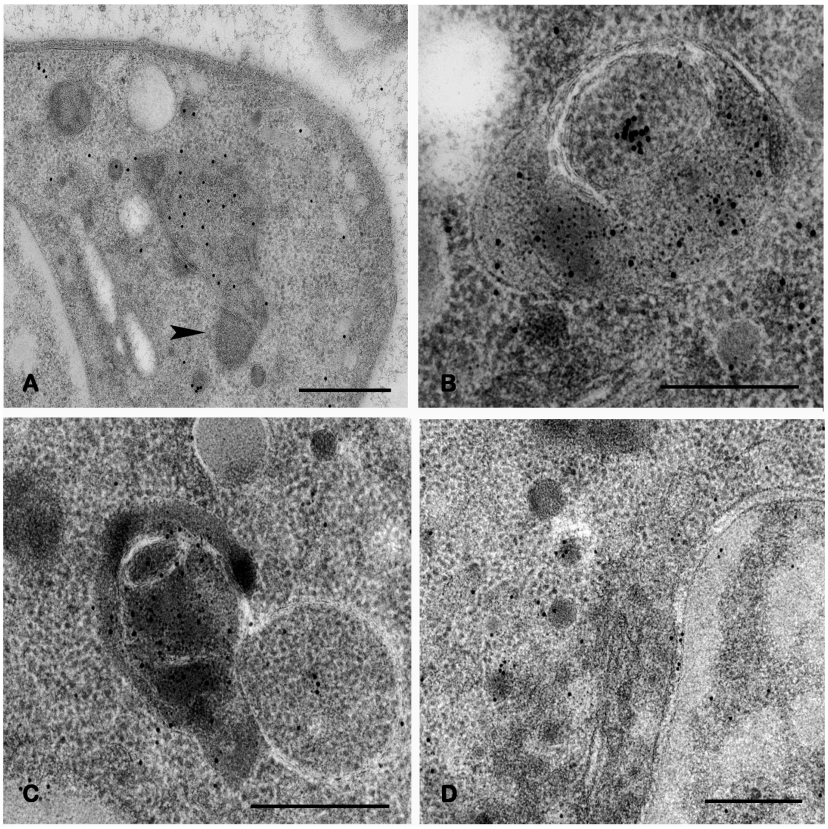

Figure 3 Micrographs of 60 nm thick sections.

All samples are HPF and FS with 0.1% uranyl acetate and embedded in HM20. **A)** Parasites of the TgTic20 KO line cultured with ATc supplement for three days. Sections are labelled for ACP (PAG 10 nm). The apicoplast is still surrounded by four membranes but exhibiting profound protuberances of the EPC (arrowhead). The sections are not post-stained. **B), C)** and **D)** Parasites of the TgTic20 KO line cultured with ATc supplement for five days. Sections are labelled for ACP (PAG 5 nm) and FNR (PAG 10 nm). The apicoplasts have lobe-subdivision morphology and surrounded by only two or three membranes. The two stromal proteins are localized in all of the compartments of the presumable plastid but mainly in cytosolic vesicles and the nuclear envelope. The sections are post-stained with 2% aqueous uranyl acetate and lead citrate. Scale bars are 200 nm.

In this study, for the first time, we document local contiguous alignment of the three inner membranes: the periplastid membrane (PPM) and the two membranes of the plastid envelope in some constrained points (Fig 4). We observed these points of tight membranous apposition in HPF material, substituted with 0.1% uranyl acetate in anhydrous acetone only, for that reason they can not be alterations introduced by changes in osmolarity, dehydration or any other artefacts imposed by chemical fixation.Therefore, this observation is of particular interest, since it might have a significant impact on our knowledge of protein trafficking in complex organelles.

At these restricted areas the periplastid membrane and the second innermost membrane of the plastid are so close, that the hydrophobic phases of the adjacent layers of the two adherent membranes seem to be continuous on leaflet contact sites (Fig.2 and Fig. 4 A, C *arrowheads*). This indicates that the distance between these leaflets is restricted to less than 2 nm. However, the resolution limitation does not allow us to define the exact relation between these leaflets at the molecular level. Despite these limitations, we can assume with certainty, that these membranes remain two distinct structures at these contact points because the distance between the outer hydrophobic phases of the adjacent bilayers equals the sum of the two membranes when measured as separate structures (appr. 8-9 nm). Comparable contact sites are described between the outer and inner envelope membranes in chloroplasts (Cremers et al., 1988).

These tight contact points between the PPM and the second innermost membrane are randomly distributed within the plastid, with no particular number per plastid (from no contact point up to six being present in an apicoplast section).

Discussion

Protein import into plastids consists of two aspects: the targeting and the translocation. Although being interconnected, these two steps require different mechanisms. The targeting step includes the components and processes responsible for the specific routing of the precursor proteins to the plastid. The translocation concerns the general question of how the protein crosses the lipid bilayers.

In this study we focused on the possible mechanisms of protein trafficking and translocation through four subsequent membranes, with different evolutionary origin and thus different morphology.

In the case of complex plastids, the majority of proteins required for their function are being encoded in the nucleus of the cell and post-translationally translocated into the plastid (Keegstra and Celine, 1999; van Dooren et al., 2001; Waller et al., 2000). The majority of the known secondary-plastid proteins have a signal sequence, suggesting that the first import step is via the ER (Cavalier-Smith, 1999). From the ER to the plastid, in principal, there are two known routes. In diatoms and cryptomonads the ER and the outer plastid membranes are continuous allowing proteins to simply diffuse from one to the other (Bhaya and Grossman, 1991; Ishida et al., 2000). In euglenids and dinoflagellates vesicular transport is required (Sulli et al., 1999; Nassoury et al., 2003).

In this study we show that apicoplast stroma-targeted proteins localise in cargo vesicles and the data we present imply that these cargo-vesicles fuse with the outer apicoplast membrane (Fig. 1). This is a strong indication both that vesicle targeting is required to convey proteins to the apicoplast and that fusion of cargo vesicles with the outermost membrane is the first step of protein translocation to the apicoplast. These results support previous hypotheses that a vesicle trafficking step is a required component of apicoplast targeting (Bodyl, 1997; Cavalier-Smith, 1999; McFadden, 1999b; Parsons et al., 2007). Previous studies have demonstrated that apicoplast targeting does not occur via the

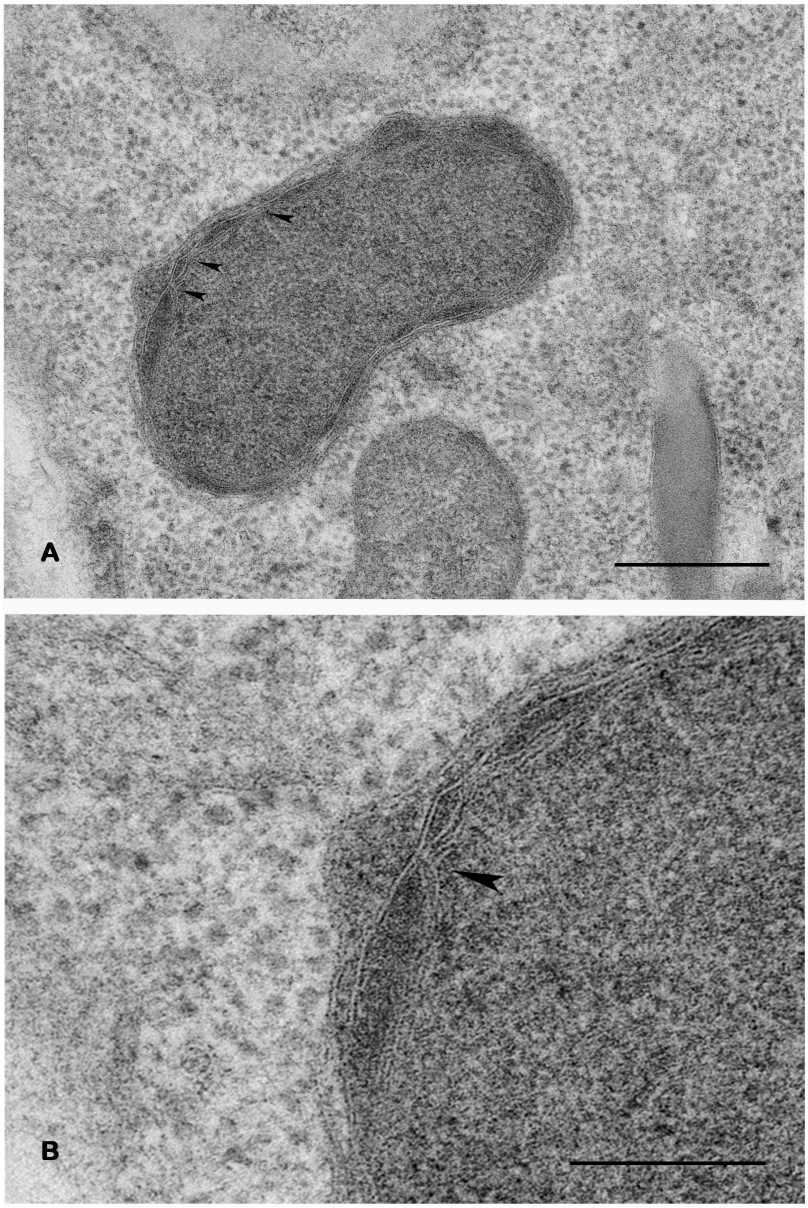

Figure 4 Micrographs of a 60 nm thick section.

Parasites were HPF and FS with 0.1% uranyl acetate and embedded in HM20. **A)** An apicoplast with its four membranes. It shows the random distribution of the tight contact points between the PPM and inner membrane (*arrowheads*). Scale bar is 200 nm **B)** Higher magnification of the same apicoplast focusing on the close alignments of the three membranes. It shows that the hydrophobic phases of the adjacent leaflets of the PPM and outer innermost membrane are difficult to distinguish, which prevents scientifically reliable interpretation of the actual relation between the two membranes at these points. Scale bar is 100 nm.

Golgi (DeRocher, 2005; Tonkin et al., 2006b), suggesting that the vesicles we observe are derived directly from the ER.

Once the plastid proteins are delivered to the exoplastid compartment (EPC) of the apicoplast, they must be further translocated across the remaining three membranes. This mechanism is still unknown. No specific targeting signals are yet identified for passing the periplastid membrane, both PPC-targeted and stroma-targeted proteins appear to have the same signal composition. However, several hypotheses have been published to explain this transport step, including vesicle-mediated transport of the proteins (Gibbs, 1981; Killian and Kroth, 2003), transport by an unspecific pore (Kroth and Strotmann, 1999), a relocated plastid translocon component (Cavalier-Smith, 1999; Bodyl, 2004), and a proteinaceous translocation pore through which proteins can cross the PPM (Cavalier-Smith, 1999; van Dooren et al., 2001). The last theory has recently been refined by Sommer, who suggests a symbiont specific ERAD-like machinery that has been relocated to the third membrane and reutilized as translocator for nuclear encoded plastid preproteins to cross the periplastid compartment (Sommer et al., 2007). The localization of stroma-targeted proteins in all three compartments (exoplastid, periplastid and stroma) of the apicoplast (Fig.1 A, B and Fig. 4 C, D, E, F arrows) in our study, also supports the idea that protein translocation occurs in three independent steps. In addition, the distribution of protein patches on the third membrane (PPM) (Fig. 4B white arrowheads) is also in favour of the translocation complex theory. The presumed protein translocation machinery, similar to the Toc complex in the chloroplast, and identical for the PPM and the outer-IM membrane, as already suggested (van Dooren et al., 2001), will facilitate translocation of all apicoplast proteins with a cleavable N-terminal targeting sequence (Foth and McFadden, 2003). It will also allow sorting between the PPC-targeted proteins and the stroma-targeted proteins to be accomplished in the PPC.

However, there are apicoplast specific proteins found in *P. falciparum Pf*APT1 (Mullin et al., 2006) and its homologous *Tg*APT1 in *T. gondii* (Karnataki et al., 2007) which lack a canonical targeting sequence, apparently, directed by a specific targeting sequence that is not yet defined. Proteomics studies have predicted a number of proteins present in plastids that apparently do not carry a plastid-targeting signal (Millar et al., 2006). Obviously, translocation via specialized complexes is not the only way for transport of proteins into plastids, but this alternative, non-canonical, mechanism is still rather neglected. A possibility for alternative import of stroma-targeted proteins is the simultaneous translocation across all three inner membranes in one step (Cavalier-Smith, 1999).

We present, for the first time, the existence of confined contact points between the third (PPM) and the second innermost membrane in the apicoplast (Fig.2 A, C and Fig.4 *arrowheads*). These local contacts may represent sites of protein import. Such translocation scenario could be facilitated by structural changes in the peptide confirmation, promoted by the contact of the proteins with the apicoplast-specific lipids (Bruce, 1998). It is interesting to point out, that the putative protein patches, previously described in

Sarcocystis sp. (Tomova et al., 2006) and also for *Toxplasma gondii* (*Chapter 3*) on the third membrane do not co-localize with the contact sites between the PPM and the second IMM (Fig.2 B). The labelling for Tic was also not directly related to these tight contacts (Fig.2 A). However, this "direct" translocation would contradict our finding that stroma-targeted proteins localize in the periplastid space, although it is not inconceivable that multiple mechanisms exist to translocate proteins into the apicoplast. Certainly, various aspects in the evolution of this plastid resulted in the development of different mechanisms ensuring the meticulous distribution of proteins.

The last biological barriers, the two inner membranes, are believed to be crossed by the stroma-targeted proteins through specialized translocation complexes. Recently, we have identified the *Tg*Tic20 protein, a component of the Tic complex, and demonstrated its apparent involvement in protein import across the innermost apicoplast membrane (van Dooren et al, 2008). Tic20 is an integral inner membrane protein in chloroplast and appears to have a role in protein conducting (Kouranov et al., 1998). This protein is a homologue of unknown function in the cyanobacterium *Synechocystis*. Tic20 was considered to be an ideal candidate for the inner membrane protein-translocating channel because of its structural similarities to prokaryotic amino acid transporters in *Bacillus subtilis* and *Methanococcus jannaschii* (Reumann and Keegstra, 1999). This is supported by the observation that Arabidopsis plants, expressing antisense Tic20, show a 50% decrease in the levels of protein import efficiency (Chen et al., 2002).

In the present study we provide ultra-structural evidence that Tic20 has an important role in the biogenesis of the apicoplast. The absence of this protein leads to inability of the stroma-targeted proteins to cross the inner two membranes, resulting in abnormal distribution of these proteins in the exoplastid and periplastid compartments. Although, we do not provide clear evidence of the direct involvement of *Tg*Tic20 in translocation of proteins we illustrate the explicit link between this protein and the normal functionality of the apicoplast. If this protein is being knocked out the apicoplast will gradually segregate and cease to exist (Fig. 3), finally leading to the malfunction of the whole parasite.

It is very probable that translocation complexes in all plastids are to some extend conservative and thus we can expect in the future more proteins from the Tic-Toc complex to be found in the apicoplast especially those of cyanobacterial (endosymbiotic) origin like the channel-forming proteins (Bhattacharya et al., 2003).

Taking into account our findings and what is already known about protein targeting and translocation in plastids with two, three or four membranes we suggest the following model for the apicoplast in *T. gondii* (Fig. 5).

The majority of proteins are delivered to the apicoplast via cargo vesicles. These vesicles fuse with the outermost membrane and their cargo is released in the exoplastid space of the apicoplast (DeRocher, 2005). Next, proteins are either "directly" translocated to the stroma of the plastid in one single step enabled by the contiguous association of the PPM with the IMs. Alternatively, import across the PPM may be independent of import

across the inner two membranes with translocation complexes being involved. Crossing the three membranes in such a serial manner permits the proteins directed for the periplastid compartment to be halted there. These two models of translocation could also act complimentary to each other.

Identifying additional proteins that function in import across each membrane should enable us to further dissect apicoplast protein import. Ultra-structural analyses such as those presented here are a key to piercing together the various steps of this fascinating and unique biological process.

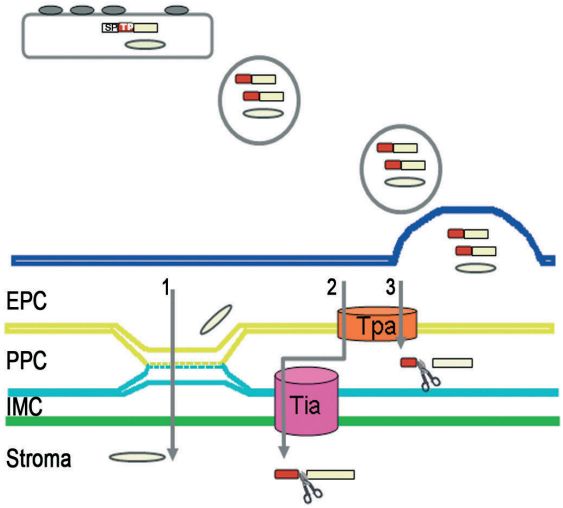

Tpa Translocation complex on the periplastid apicoplast membrane

Tia Translocation complex on the inner apicoplast membranes

IMC inner membranes compartment

PPC periplastid compartment

EPC exoplastid compartment

SP TP A protein with the classical, bipartite, N-terminus sequence (SP-signal peptide; TP-transit peptide).

A protein with a non-canonical signal sequence.

Figure 5 Model of protein trafficking to the apicoplast of *T. gondii*

The majority of proteins, those possessing the predicted transit peptide and those without it, are being routed to the apicoplast via vesicles. These vesicles fuse with the outermost membrane delivering the cargo to the first compartment of the plastid- the exoplastid compartment (EPC). Next, some of the proteins are being translocated directly from the EPC to the stroma crossing simultaneously the three inner membranes, facilitated by the contiguous alignments of the PPM with the IMs (*pathway* **1).** The proteins with the canonical signal sequence are being translocated via translocation complexes, one located on the PPM and another on the inner two membranes. This process is being performed in series allowing the proteins designed for the PPC to be halted there (*pathway* **3**) and those for the stroma to continue (*pathway* **2**).

References

Bhattacharya, D., Yoon, H.S. and Hackett, J.D. 2003. Photosynthetic eukaryotes unite: endosymbiosis connects the dots. BioEssays. 26:50-60.

Bhaya, D. and Grossman, A. 1991. Targeting proteins to diatom plastids involves transport through an endoplasmic reticulum. Molecular and General Genetics. 229:400-404.

Bodył, A. 1997. Mechanism of protein targeting to the chlorarachnophyte plastids and the evolution of complex plastids with four membranes-a hypothesis. Botanica Acta. 110:395-400.

Bodył, A. 2004. Evolutionary origin of a preprotein translocase in the periplastid membrane of complex plastids: a hypothesis. Plant Biotechnology. 6:513–518.

Bruce, B.D. 1998. The role of lipids in plastid protein transport. Plant Molecular Biology. 38:223-246.

Cavalier-Smith, T. 1999. Principles of protein and lipid targeting in secondary symbiogenesis: euglenoid, dinoflagellate, and sporozoan plastid origins and the eukaryotic family tree. Journal of Eukaryotic Microbiology. 46:347-366.

Chen, X., Smith, M.D., Fitzpatrick, L. and Schnel, D.J. 2002. In vivo analysis of the role of atTic20 in protein import into chloroplasts. Plant Cell. 14:641– 654.

Cremers, F.F.M., Voorhout, W.F., van der Krift, T.P., Leunissen-Bijvelt, J.J.m. and Verkleij, A.J. 1988. Visualisation of contact sites between outer and inner envelope membranes in isolated chloroplasts. Biochimica and Biophysica Acta. 933:334-340.

Delwiche, C.F. and Palmer, J.D. 1997. The origin of plastids and their spread via secondary endosymbiosis. Plant Systematics and Evolution. Suppl. 11:53-86.

DeRocher, A., B., Gilbert, J. E., Feagin, Parsons, M. 2005. Dissection of brefeldin A-sensitive and -insensitive steps in apicoplast protein targeting. Journal of Cell Science. 118:565–574.

DeRocher, A., Hagen, C.B., Froehlich, J.E., Feagin, J.E. and Parsons, M. 2000. Analysis of targeting sequences demonstrates that trafficking to the *Toxoplasma gondii* plastid branches off the secretory system. Journal of Cell Science. 113:3969–3977.

Fichera, M.E. and Roos, D.S. 1997. A plastid organelle as a drug target in apicomplexan parasites. Nature. 390:407–409.

Foth, B.J. and McFadden, G.I. 2003. The apicoplast: a plastid in *Plasmodium falciparum* and other Apicomplexan parasites. International Review of Cytology. 224:57-110.

Foth, B.J., Ralph, S.A., Tonkin, C.J., Struck, N.S., Fraunholz, M., Roos, D.S., Cowman, A.F. and McFadden, G.I. 2003. Dissecting apicoplast targeting in the malaria parasite *Plasmodium falciparum*. Science. 299:705-708.

Gibbs, S.P. 1981. The chloroplast endoplasmic reticulum, structure, function, and evolutionary significance. International Review of Cytology. 72:49-99.

Gross, U., Muller, W.A., Knapp, S. and Heesemann, J. 1991. Identification of a Virulence-Associated Antigen of *Toxoplasma gondii* by Use of a Mouse Monoclonal Antibody. Infection and Immunity. 59:4511-4516.

Hempel, F., Bozarth, A., Sommer, M.S., Zauner, S., Przyborski, J.M. and Maier, U.G. 2007. Transport of nuclear-encoded proteins into secondarily evolved plastids. Biochemical Chemistry. 388:899-906.

Ishida, K., Cavalier-Smith, T. and Green, B., R. 2000. Endomembrane structure and the chloroplast protein targeting pathway in *Heterosigma akashiwo* (*Raphidophyceae*, *Chromista*). Journal of Phycology. 36:1135-1144.

Jomaa, H., Wiesner, J., Sanderbrand, S., Altincicek, B., Weidemeyer, C., Hintz, M., Türbachova, I., Eberl, M., Zeidler, J., Lichtenthaler, H.K., Soldati, D. and Beck, E. 1999. Inhibitors of the nonmevalonate pathway of isoprenoid biosynthesis as antimalarial drugs. Science. 285:1573-1576.

Karnataki, A., Derocher, A.E., Coppens, I., Feagin, J.E. and Parsons, M. 2007. Membrane Protease is Targeted to the Relict Plastid of *Toxoplasma* via an Internal Signal Sequence. Traffic. 8:1543-53.

Keegstra, K. and Celine, K. 1999. Protein import and routing systems of chloroplasts. The Plant Cell. 11:557-570.

Killian, O. and Kroth, P.G. 2003. Evolution of protein targeting into "complex" plastids: the "secretory transport hypothesis". Plant Biology. 5:350– 358.

Köhler, S., Delwiche, C.F., Denny, P.W., Tilney, L.G., Webster, P., Wilson, R.J.M., Palmer, J.D. and Roos, D.S. 1997. A plastid of probable green algal origin in apicomplexan parasites. Science. 275:1485–1489.

Kouranov, A., Chen, X., Fuks, B. and Schnell, D., J. 1998. Tic20 and Tic22 are new components of the protein import apparatus at the chloroplast inner envelope membrane. Journal of Cell Biology. 143:991–1002.

Kremer, J.R., Mastronarde, D.N. and McIntosh, J.R. 1996. Computer visualization of three-dimensional image data using IMOD. Journal of Structural Biology. 116:71-76.

Kroth, P. and Strotmann, H. 1999. Diatom plastids: Secondary endocytobiosis, plastid genome and protein import. Physiology of Plants. 107:136-141.

Liou, W., Geuze, H.J. and Slot, J.W. 1996. Improving structural integrity of cryosections for immunogold labeling. Histochemical Cell Biology. 106:41-58.

Martin, W. and Herrmann, R., G. 1998. Gene transfer from organelles to the nucleus: how much, what happens, and Why? Plant Physiology. 118:9-17.

Mazumdar, J., Wilson, E.H., Masek, K., Hunter, C.A. and Striepen, B. 2006. Apicoplast fatty acid synthesis is essential for organelle biogenesis and parasite survival in *Toxoplasma gondii*. Proceedings of the National Academy of Science of the Unated States of America. 103:13192–13197.

McFadden, G. and Gilson, P. 1995. Something borrowed, something green: lateral transfer of chloroplasts by secondary endosymbiosis. Trends in Ecological Evolution. 10:12-17.

McFadden, G.I. 1999a. Endosymbiosis and evolution of the plant cell. Currunt Opinion in Plant Biology. 2:513–519.

McFadden, G.I. 1999b. Plastids and protein targeting. Journal of Eukaryotic Microbiology. 46:339-346.

Millar, A.H., Whelan, J. and Small, I. 2006. Recent surprises in protein targeting to mitochondria and plastids. Current Opinion in Plant Biology. 6:610-615.

Müller, M., Marti, T. and Kriz, S. 1980. Improved structural preservation by freeze substitution. In: Proceedings of the 7th European Congress on Electron Microscopy. P. Brederoo and W. de Priester, editors:720-721.

Mullin, K.A., Lim, L., Ralph, S.A., Spurck, T.P., Handman, E. and McFadden, G.I. 2006. Membrane transporters in the relict plastid of malaria parasites. Proceedings of the National Academy of Science of the Unated States of America. 130:9572–9577.

Nassoury, N., Cappadocia, M. and Morse, D. 2003. Plastid ultrastructure defines the protein import pathway in dinoflagellates. Journal of Cell Science. 116:2867– 2874.

Nassoury, N. and Morse, D. 2005. Protein targeting to the chloroplasts of hotosynthetic eukaryotes: Getting there is half the fun. Biochimica et Biophysica Acta. 1743:5-19.

Palmer, J.D. and Delwiche, C.F. 1996. Second-hand chloroplasts and the case of the disappearing nucleus. Proceedings of the National Academy of Science of the Unated States of America. 93:7432-1435.

Parsons, M., Karnatak, i.A., Feagin, J.E. and DeRocher, A. 2007. Protein Trafficking to the Apicoplast: Deciphering the Apicomplexan Solution to Secondary Endosymbiosis. Eukaryotic Cell. 6:1081–1088.

Penczek, P., Marko, M., Buttle, K. and Frank, J. 1995. Double-tilt electron tomography. Ultramicroscopy. 60:393-410.
Reumann, S. and Keegstra, K. 1999. The endosymbiotic origin of the protein import machinery of chloroplastic envelope membranes. Trends in Plant Science. 4:302–307.
Reynolds, E.S. 1963. The use of lead citrate at high pH as an electron-opaque stain in electron microscopy. Journal of Cell Biology. 17:208-212.
Roos, D., S., Donald, R.G., Morrissette, N.S. and Moulton, A.L. 1994. Molecular tools for genetic dissection of the protozoan parasite *Toxoplasma gondii*. Methods Cell Biol. 45:27-63.
Schliwa, M. and van Blerkom, J. 1981. Structural Interaction of Cytoskeletal Components. The Journal of Cell Biology. 90:222-235.
Slot, J.W. and Geuze, H.J. 2007. Cyosectioning and immunolabeling. Nature Protocols. 2:2480-2491.
Sommer, M., S., Gould, S., B., Lehmann, P., Gruber, A., Przyborski, J.M. and Maier, U., G. 2007. Der1-mediated pre-protein import into the periplastid compartment of chromalveolates. Molecular Biology Evolution. 24:918–928.
Sulli, C., Fang, Z., Muchhal, U. and Schwartzbach, S.D. 1999. Topology of Euglena chloroplast protein precursors within endoplasmic reticulum to Golgi to chloroplast transport vesicles. Journal of Biological Chemistry. 274:457–463.
Tokuyasu, K.T. 1973. A technique for ultracryotomy of cell suspensions and tissues. Journal of Cell Biology. 57:551-565.
Tokuyasu, K.T. 1980. Immunochemistry on ultrathin frozen sections. Histochemical Journal. 12:381-403.
Tomova, C., Geerts, W.J.C., Müller-Reichert, T., Entzeroth, R. and Humbel, B.M. 2006. New comprehension of the apicoplast of Sarcocystis by transmission electron tomography. Biology of the Cell. 98:535–545.
Tonkin, C., J., Kalanon, M. and McFadden, G., I. 2008. Protein Targeting to the Malaria Parasite Plastid. Traffic. 9:166–175.
Tonkin, C.J., Roos, D.S. and McFadden, G.I. 2006a. N-terminal positively charged amino acids, but not their exact position, are important for apicoplast transit peptide fidelity in *Toxoplasma gondii*. Molecular & Biochemical Parasitology. 150:192-200.
Tonkin, C.J., Struck, N.S., Mullin, K.A., Stimmler, L.M. and McFadden, G.I. 2006b. Evidence for Golgi-independent transport from the early secretory pathway to the plastid in malaria parasites. Molecular Microbiology. 61:614–630.
van Dooren, G.G., Schwartzbach, S.D., Osafune, T. and McFadden, G.I. 2001. Translocation of proteins across the multiple membranes of complex plastids. Biochimica et Biophysica Acta. 1541:34-53.
van Dooren, G.G., Tomova, C., Agrawal, S., Humbel, B.M. and Striepen, B. 2008. *Toxoplasma gondii* Tic20 is essential for apicoplast protein import. Proceedings of the National Academy of Science of the Unated States of America. 105:13574–13579.
Waller, R.F., Keeling, P.J., Donald, R.G.K., Striepen, B., Handman, E., Lang-Unnasch, N., Cowman, A.F., Besra, G.S., Roos, D.S. and McFadden, G.I. 1998. Nuclear-encoded proteins target to the plastid in *Toxoplasma gondii* and *Plasmodium falciparum*. Proceedings of the National Academy of Science USA. 95:12352-12357.
Waller, R.F., Reed, M.B., Cowman, A.F. and McFadden, G.I. 2000. Protein trafficking to the plastid of *Plasmodium falciparum* is via the secretory pathway. EMBO Journal. 19:1794–1802.
Yung, S., Unnasch, T.R. and Lang-Unnasch, N. 2001. Analysis of apicoplast targeting and transit peptide processing in *Toxoplasma gondii* by deletional and insertional mutagenesis. Molecular & Biochemical Parasitology. 118:11-21.

Chapter 6

SUMMARY AND CONCLUSION

SUMMARY AND CONCLUSION

The aim of this research was to reveal the architecture of the apicoplast, a non-photosynthetic plastid found in almost all protozoan parasites of the phylum Apicomplexa. This organelle changed the focus of research in evolutionary biology and molecular Parasitology since the moments of its discovery some 15 years ago. It is now commonly accepted that the apicoplast was acquired by secondary endosymbiosis (Delwiche and Palmer, 1997; McFadden and Gilson, 1995). As a result of the evolutionary incorporation of this organelle into the ancestral parasite the vast majority of its protein genes have been transferred to the nuclear genome. Although the apicoplast has its own genome (only 35 kb) over 500 proteins are predicted to be targeted back to the apicoplast post-translationally (Foth et al., 2003). In the last decade several studies directly addressed issues of organellar protein targeting, especially transgenic experimentation in *Toxoplasma gondii* and *Plasmodium falciparum* (DeRocher et al., 2000; Foth et al., 2003; Nielsen et al., 1997; Ralph et al., 2004; Waller et al., 2000; Yung and Lang-Unnasch, 1999), but the question of how trafficking of apicoplast proteins is accomplished is still open.

The other important consequence of the secondary endosymbiosis is the number of membranes surrounding the apicoplast. The membranous enclosure is not only an indication for the endosymbiotic origin of the apicoplast, but is of critical importance for understanding the accessibility and the relation between the plastid and the parasite cell.

The knowledge of the apicoplast ultrastructure was incomplete and based on thin (some times serial) sections from chemically fixed material. The reports in the literature concerning structure and number of membranes were contradictive (Hopkins et al., 1999; Köhler, 2005) .

The first challenge in our endeavour was to answer the question: how many membranes surround the plastid?

It is known that especially membranous continuities are vulnerable to chemical fixation artefacts and during dehydration and resin embedding most of the lipids are extracted and lost (Dubochet et al., 1983; Ebersold et al., 1981; Murk et al., 2003). It is generally accepted that cryofixation methods provide better ultra-structural preservation (Dubochet et al., 1988; Müller, 1992; Steinbrecht and Zierold, 1987). High-pressure freezing (HPF) is generally acknowledged as the method of choice for cryofixation of biological samples. The subsequent imaging of the sample in the frozen-hydrated stage as the method for examining the cellular structure as close as possible to the native (Dubochet et al., 1988). As a compromise, cryofixation followed by freeze-substitution and embedding in Epon has proven to give a reliable view of the cellular architecture (Ebersold et al., 1981; Engfeldt et al., 1994; Humbel and Schwarz, 1989; Kaneko and Walther, 1995; Steinbrecht, 1980; van Harreveld et al., 1965). In addition, this approach allows the sectioning of thick sections, suitable for electron tomography, to be sectioned. Therefore, to investigate the architecture of the apicoplast, we choose to combine high-pressure freezing, freeze-substitution,

resin embedding, and electron tomography. As a result, we obtained 3-D models of the subcellular structure of the apicoplast that closely resemble the living state. This allowed us to examine computationally the apicoplast structure in its three dimensions, so that the acquired information gave answers to our specific questions.

We clearly show that four membranes surround the apicoplast (Tomova et al., 2006) (Chapter *2*). Two regularly shaped almost circular, inner membranes. The third (periplastid) and the fourth membranes show some variations, most probably representation of the dynamic processes these membranes were part of. The clearly visible mass densities, patches, between the two inner membranes and in the periplastid membrane most likely represent protein complexes.

An important observation in the tomograms was the proximity of the ER sheets to the outermost-apicoplast membrane. The exact relation between these subcellular compartments is the key step in apprehending the substrate transport to and from the apicoplast. Despite the improved ultra-structural preservation in the HPF/FS samples the membrane contrast and visualisation of the apicoplast and the ER was not adequate to determine the relation of these closely apposed membranes.

In the process of freeze-substitution, heavy metal stains are added in the substitution cocktails to enhance specimen contrast. However, visualization of a number of cellular membranes, in particular those of the nuclear envelope, endoplasmic reticulum (ER) and Golgi, are often not well contrasted after FS. Three major parameters affect the visibility of membranes. First and most important is the type of specimen and the nature of the investigated structure. Membranes are usually well visible in neuronal structures (Szczesny et al., 1996) but poorly visible in yeast cells, especially in mitochondria (Erk et al., 1998; Hohenberg et al., 1994). Second criterion is the quality of freezing. When the samples are not well frozen, and contain ice crystal segregation patterns the contrast in the sample is enhanced and membranes are better visible. Third parameter is the freeze-substitution, plastic embedding and post-staining protocol. Only this parameter (substitution, embedding and staining) can be experimentally altered and improved.

Even though numerous different substitution protocols exist in literature there are only a few methodological investigations concerning the process of freeze-substitution. These studies examined the replacement of ice by an organic solvent at temperatures of -90°C to 0°C (e.g. (Müller et al., 1980)), the substitution capacities of different organic solvents in the presence of water (Humbel and Müller, 1986) and the influence of the different solvents on the ultra-structural preservation of high-pressure frozen, freeze-substituted sample (Studer et al., 1995). Yet, little is known about what exactly is the influence of the heavy metals on the structure preservation and contrast enhancing at low temperatures. The reagents included in FS protocols are typically the same as those used for aqueous phase fixation and staining, but can yield significantly different staining patterns following FS. In principle, this problem may arise from a variety of causes, including extraction of lipids during FS, failure to bind an electron-dense fixative such as osmium or failure of

post embedding stains.

A number of methods have been developed to overcome the problem of insufficient membrane contrast in FS such as the addition of water to the FS solution (Walther and Ziegler, 2002), the combination of tannic acid and glutaraldehyde in acetone, or freeze-substitution with potassium permanganate in acetone (Giddings, 2003).

Membrane contrast can also be increased by enhancing the intensity of the post-section-stain, e.g. introducing an additional step with tannic acid (McDonald and Müller-Reichert, 2002), or with aqueous potassium permanganate solutions, especially for Lowicryl embedded samples (Sawaguchi et al., 2002).

However, increased membrane staining of different structures or vesicle coats can become excessive, grainy of fussy to the point that resolution of fine detail deteriorates. This problem can limit the information obtained from high-resolution techniques such as tomography.

At present, no freeze-substitution protocol described overcomes the limitations of membrane contrast and still being suitable for all types of analysis like high-resolution electron microscopy, electron tomography and immunolocalization. Therefore, optimizing the substitution and embedding step for improved preservation and visualization of a complex membranous structure, as the apicoplast was a key subject of the present study.

We described a FS protocol that provides adequate contrast on cellular membranes and yielded specimens suitable for high-resolution electron microscopy and tomography. In addition, the samples substituted in 0.1% uranyl acetate in acetone, followed by embedding in Lowicryl HM20, are suitable for both immunolocalization and high-resolution structural studies. Membranes are typically lightly stained but very well defined, not only in thin 60 nm sections but also in a thick 200 nm section (Fig.1). In the samples we examined the lamellar structure of the membrane bilayer is clearly visible without any additives of osmium, tannic acid or water in the FS cocktail which, might cause some alterations in the structure preservation, thus leading to ambiguous interpretations. The contrast of the samples was sufficient to allow us the direct examination of the sections in the electron microscope without any additional post-sectioning contrasting. It is known that the position of the stain might not accurately reflect the shapes of the macromolecules to which it binds. Furthermore, the electron doses required for ET can cause the stain to migrate and to agglomerate, which additionally compromises the resolution. Therefore, we believe that this optimized method of sample processing reduces alterations of the cellular structure to a minimum and improves the resolution of our tomograms. The resolution of a tomogram depends on many practical factors, such as the angle between tilted views (Crowther, 1970), the total tilt range (Radermacher, 1992), the precision with which the tilted views are aligned before their back projection (Frank, 1992), the use of images from two as opposed to one tilt axis (Mastronarde, 1997; Penczek et al., 1995), and the electron dose used for all of the images (McEwen, 1995). Taking all this into account, we estimate a

resolution of approximately 2 nm.

Our optimized sample preparation method allowed us to demonstrate that the ER membrane does not fuse with the outermost membrane of the apicoplast and to reveal the existence of 'membrane contact sites' (MCS) between the apicoplast and the ER (*Chapter 3*). The cytosolic gap between the apicoplast outermost membrane and the most closely positioned ER membrane is 8-10 nm. This close membrane association has a random spatial distribution and is restricted to 40-60 nm in z direction of the sample volume and 30-40 nm parallel to the direction of the membranes. The distance of 8-10 nm between the associating membranes of the two organelles, is sufficiently small to facilitate contact formation by membrane-active binding proteins to effectively assist the inter-membrane flux (Holthuis and Levine, 2005; van Meer et al., 2008; Weisiger and Zucker, 2002). Based on the structural organization of these membrane associations and the significant role of the apicoplast in the lipid metabolism in the parasite cell (Bisanz et al., 2006; Jomaa et al., 1999; Ralph et al., 2004; Roos et al., 1999; Waller et al., 1998), we suggest that these MCSs between the ER and the apicoplast in *Toxoplasma gondii* are specialized units in a complex transport pathway for fast and accurate allocation of lipids.

We studied and identified a highly diverged member of the Tic20 protein family in the phylum Apicomplexa (Chapter 4). We demonstrate that Tic20 of *Toxoplasma gondii* is an integral protein of the innermost apicoplast membrane. Further, we examined the effects of *Tg*Tic20 knockout on apicoplast protein import, and conclude that *Tg*Tic20 is essential for protein import across the inner apicoplast membrane (van Dooren et al., 2008). As such, *Tg*Tic20 is the first functionally characterised apicoplast import protein identified in the Apicomplexa.

We provide an unequivocal prove that Tic20 has an important role in the biogenesis of the plastid. Absence of this protein leads to the abnormal distribution of the stroma-targeted proteins in the exoplastid and periplastid compartments of the plastid and finally causes the gradual segregation and loss of the apicoplast (see *Chapter 5*). Although we do not provide clear evidence of the direct involvement of Tic20 in the translocation of proteins, we illustrate the explicit link between this protein and the normal functionality of the apicoplast.

The developed protocol combines structure preservation as close as possible to the native, optimized membrane visualisation and possibility for immunolocalization studies. This allowed us to identify the precise distribution of the stromal proteins within the parasite cell. We show that apicoplast stroma-targeted proteins localise in cargo vesicles and in the protrusions of the EPC. The data from the 3D electron tomographic analysis imply that, these cargo-vesicles fuse with the outer apicoplast membrane and strongly support the vesicular transport theory (*Chapter 5*).

We present, for the first time, the existence of confined contact points between the third periplastid (PPM) and the outer innermost membrane. We hypothesize that these local contacts very likely facilitate an alternative way for transport of the stromal proteins

through three inner membranes (Cavalier-Smith, 1999). However, this “direct” translocation scenario is in contradiction with our finding that stroma-targeted (ACP and FNR-DHFR) proteins localize in the periplastid space. Still, it is possible that multiple mechanisms exist to translocate proteins into the apicoplast.

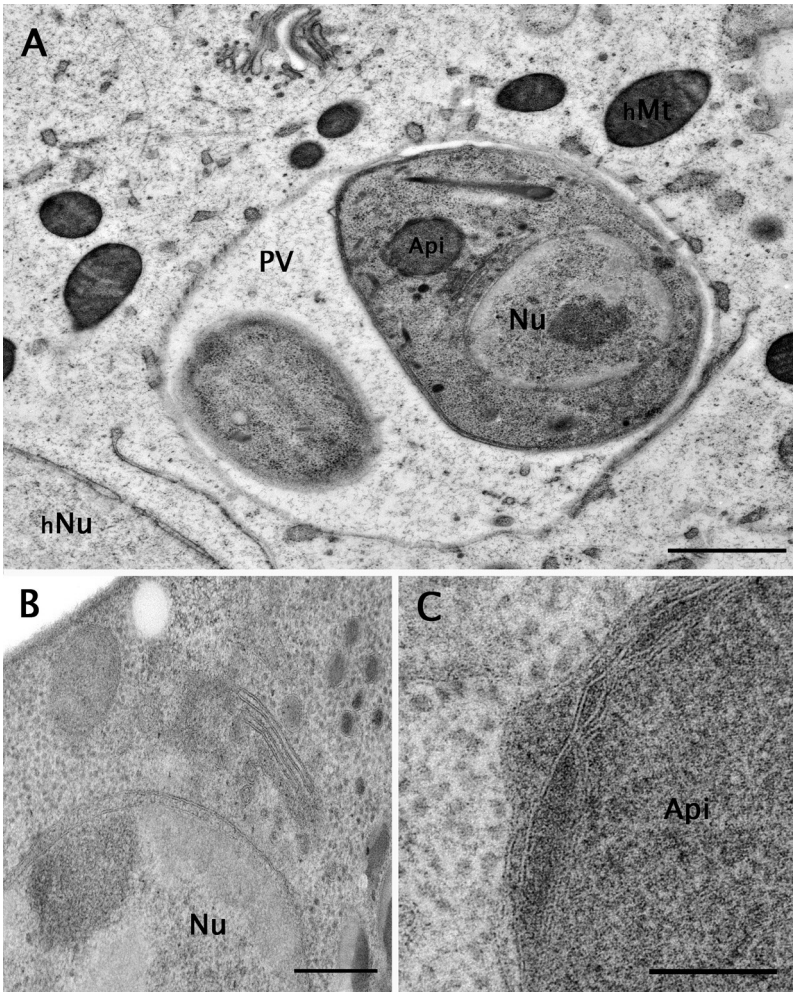

Figure 1 Illustration of our optimized sample preparation

Samples freeze substituted in 0.1% uranyl acetate in acetone and low-temperature embedded in HM20. Sections are not post-stained. **A)** Overview of a parasite cell within the parasitophorous vacuole inside the host cell. **B)** is a close up of the nucleus and Golgi and **C)** is the apicoplast with its four membranes. The laminar structure of the membranes is clearly visible without any additional post-staining. This figure clearly indicates the advantage of this method in optimal visualization of all membranous structures in the parasite cell without alterations caused by heavy metals or water.
hNu-host nucleus; **hMt**-host mitochondrion; **PV**-parasitophorous vacuole; **Nu**-parasite nucleus; **Api**-apicoplast. Scale bars: in **A** 1000nm in **B** and **C** 200nm.

Based on our findings and the current knowledge on protein targeting and translocation in primary and secondary plastids we suggest the following model for the apicoplast in *T. gondii* (Fig. 2 **E**)

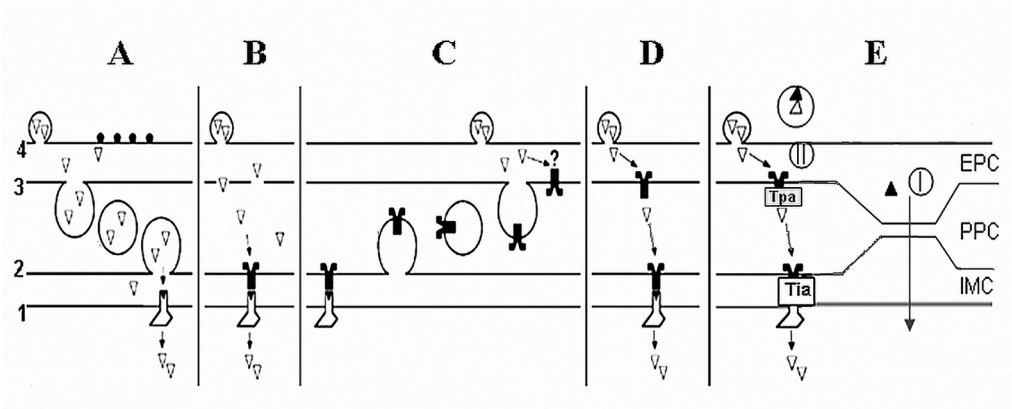

Figure 2 Schematic representations of the current hypotheses for protein import to the apicoplast

A) According to Gibbs (Gibbs, 1981)
B) According to Kroth and Strotmann (Kroth and Strotmann, 1999)
C) According to Cavalier-Smith (Cavalier-Smith, 1999)
D) According to van Dooren (van Dooren et al., 2001)
E) Our model of protein trafficking to the apicoplast of *T. gondii*
The majority of proteins, those possessing the predicted transit peptide and those without it, are targeted to the apicoplast via vesicles. The cargo vesicles fuse with the outermost membrane and deliver the proteins to the outermost, exoplastid compartment of the plastid (EPC). Next, some of the proteins translocate directly from the EPC to the stroma, crossing the three inner membranes simultaneously, which is facilitated by the contiguous alignments of the PPM with the IMs (*pathway* **I**).
The proteins with a canonical signal sequence translocate via translocation complexes, one located on the PPM, the other across the inner two membranes. This process is performed in series allowing the proteins designed for the PPC to be halted there and those for the stroma to continue (*pathway* **II**).
EPC - exoplastid compartment; **PPC** - periplastid compartment; **IMC** - inner membranes compartment; **Tpa** – Translocation complex on the periplastid apicoplast membrane; **Tia** - Translocation complex on the inner apicoplast membranes. **1** and **2**- inner membranes; **3** - periplastid membrane (PPM); **4** – outermost membrane

References

Bisanz, C., Bastien, O., Grando, D., Jouhet, J., Marechal, E. and Cesbron-Delauw, M.F. 2006. *Toxoplasma gondii* acyl-lipid metabolism: de novo synthesis from apicoplast-generated fatty acids versus scavenging of host cell precursors. J.Biochem. 394:197-205.

Cavalier-Smith, T. 1999. Principles of protein and lipid targeting in secondary symbiogenesis: euglenoid, dinoflagellate, and sporozoan plastid origins and the eukaryotic family tree. Journal of Eukaryotic Microbiology. 46:347-366.

Crowther, R.A.e.a. 1970. Three dimensional reconstructions of spherical viruses by Fourier synthesis from electron micrographs. Nature. 226:421–425.

Delwiche, C.F. and Palmer, J.D. 1997. The origin of plastids and their spread via secondary endosymbiosis. Plant Systematics and Evolution. Suppl. 11:53-86.

DeRocher, A., Hagen, C.B., Froehlich, J.E., Feagin, J.E. and Parsons, M. 2000. Analysis of targeting sequences demonstrates that trafficking to the *Toxoplasma gondii* plastid branches off the secretory system. Journal of Cell Science. 113:3969–3977.

Dubochet, J., Adrian, M., Chang, J.J., Homo, J.C., Lepault, J., McDowall, A.W. and Schultz, P. 1988. Cryo-electron microscopy of vitrified specimens. Quarterly Reviews of Biophysics. 21:129-228.

Dubochet, J., McDowall, A.W., Menge, B., Schmid, E.N. and Lickfeld, K.G. 1983. Electron microscopy of frozen-hydrated bacteria. Journal of Bacteriology. 155:381-390.

Ebersold, H.R., Cordier, J.L. and Lüthy, P. 1981. Bacterial mesosomes: method dependent artifacts. Archives of Microbiology. 130:19-22.

Engfeldt, B., Reinholt, F.P., Hultenby, K., Widholm, S.M. and Müller, M. 1994. Ultrastructure of hypertrophic cartilage: histochemical procedures compared with high pressure freezing and freeze substitution. Calcified Tissue International. 55:274-280.

Erk, I., Nicolas, G., Caroff, A. and Lepault, J. 1998. Electron microscopy of frozen biological objects: a study using cryosectioning and cryosubstitution. Journal of Microscopy. 189:236-248.

Foth, B.J. and McFadden, G.I. 2003. The apicoplast: a plastid in *Plasmodium falciparum* and other Apicomplexan parasites. International Review of Cytology. 224:57-110.

Foth, B.J., Ralph, S.A., Tonkin, C.J., Struck, N.S., Fraunholz, M., Roos, D.S., Cowman, A.F. and McFadden, G.I. 2003. Dissecting apicoplast targeting in the malaria parasite *Plasmodium falciparum*. Science. 299:705-708.

Frank, J. 1992. Electron Tomography: Three-dimensional imaging with the transmission electron microscope. Plenum Press, New York, London.

Gibbs, S.P. 1981. The chloroplast endoplasmic reticulum, structure, function, and evolutionary significance. International Review of Cytology. 72:49-99.

Giddings, T.H. 2003. Freeze-substitution protocols for improved visualization of membranes in high-pressure frozen samples. Journal of Microscopy. 212:53-61.

Hohenberg, H., Mannweiler, K. and Mueller, M. 1994. High-pressure freezing of cell suspensions in cellulose capillary tubes. Journal of Microscopy. 175:34-43.

Holthuis, J.C.M. and Levine, T.P. 2005. Lipid Traffic: Floppy Drives and a Superhighway. Nature Reviews Molecular Cell Biology. 6:209-220.

Hopkins, J., Fowler, R., Krishna, S., Wilson, I., Mitchell, G. and Bannister, L. 1999. The plastid in *Plasmodium falciparum* asexual blood stages: a three-dimensional ultrastructural analysis. Protist. 150:283-295.

Humbel, B. and Müller, M. 1986. Freeze substitution and low temperature embedding. In The Science of Biological Specimen Preparation 1985. M. Müller, R.P. Becker, A. Boyde, and J.J. Wolosewick, editors. SEM Inc., AMF O'Hare. 175-183.

Humbel, B.M. and Schwarz, H. 1989. Freeze-substitution for immunochemistry. In Immuno-

Gold Labeling in Cell Biology. A.J. Verkleij and J.L.M. Leunissen, editors. CRC Press, Boca Raton. 115-134.
Jomaa, H., Wiesner, J., Sanderbrand, S., Altincicek, B., Weidemeyer, C., Hintz, M., Türbachova, I., Eberl, M., Zeidler, J., Lichtenthaler, H.K., Soldati, D. and Beck, E. 1999. Inhibitors of the nonmevalonate pathway of isoprenoid biosynthesis as antimalarial drugs. Science. 285:1573-1576.
Kaneko, Y. and Walther, P. 1995. Comparison of ultrastructure of germinating pea leaves prepared by high-pressure freezing-freeze substitution and conventional chemical fixation. Journal of Electron Microscopy. 44:104-109.
Köhler, S. 2005. Multi-membrane-bound structures of Apicomplexa: I. the architecture of the *Toxoplasma gondii* apicoplast. Parasitology Research. 96:258-272.
Kroth, P. and Strotmann, H. 1999. Diatom plastids: Secondary endocytobiosis, plastid genome and protein import. Physiology of Plants. 107:136-141.
Mastronarde, D.N. 1997. Dual-axis tomography: an approach with alignment methods that preserve resolution. Journal of Structural Biology. 120:343-352.
McDonald, K.L. and Müller-Reichert, T. 2002. Cryomethods for thin section electron microscopy. Methods in Enzymology. 351:96-123.
McEwen, B.F.e.a. 1995. The relevance of dose-fractionation in tomography of radiation-sensitive specimens. Ultramicroscopy. 60:357–373.
McFadden, G. and Gilson, P. 1995. Something borrowed, something green: lateral transfer of chloroplasts by secondary endosymbiosis. Trends in Ecological Evolution. 10:12-17.
Müller, M. 1992. The integrating power of cryofixation-based electron microscopy in biology. Acta Microscopica. 1:37-44.
Müller, M., Marti, T. and Kriz, S. 1980. Improved structural preservation by freeze substitution. In: Proceedings of the 7th European Congress on Electron Microscopy. P. Brederoo and W. de Priester, editors:720-721.
Murk, J.L.A.N., Posthuma, G., Koster, A.J., Geuze, H.J., Verkleij, A.J., Kleijmeer, M.J. and Humbel, B.M. 2003. Influence of aldehyde fixation on the morphology of endosomes and lysosomes: Quatitative analysis and electron tomography. Journal of Microscopy. 212:81-90.
Nielsen, H., Engelbrecht, J., Brunak, S. and von Heijne, G. 1997. A neural network method for identification of prokaryotic and eukaryotic signal peptides and prediction of their cleavage sites. International Journal of Neural Systems. 8:581-599.
Penczek, P., Marko, M., Buttle, K. and Frank, J. 1995. Double-tilt electron tomography. Ultramicroscopy. 60:393-410.
Radermacher, M. 1992. Weighted back projection methods. In Electron Tomography: Three Dimensional Imaging with the Transmission Electron Microscope. J. Frank, editor. Plenum Press. 91–115.
Ralph, S.A., van Dooren, G.G., Waller, R.F., Crawford, M.J., Fraunholz, M.J., Foth, B.J., Tonkin, C.J., Roos, D.S. and McFadden, G.I. 2004. Methabolic Maps and Functions of the *Plasmodium falciparum* Apicoplast. Nature Reviews | Microbiology. 2:204-216.
Roos, D.S., Crawford, M.J., Donald, R.G., Kissinger, J.C., Klimczak, L.J. and Striepen, B. 1999. Origin, targeting, and function of the apicomplexan plastid. Current Opinion in Microbiology. 2:426-432.
Sawaguchi, A., McDonald, K.L., Karvar, S. and Forte, J.G. 2002. A new approach for high-pressure freezing of primary culture cells: the fine structure and stimulation-associated transformation of cultured rabbit gastric parietal cells. Journal of Microscopy. 208:158-166.
Steinbrecht, R.A. 1980. Cryofixation without cryoprotectants. Freeze substitution and freeze etching of an insect olfactory receptor. Tissue and Cell. 12:73-100.

Steinbrecht, R.A. and Zierold, K. 1987. Cryotechniques in Biological Electron Microscopy. Springer-Verlag, Berlin, Heidelberg.

Studer, D., Michel, M., Wohlwend, M., Hunziker, E.B. and Buschmann, M.D. 1995. Vitrification of articular cartilage by high-pressure freezing. Journal of Microscopy. 179:321-332.

Szczesny, P.J., Walther, P. and Müller, M. 1996. Light damage in rod outer segments: the effects of fixation on ultrastructural alterations. Current Eye Research. 15:807-814.

Tomova, C., Geerts, W.J.C., Müller-Reichert, T., Entzeroth, R. and Humbel, B.M. 2006. New comprehension of the apicoplast of Sarcocystis by transmission electron tomography. Biology of the Cell. 98:535–545.

van Dooren, G.G., Schwartzbach, S.D., Osafune, T. and McFadden, G.I. 2001. Translocation of proteins across the multiple membranes of complex plastids. Biochimica et Biophysica Acta. 1541:34-53.

van Dooren, G.G., Tomova, C., Agrawal, S., Humbel, B.M. and Striepen, B. 2008. *Toxoplasma gondii* Tic20 is essential for apicoplast protein import. Proceedings of the National Academy of Science of the Unated States of America. 105:13574–13579.

van Harreveld, A., J., C. and Malhotra, S.K. 1965. A study of extracellular space in central nervous tissue by freeze-substitution. Journal of Cell Biology. 25:117-137.

van Meer, G., Voelker, D.R. and Feigenson, G.W. 2008. Membrane lipids: where they are and how they behave. Nature Reviewsws | molecular cell biology. 9:112-124.

Waller, R.F., Keeling, P.J., Donald, R.G.K., Striepen, B., Handman, E., Lang-Unnasch, N., Cowman, A.F., Besra, G.S., Roos, D.S. and McFadden, G.I. 1998. Nuclear-encoded proteins target to the plastid in *Toxoplasma gondii* and *Plasmodium falciparum*. Proceedings of the National Academy of Science USA. 95:12352-12357.

Waller, R.F., Reed, M.B., Cowman, A.F. and McFadden, G.I. 2000. Protein trafficking to the plastid of *Plasmodium falciparum* is via the secretory pathway. EMBO Journal. 19:1794–1802.

Walther, P. and Ziegler, A. 2002. Freeze substitution of high-pressure frozen samples: the visibility of biological membranes is improved when the substitution medium contains water. Journal of Microscopy. 208:3-10.

Weisiger, R.A. and Zucker, S.D. 2002. Transfer of fatty acids between intracellular membranes: roles of soluble binding proteins, distance, and time. Journal of Gastrointestinal and Liver Physiology. 282:G105–G115.

Yung, S. and Lang-Unnasch, N. 1999. Targeting of a nuclear encoded protein to the apicoplast of *Toxoplasma gondii*. Journal of Eukaryotic Microbiology. 46:79S-80S.

SAMENVATTING

NEDERLANDSE SAMENVATTING

Tijdens de evolutie heeft het proces van endosymbiose geleid tot een significante verscheidenheid aan plastid-dragende organismen. Ondanks hun verschillen in morfologie en fysiologie komen zij allen voort uit één enkele succesvolle integratie van een cyano-bacterie-achtige voorvader in een eukaryotic phagotroof (Delwiche en Palmer, 1997). Het product van deze primaire symbiotische gebeurtenis, een alg, is vervolgens opnieuw geintegreerd in een andere vrij levende eukaryoot tijdens een proces dat secundaire endosymbiose genoemd wordt. Deze gebeurtenis had de vorming van meer complexe organellen tot gevolg die nu als zogenaamde “secundaire plastiden” bekend zijn (McFadden en Gilson, 1995; Palmer en Delwiche, 1996). Deze plastiden worden omgeven door drie of vier membranen en komen voor in talrijke organismen. Hoofdzakelijk in algen maar ook in een zeer opmerkelijke groep van protozoa, namelijk de intracellulaire parasieten van het phylum Apicomplexa. In dit phylum vinden we onder andere de veroorzakers van malaria en toxoplasmose bij mensen of coccidiosis in gevogelte en vee.
Een cruciale stap bij de totstandkoming van een nieuw gecompliceerd organisme, het resultaat van de secundaire endosymbiose, is de regulering van metabole processen. Tijdens het proces van symbiont integratie is namelijk een groot deel van het genetisch materiaal onder gebracht in de kern van de gastheercel (Martin en Herrmann, 1998). Hierdoor moeten de in de gastheer gecodeerde eiwitten getransporteerd worden naar het organel. De vraag van hoe de plastid-eiwitten door en over de verschillende membraan-bilagen worden vervoerd is nog steeds een onopgeloste kwestie, met name in de gecompliceerde (secundaire) plastiden.
Het plastide van de Apicomplexa parasieten (de apicoplast) heeft een secundair endosymbiotische oorsprong en wordt vaak als een plastide overblijfsel beschouwt omdat het geen fotosynthetische eigenschappen meer bezit. Genoom sequenties van *Plasmodium falciparum* en van *Toxoplasma gondii* voorspellen dat de meeste genen die apicoplast eiwitten coderen, een rol spelen in anabole processen. De eiwitten zijn betrokken bij de vetzuur synthese (Waller et al., 1998; Jelenska et al., 2001; Crawford et al., 2003; Fleige et al., 2007) en de non-mevalonate synthese van het isopen-tenyldifosfaat (Jomaa et al., 1999; Ralph et al., 2004). De producten van deze metabole paden hebben waarschijnlijk functies in de apicoplast. Een aantal van deze producten zullen waarschijnlijk voor de gehele parasietcel essentieel zijn. Vrij snel na zijn ontdekking werd duidelijk dat de apicoplast onontbeerlijk is voor de parasiet (Fichera en Roos, 1997a; Mazumdar et al., 2006).
In dit proefschrift is onomstotelijk vastgesteld dat de apicoplast van *Toxoplasma gondii* wordt omringd door een viertal membranen. De binnenste twee membranen zijn vermoedelijk afkomstig van de pro-plastide binnen- en buitenmembraan, welke het resultaat zijn van de eerste endosymbiotische gebeurtenis (McFadden, 1999a). De derde membraan is vermoedelijk afkomstig van de endosymbiont plasma membraan en de buitenmembraan van de phagocytic vacuole van een voorouderlijke apicomplexa. De twee binnen membranen zijn cirkel vormig en hebben een constante afstand van elkaar. Het lijkt erop dat er grote eiwitcomplexen tussen hen aanwezig zijn. De beide buiten membranen zijn veel onregelmatiger van vorm. De periplastid membraan (derde membraan) bevat grote eiwit complexen, terwijl de buiten membraan flinke uitstulpingen in het parasiet cytoplasma vertoont. Daarnaast zien we dat het nauw verbonden is met het endoplasmatisch reticulum (ER) door middel van `contactplaatsen' (Tomova et.al., 2006). In dit proefschrift hebben we de structurele eigenschappen van deze membraancontact plaatsen tussen het ER en de buitenste membraan van de apicoplast in T. Gondii, bepaald. Gebaseerd op onze huidige kennis van lipiden transport en de rol van de apicoplast in een eukaryote cel denken we dat deze membraan contact plaatsen (MCS)

een belangrijke rol spelen bij het lipiden transport in de parasiet cel.
Het 35 kb grote apicoplast genoom is het kleinste plastide genoom dat tot dusver beschreven is. Het codeert voor slechts 30 eiwitten (Köhler et al., 1997). De meeste apicoplast eiwitten worden dus in de kern gecodeerd. Een aantal van deze kern-gecodeerde-plastid-eiwitten van T. gondii zijn geïdentificeerd en zij bevatten een dubbel target peptide aan het N-terminale uiteinde (Waller et al., 1998). Het eerste gedeelte van dit target peptide bepaald de toegang tot het endoplasmic reticulum, terwijl het tweede gedeelte het verdere transport naar het plastide toe, bepaald (Hempel et al., 2007; Nassoury en Morse, 2005).
In apicomplexa worden luminale eiwitten via de secretoire route getransporteerd en schijnt het Golgi omzeilt te worden (DeRocher, 2005; Tonkin et al., 2006b). De route die oplosbare eiwitten van het ER naar de apicoplast afleggen, wordt bepaald door de "transit" regio (DeRocher et al., 2000; Waller et al., 2000; Yung et al., 2001). In zowel *Plasmodium falciparum* (Foth et al., 2003) als *Toxoplasma gondii* (Tonkin et al., 2006a) is het positief geladen N-terminale gedeelte van de transit regio essentieel voor het nauwkeurig leiden van de eiwitten. Daarbij moeten de apicoplast stromal-proteïnen, vier membranen passeren. Hoewel er diverse modellen zijn (b.v. (Foth en McFadden, 2003; Parsons et al., 2007; Tonkin et al., 2008; van Dooren et al., 2001) is de vraag hoe de eiwitten deze uitdaging aanpakken, onbeantwoord.
In dit proefschrift is een moleculaire benadering gecombineerd met 3D elektronen microscopie, om een beter begrip te krijgen van het eiwit transport naar de apicoplast. Uit de resultaten blijkt dat "blaasjes" ofwel "vesicles" de manier van transport zijn om de door de kern gecodeerde eiwitten naar hun functionele plaats, de apicoplast te transporteren. We analyseerden de distributie van stroma-gerichte proteïnen (ACP en FNR) in de geconditioneerde *Tg*Tic20KO fnr-DHFR mutantlijn (van Dooren et al., 2008). De resultaten bevestigen de vesicle hypothese en ondersteunen de significante rol van *Tg*Tic20 in de biogenesis van de apicoplast. We tonen aan dat Tic20 in T. gondii een integraal eiwit is van de binnenste plastid membraan en dat verlies van *Tg*Tic20 tot een ernstige verstoring van plastide eiwitinvoer, leidt. *Tg*Tic20 is daarmee de eerste experimenteel geidentificeerde invoerfactor in T. gondii (van Dooren et al., 2008). Als laatste stellen we een nieuw model voor waarin de huidige kennis van eiwit transport over de 4 membranen van de apicoplast, zijn verwerkt.

ACKNOWLEDGEMENTS

I would like to express my gratitude to my Supervisor Prof. Arie J. Verkleij for making this work possible, for his support and understanding in every step of the way, but most of all for his wonderful personality!
I also would like to sincerely acknowledge Prof.Dr. R. Entzeroth (Institute of Zoology, TU Dresden, Germany) for initiating this project and for the support and freedom he gave me in my scientific career during my assistantship in his laboratory (2004-2006). I would like to acknowledge my colleagues from Dresden: Christine, Regina, Gudrun, Michael, Sacha, Susane, Steffi, which contributed to this work in different ways and some of them became my friends.
Turning point in this research was my first visit in Utrecht University as a student from the 3D Network of Excellence in April 2005. During this 2 months period my contact person and daily supervisor, Dr. Willie J.C. Geerts, taught me how to do tomography and ever since I have his support and care. Thank you very much, Willie!
I do thank Dr. B.M. Humbel for accepting the obligation of being a co-supervisor of this work and thus enabling the beginning of my PhD studies in Utrecht. I am thankful for his criticism, which turned to be very helpful in finding “my way” in this research.
I would like to express my sincere thankfulness and appreciation to Prof. Boris Striepen and Dr. Giel G. van Dooren (Centre for Tropical and Emerging Global Diseases and Department of Cellular Biology, University of Georgia, Athens, USA). Their professionalism, knowledge and support are of enormous value for the successful accomplishment of this work.
I am especially thankful to Prof. J.C.M. Smeekens, Dr. J.C. Holthuis, Prof. A.J. Koster for the support and the useful discussions. I am indebt to Prof. J. Klumperman for her proficiency and valuable help in my professional self-awareness.
My most special Thank You is for the colleagues from the EM part of the CAD Department (UU). Most of all to:
Elly van Donselaar for sharing her priceless experience with me, for the numerous discussions, for her precision, for the support and trust she gave me. Thank you Elly!
Dr. Nuria Jimenez-Gil, the best office-mate, a friend in good and bad times, I cherish our loud laughter and silent understanding.
Hans Meeldijk and Chris Schneijdenberg Thank you for teaching me so much about microscopes, for being always there for me (for scientific and not so scientific problems), for making me smile no matter what, for being such wonderful people!
Dr. W.H. Müller for being there and pulling me out in moments of hardship and isolation, for teaching me that there are “no bad days, but only good days, occasionally some better days and very seldom best days”. Thank you Wally!
Montse, Alya, Daniëlle, Matthia, Karin, Miriam, Liesbeth, Elsa, Laura, Theo, Misjaël, Bart, Marco, Matthijs, Heiner, Rahmat, Mark for the help, the nice moments and friendly attitude, and all the colleagues from the CAD Department for their kindness.

I am grateful to my family for their unconditional support and love!

Curriculum Vitae

Cveta B. Tomova born in Ruse, Bulgaria, on the 18th of June 1976.
1989-1994 Gymnasium with high profile in Natural Sciences, Ruse, Bulgaria
1994-2000 University Plovdiv, Faculty of Biology, Plovdiv, Bulgaria
Degree: MSc Ecology obtained in July 2000 after public defence of the diploma thesis under the supervision of Prof. V. Golemansky and Prof. G. Bychvarov.
1997-1999 Specialization of Parasitology with internships in:
Medical Parasitology under the supervision of Prof. M.D. M. Andreeva (Medical Academy, Plovdiv,) Medical Entomology under the supervision of Prof. T. Hristova (Medical Academy, Sofia), Veterinary Parasitology under the supervision of Prof. V.M.D. A. Arnaudov (Veterinary Academy, Plovdiv) and Histology of Helminths under the supervision of Prof. G. Bychvarov and Dr. D. Kirin (Plovdiv University).
2000-2001 Internship in Protoparasitology and latter assistant position in Institute of Zoology /Bulgarian Academy of Science/ Sofia, Bulgaria, Department of Protozoology under the supervision of Prof. V. Golemansky.
2001-2002 Scientific assistant at the Institute of Veterinary Medicine, Ruse, Bulgaria
2004-2006 Research Associate /basic and advanced teaching/ in the Institute of Zoology, Spezielle Zoologie und Parasitologie, TU Dresden, Dresden, Germany
Scientific research: Structural studies of the apicoplast in Toxoplasma, Besnoitia and Sarcocystis under the supervision of Prof.Dr. R. Entzeroth.
2006 –2008 PhD position at the department of Cellular Architecture and Dynamics, University Utrecht, The Netherlands, under the supervision of Prof. A.J. Verkleij.

Publications:

Protozoan parasites in Amphibians /*Amphibia:Anura*/ and Reptiles /*Reptilia: Squamta*/ from Bulgaria. Golemansky, V. and Tomova, C.Actazool. Bulg., 53(1):41-46, 2001

New Comprehension of the Apicoplast of *Sarcocystis* by Transmission Electron Tomography. Tomova, C., Geerts, W. J.C., Müller-Reichert, T., Entzeroth, R., Humbel, B. M. Biology of the Cell, 98, 535–545, 2006

A Tic20 homologue in *Toxoplasma gondii* is essential for plastid protein import and biogenesis. G. G. van Dooren, C. Tomova, S. Agrawal, B. M. Humbel and B. Striepen PNAS,105,13574-13579,2008

Papers in preparation:

Membrane Contact Sites between the Apicoplast and the Endoplasmic Reticulum in *Toxoplasma gondii* Revealed by Electron Tomography. C. B., Tomova, B. M., Humbel, W. J., Geerts, R., Entzeroth,J. C. M., Holthuis and A.J., Verkleij

Vesicular trafficking of proteins to the apicoplast of *Toxoplasma gondii* the first step for stromal proteins to cross multiple bilayers. C. Tomova, G. G. van Dooren, B. Striepen, E. G. van Donselaar, W. H. Müller, B. M. Humbel and A. J. Verkleij

An novel dynamin-related protein has been recruited for apicoplast fission in *Toxoplasma gondii.* Giel G. van Dooren, Sarah B. Reiff, Cveta Tomova, Markus Meissner, Bruno M. Humbel and Boris Striepen